AD_____

Award Number: DAMD17-01-1-0688

TITLE: Novel Tissue Models of Junctional Epidermolysis Bullosa to Characterize Functional Mechanisms of Sulfur Mustard Injury to Human Skin

PRINCIPAL INVESTIGATOR: Jonathan A. Garlick, Ph.D.

CONTRACTING ORGANIZATION: The Research Foundation of
State University of New York
Stony Brook, NY 11794-3362

REPORT DATE: May 2004

TYPE OF REPORT: Annual

PREPARED FOR: U.S. Army Medical Research and Materiel Command
Fort Detrick, Maryland 21702-5012

REPORT DOCUMENTATION PAGE

Form Approved
OMB No. 074-0188

1. AGENCY USE ONLY (Leave blank)	2. REPORT DATE	3. REPORT TYPE AND DATES COVERED
	May 2004	Annual (1 May 2003 - 30 Apr 2004)

4. TITLE AND SUBTITLE
Novel Tissue Models of Junctional Epidermolysis Bullosa to Characterize Functional Mechanisms of Sulfur Mustard Injury to Human Skin

5. FUNDING NUMBERS
DAMD17-01-1-0688

6. AUTHOR(S)

Jonathan A. Garlick, Ph.D.

7. PERFORMING ORGANIZATION NAME(S) AND ADDRESS(ES)

The Research Foundation of
State University of New York
Stony Brook, NY 11794-3362

E-Mail: jgarlick@sunysb.edu

8. PERFORMING ORGANIZATION REPORT NUMBER

9. SPONSORING / MONITORING AGENCY NAME(S) AND ADDRESS(ES)
U.S. Army Medical Research and Materiel Command
Fort Detrick, Maryland 21702-5012

10. SPONSORING / MONITORING AGENCY REPORT NUMBER

11. SUPPLEMENTARY NOTES
Original contains color plates: ALL DTIC reproductions will be in black and white

12a. DISTRIBUTION / AVAILABILITY STATEMENT
Approved for Public Release; Distribution Unlimited

12b. DISTRIBUTION CODE

13. ABSTRACT (Maximum 200 Words)

We first measured dose-time responses in 2-D and 3-D cultures (TASK 1) and discovered that an SM dose of 150uM induced significant apoptotic cell death. We next compared the SM response of 3-D cultures grown in the absence or presence (AlloDerm) of structured basement membrane (BM) (TASK 8) and found that the presence of BM led to resistance to SM-induced damage, suggesting that BM could protect basal keratinocytes from SM-induced apoptosis. To further explore the role of BM in decreased SM susceptibility, primary keratinocytes harvested from Junctional Epidermolysis Bullosa (JEB) patients (#552), that lack a functional γ2 chain of laminin 5 and do not adhere to BM, were transduced with retroviral vectors (TASK 4) to restore or abrogate laminin 5-mediated adhesion. We constructed 3-D tissues with these "reverted" JEB cells (TASK 5,6 and 7) and their phenotypic analysis showed that only JEB cells with restored laminin 5 function (F-GAL) were resistant to apoptosis when exposed to SM (150uM), thereby implicating laminin 5-mediated attachment as being important in limiting SM damage. These studies provide important evidence that bioengineered, *in vitro* tissues mimic many skin alterations previously found in vivo and that adhesion to BM enables epithelial resistance to SM damage.

14. SUBJECT TERMS	15. NUMBER OF PAGES
Sulfur mustard, basement membrane, organotypic culture, keratinocytes	70
	16. PRICE CODE

17. SECURITY CLASSIFICATION OF REPORT	18. SECURITY CLASSIFICATION OF THIS PAGE	19. SECURITY CLASSIFICATION OF ABSTRACT	20. LIMITATION OF ABSTRACT
Unclassified	Unclassified	Unclassified	Unlimited

Table of Contents

Cover.....1

SF 298.....2

Table of Contents.....3

Introduction.....4

Body.....4

Key Research Accomplishments.....12

Reportable Outcomes.....13

Conclusions..... 14

References.....none

Appendices.....15

INTRODUCTION

A major reason for our limited understanding of what triggers SM injury is that detailed mechanistic studies using human skin have not been possible for ethical reasons. Therefore, we have used an approach that has allowed us to identify sites and pathways of sulfur mustard (SM)-induced vesication using engineered human skin that mimics the clinical and histologic features of this tissue. Through research conducted this past year, our laboratory has extensively studied the pathophysiology of bioengineered, *in vitro,* 3-D human skin in response to SM by establishing dose/time responses of these human, skin-like tissues that lead to dermal-epidermal separation. We have developed and adapted novel tissue models that have found that structured basement membrane can alter the response to SM injury by making the tissue less susceptible to SM-mediated damage. We used immunohistochemical, morphologic and biochemical analyses to characterize the influence of these ECM and BM subtrates on the morphogenesis, survival, differentiation and growth of NHK. We have found that the presence of individual BM components, Type IV and tissues grown on intact complete BM (de-epidermalized dermis) in organotypic cultures supports the survival of these skin-like tissues. Since there is a significant linkage between the pathologic alterations in Junctional Epidermolysis Bullosa (JEB) and SM injury, our understanding of he molecular defects in in BM causing JEB should shed light on the pathogenesis of SM-induced blistering. To further explore the role of basement membrane proteins in keratinocyte resistance to SM-induced damage, we directly studied the role of laminin 5 in this process. Primary keratinocytes harvested from patients with the blistering skin disease Junctional Epidermolysis Bullosa (JEB), that lack a functional gamma 2 chain of laminin 5 and are not able to adhere to basement membrane, were transduced with retroviral vectors designed to restore laminin 5-mediated adhesion. We found that only JEB cells in which laminin 5 adhesive function was restored (F-GAL) were resistant to apoptosis when exposed to SM (150 ug/ml), thereby implicating laminin 5-mediated attachment as being important in limiting SM damage. These studies provide important proof of concept that *in vitro* and *in vivo* tissue models mimic many of the tissue alterations previously found in animal models of SM injury. Our findings show that adhesion to basement membrane proteins enables subsets of keratinocytes to resist SM damage. Since we have previously found that only specific subsets of basal keratinocytes underwent cellular damage leading to apoptosis in our *in vivo* engineered tissue models, we have taken an important step towards defining the ECM or BM components that provide survival signals that can protect cells when challenged with SM. These human tissue models will be of great relevance in understanding functional mechanisms of SM injury and in testing new countermeasures to limit its morbidity and mortality.

EXPERIMENTAL RESULTS:

PART I: ESTABLISHMENT OF CONDITIONS UNDER WHICH SULFUR MUSTARD CAN ALTER THE SURVIVAL AND VIABILITY OF NORMAL HUMAN KERATINOCYTES AND JUNCTIONAL EPIDERMOLYSIS BULLOSA CELLS GROWN ON A VARIETY OF BASEMENT MEMBRANE COMPONENTS IN 2-D MONOLAYER CULTURES

TASK 1: To determine the dose/time responses of normal keratinocytes to sulfur mustard exposure

1. **Determination of the effects of ethanol on human keratinocytes:** Prior to the application of sulfur

mustard (SM) on cultured cells, we conducted a series of experiments using various concentrations of pure ethanol to determine the effects of this solvent on keratinocyte growth and survival. This was done because SM was dissolved in pure ethanol and it was important to determine if this vehicle would induce alterations in cultured cells at the SM concentrations needed. Experiments were carried out in p60 plates and keratinocytes were grown on feeder layers of γ-irradiated 3T3 cells until colonies were 60% confluent. Cultures were then exposed to different doses of ethanol (0.4%, 0.8%, 1.6%) for 30 min and compared to untreated controls. Plates were then rinsed three times with fresh media and were grown for an additional week. Colonies were stained using crystal violet and the diameter of colonies exposed to ethanol doses were measured. ***Based on our experiments we concluded that ethanol did not greatly alter the growth of keratinocytes compared to the non-exposed controls as the size of individual colonies was not altered upon exposure to ethanol (Figure 1).***

2. Staining for cellular apoptosis to determine the dose and time response of cultured keratinocytes to sulfur mustard: To establish the SM doses that could induce alterations in keratinocyte growth, a dose and time study was performed to measure the response of human keratinocytes to SM. Keratinocytes were seeded on sterile coverslips with 3T3 feeder layers (10,000 cells/p60) for six days in p60 plates until the colonies became 70% confluent. Cultures were then exposed to different doses of SM and compared to ethanol-exposed controls. We initially selected four different doses 37.5, 75, 150, 300μM of SM and compared these to 0.25, 0.5, 1, 2% ethanol upon exposure for 7 min. Cells on coverslips that were exposed to agents were then processed 24 hours later for immunofluorescent staining for the presence of apoptotic cells using a monoclonal antibody that detects the cleavage product of keratin 18 that is the end result of apoptotic pathways (M30 Cytodeath-stain, Roche, Inc.). Fig. 3 shows the appearance of apoptotic cells that demonstrated M30 staining in the cytoplasm (red stain) for different doses of SM when compared to corresponding ethanol controls. At low SM doses of (37.5μM, 75μM), fewer apoptotic cells were seen when compared to 150 and 300μM SM doses. All doses of ethanol showed fewer apoptotic cells than SM-exposed cells. ***Thus a dose-dependent increase in the number of apoptotic cells was seen after SM treatment. Based on these findings, we selected 150μM as a standard SM dose that induced a maximum number of apoptotic cells.***

An additional experiment was performed to study the effect of the length of exposure to SM on cell survival and death. We selected a dose of 150μM to study the effects of SM exposure for 1,3, 7, 14, and 28 min. Staining was performed for apoptotic keratinocytes grown on coverslips using the M30 stain the numbers of apoptotic cells on 3 coverslips were counted for each length of exposure. A sharp increase in the number of apoptotic cells was seen for 7 min exposures when compared to 1 and 3 min exposures. Longer exposures (14 min and 28 min) resulted in an 8–10 fold increase in numbers of apoptotic cells when compared to cultures exposed for 7 min (Fig. 5). In comparison, untreated controls showed a very small number of apoptotic cells while ethanol showed very small changes in the number of apoptotic cells. Fig. 6 demonstrates the appearance M30 positive cell after exposure to SM and to 1% ethanol for 7 min. ***These findings demonstrated that a SM dose of 150μM at an exposure time of 7 min was sufficient to induce significant apoptotic cell damage in 2-D cultures of keratinocytes. As a result, it was decided to use 7 min as the standard SM exposure time for all future studies.***

3. MTT viability/survival assays to determine keratinocyte survival after SM exposure: We next performed the MTT assay to evaluate the viability of normal keratinocytes after exposure to SM. In this assay, the yellow tetrazolium salt MTT is reduced in metabolically active cells to form insoluble purple formazan crystals that are solubilized by the addition of a detergent. The purple color can then be

quantified by spectrophotometric means and provides a direct measure of cell viability upon exposure to SM. Conversely, a reduction in spectrophotometric measurement reflects the loss of cell viability. We performed MTT assays using normal human keratinocytes (NHK) at different cell densities to establish if varying cell density could alter cell viability in response to SM. NHK's were plated at densities of $5X10^4$, $2.5X10^4$, $1X10^4$ and $1X10^3$ and exposed to either 150μM of SM or to 1% ethanol control. Fig. 7 demonstrates that cells seeded at low densities (1,000 and 10,000 cells) showed no difference in cell viability when SM exposures were compared to ethanol controls (Fig. 7). However, at high cell densities (25,000 and 50,000 cells), SM exposure significantly decreased cell viability when compared to ethanol-exposed controls. ***This demonstrated that the sensitivity of detection of MTT assay required a threshold number of cells greater than 25,000 to yield differences in cell survival between SM- and ethanol-exposed cells. These studies laid the groundwork for all experiments by establishing parameters required for length and concentration of SM exposure needed to alter cell viability and to induce apoptosis.***

TASK 8 : Dose-time response to establish the role of basement membrane components to SM in 2-D cultures

4. The role of basement membrane components on the survival and viability of keratinocytes exposed to sulfur mustard - We next performed experiments to establish the importance of (BM) or extracellular matrix components (EMC) on cell viability and cell survival when exposed to different doses of SM compared to ethanol controls. To establish if the basement membrane (BM) protein Type IV collagen could alter the sensitivity of normal keratinocytes to SM, we seeded different numbers of keratinocytes on Type IV Collagen-coated, 24-well plates and performed MTT viability assays (Fig.8). Results were similar to those seen when cells were plated on tissue culture plastic as SM-exposed cells showed lower viability when compared to those ethanol-exposed at higher cell density (50,000 and 25,000). Similar differences were seen when cells were exposed to SM and ethanol after seeding onto Type I Collagen coated plates (Fig. 9). These experiments demonstrated that an SM dose of 150μM for 7 min reduced cell survival compared to ethanol exposure. Fig.10 presents MTT viability assays when 50,000 cells were plated on different substrates including plastic, Type I Collagen, Type IV Collagen, Fibronectin, Laminin and Poly D-lysine in monolayer, 2-D cultures. 24 hours after seeding, cells were exposed to 150μM SM or 1% ethanol for 7min. All the plates showed a decrease in cell viability when treated with SM compared to ethanol controls. However, the greatest reduction in viability (50%) upon SM exposure was seen for cells grown on Type IV Collagen. Since cells grown on this substrate also demonstrated the highest cell viability when exposed to ethanol, it is possible that the elevated cell growth on Type IV Collagen made cells more vulnerable to SM damage. Other substrates (Type I Collagen, Fibronectin and Laminin) demonstrated decreased viability upon SM exposure, but to a lesser degree than Type IV Collagen. Poly-D-lysine and plastic-coated dishes demonstrated the smallest loss of viability upon SM exposure. This may be due to the poor attachment of keratinocytes to poly D-lysine-coated plates compared to other substrates.

MTT assays were carried out for varied doses of SM and ethanol on different substrates (Fig. 11). Four different doses of SM were tested (37.5, 75, 150, 300μM) and were compared to controls (0.25, 0.5, 1, 2% ethanol) when cells were seeded onto tissue culture plastic, Type I Collagen, Type IV Collagen, Fibronectin and Laminin. As described above, the greatest decrease in viability after SM exposure was seen for cells grown on Type IV Collagen. Interestingly, this was the only substrate that demonstrated loss of cell survival even at low SM doses (37.5μM and 75μM). Other substrates showed no loss of viability for these low SM doses but did show a moderate decrease at higher SM doses. Thus, while

ECM components were protective at low SM doses, they did not provide a survival advantage at higher SM doses. ***Significantly, cells grown on the BM component Type IV Collagen demonstrated the greatest sensitivity of cells to SM-induced damage in 2-D cultures. These findings demonstrated that individual ECM or BM components were not able to provide protection from SM damage in 2-D cultures and intact BM may be required to mediate this event.***

TASK 5: Dose-time response to establish the response of JEB cells to low dose SM exposure

5. <u>MTT Assay to determine the response of Junctional Epidermolysis Bulllosa (JEB) cells to SM:</u>
There is a significant linkage between the pathologic alterations seen in Junctional Epidermolysis Bullosa (JEB) and those seen in vesicant injury induced by SM. To determine if cells lacking the ability to synthesize a functional laminin 5 molecule would demonstrate an altered sensitivity to SM exposure, we utilized primary keratinocytes that were derived from patients with JEB that were deficient in laminin 5 function. JEB cell lines were initially harvested from the skin of a patient with JEB (552) by the laboratory of Dr. Guerrino Meneguzzi (INSERM, Nice, France). Cells were infected with retroviral vectors that were previously shown in our lab (Progress Report 1) to modify laminin 5 function and restore cell-substrate adhesion in cells that were adhesion-deficient due to the absence of Gamma 2 chain (Phoenix producer cells courtesy of Nolan lab). The following vectors were used to modify laminin 5 function in 552 cells:
Delta BC: Cleaved variant of Gamma 2 chain of laminin 5 with a shortened 80 kd Gamma 2 chain. This generates cells that do not adhere well to connective tissue substrates.
FGAL: Non-cleaved variant of Gamma 2 chain. The chain remains intact and is not cleaved at it's BMP-1 site to generate a 155kd chain that restores adhesion.
Pfu: A Gamma 2 mutant that encodes cDNA for the constitutively cleaved form of this chain that has been truncated at the proteolytic cleavage site to generate a 105kd chain. These cells do not adhere well to connective tissue substrates.
Wild type (Gamma 2 WT): This has a full-length Gamma 2 chain and cells infected with this variant restore their laminin 5 function.
Delta C115: This is an empty vector that does not correct laminin 5 due to the absence of Gamma 2 chain and so that cells retain the properties of the mutant cells.

We used the MTT cell proliferation assay to study the effects of SM on JEB cells that were seeded on different BM and ECM components such as Type I Collagen, Type IV Collagen, Fibronectin and Laminin, as well as control plastic plates. Cells were seeded into 24-well plates on these substrates and exposed to 150μM of SM or 1% ethanol on the following day for an exposure time of 7min, rinsed three times with fresh media and incubated for an additional 24 h. Fig. 12 represents results of MTT assays for these JEB cells grown on different ECM or BM substrates. In general, there was an increase in cell viability for the Gamma 2 WT, Delta C115 and FGAL cells, demonstrating that these cells survived the exposure on different substrates to a greater degree when compared to Delta BC and Pfu. However, the degree to which cell viability was altered was dependent on the substrate on which the JEB cells were plated. For example, cells that had restored their laminin 5-mediated adhesive function (FGAL and Gamma 2 WT) showed a minimal loss of viability on Type I and Type IV Collagen and tissue culture plates when compared to JEB cells restored with a gamma 2 chain that did not support adhesion (Delta BC). However, SM-induced loss of cell viability was not as great with Delta BC-restored cells on Fibronectin as had been seen on other substrates. ***These findings demonstrated that restoration of***

adhesive function mediated by laminin 5 was able to provide decreased cell vulnerability and increased cell survival upon SM exposure.

In light of these findings, we next performed MTT assays for JEB cells on these substrates at an elevated dose (300μM) of SM and compared this to control exposures of 2% ethanol (Fig. 13). As a control, we compared the SM response of JEB cells to that of normal keratinocytes, as well. JEB cells whose laminin 5-mediated adhesion was restored (FGAL and Gamma 2 WT) showed a similar susceptibility to this dose of SM, as did cells whose adhesion was not restored (Delta BC). Interestingly, all cells grown on Type IV collagen showed a 2 to 3 fold decrease in cell viability even in the presence of 2% ethanol, suggesting that this substrate rendered cells more susceptible to cell death. ***Thus, it appears that restoration of laminin 5 function could provide protection from SM damage only if the SM dose was lower than a threshold amount (150μM) in 2-D culture. Above this dose, even cells with intact laminin 5-mediated adhesion could not withstand SM-induced damage (300μM).***

To further confirm these observations regarding threshold doses of SM, JEB cells were tested on the three substrates that showed the maximum difference in cell viability when treated with SM and ethanol. To accomplish this, JEB cells were exposed to doses of SM (75, 150, 300 μM) and corresponding doses of ethanol controls (0.5, 1, 2 %) for 7 min. Fig. 14 presents results of the MTT assay for the 5 different JEB cell types and human keratinocytes seeded on three different substrates (Type I Collagen, Type IV Collagen, Fibronectin) that were exposed to 75μM of SM or 0.5% ethanol. At lowest SM doses (75μM, 150μM), FGAL cells showed sensitivity to SM damage on Type I Collagen and Fibronectin, but not on Type IV Collagen (Fig. 14). This supported the observation that restoration of laminin 5-mediated adhesion and resistance to M damage were optimal on proteins present in the BM such as Type IV Collagen at low SM doses. This may occur as Type IV Collagen is known to interact with laminin 5 and may provide apoptosis resistance as due to this adhesive association. This also suggested that restoration of laminin 5 function will not reduce the sensitivity to SM damage when cells are grown on a substrate that is not found in BM, such as Type I Collagen. This apoptosis resistance seen for FGAL cells was lost at higher SM doses (300μM, Fig. 16) and was similar to that seen for cells that did not undergo restoration of laminin 5 function (Delta BC) at low SM doses on Type IV Collagen. However, the loss of viability for Delta BC cells was greater than that seen for FGAL cells on Type IV Collage substrates, even at the elevated SM dose (300μM).

A final experiment in monolayer, 2-D culture was performed to compare SM damage between Delta BC and FGAL cells on two substrates (Type I Collagen and Type IV Collagen) that showed the maximum difference in cell viability after SM and ethanol exposure (Fig. 17-20). MTT assays were carried out using 8 different SM doses (75, 150,300, 450, 600, 750, 900, 1200μM) and compared to their corresponding ethanol controls (0.5, 1,2, 3, 4, 6, 8 %). Both FGAL and Delta BC cells showed a threshold, SM dose below which no decrease in cell viability was seen. Surprisingly this threshold was highest (450μM) for Delta BC cells grown on Type IV Collagen plates. In contrast, FGAL cells grown on both Type IV collagen and Type I collagen, as well as Delta BC cells grown on Type I collage showed a small SM-induced decrease in cell viability below 150μM SM. However, as SM dose was increased to 1200μM a gradual dose-dependent decrease in cell viability was seen for both cell types on both Type I and Type IV Collagen substrates. *At this point, we are unable to explain this greater sensitivity of SM exposed cells in 2-D cultures grown on basement membrane composed of only Type IV collagen. It is possible that matrix proteins are seeded de novo, after cell seeding, that masks the supportive effect of Type IV collagen. This may also explain the minimal loss of sensitivity to SM seen on Type 1 collagen.*

PART II: EXPOSURE OF THREE-DIMENSIONAL, HUMAN ORGANOTYPIC CULTURES HARBORING NORMAL HUMAN KERATINOCYTES AND JEB KERATINOCYTES TO DETERMINE THE ROLE OF BASEMENT MEMBRANE ON THE INDUCTION OF SULFUR MUSTARD INJURY

We next generated 3-D, organotypic cultures to identify pathways of SM induced vesication by using engineered human skin that mimics the clinical and histological features of this tissue. Organotypic cultures grown in the absence of pre-existing BM components ("Raft" cultures) were prepared according to our lab protocol. To accomplish this, early passage human dermal fibroblasts were added to neutralized Type I Collagen to a final concentration of $2.5X10^4$ cells per ml. This mixture (3ml) was added to each 35mm well insert of a six-well plate and incubated for 4-6 days in media containing Dulbecco's Modified Eagle's Medium and 10% fetal calf serum, until the collagen matrix showed no further shrinkage. At this time, a total of $5X10^5$ normal human epidermal keratinocytes were seeded directly on the contracted collagen gel. Alternatively, to generate cultures in the presence of BM, cells were seeded onto a de-epidermalized human dermis (AlloDerm) that was layered onto the contracted Type I Collagen gel. Organotypic cultures were maintained submerged in low calcium, epidermal growth media for 2 days , submerged for 2 days in normal calcium epidermal growth media and raised, to the air-liquid interface by feeding tissues from below with cornification media for an additional 2 days. At this point, cultures were exposed to different doses of SM or ethanol that were added to fresh media on day 7 of culture. Tissues were exposed for 7 min based on our previous results with 2-D monolayer cultures (see above). In addition to ethanol treated cultures, untreated cultures were used as controls by not adding ethanol to the media. After exposure, tissues were rinsed three times with fresh media and incubated for an additional 24 h. The following day, tissues were pulsed with 10μm bromodeoxyuridine (BrdU) 6h prior to terminating experiments to allow assay of proliferation in exposed tissues. Tissues were then bisected and one-half was snap-frozen in liquid nitrogen, while the other half of the tissue was formalin-fixed, paraffin-embedded and Hematoxylin and Eosin sections were prepared.

1. Establishing SM doses that induce tissue damage in 3-D organotypic cultures- morphologic and apoptotic alterations - To gain an understanding of SM doses needed to induce tissue damage in 3-D tissues, cultures were first treated with 75 and 150μm SM and compared to untreated cultures and those exposed to 1% ethanol. Figures 21 and 22 demonstrate the appearance of collagen Raft cultures grown in the absence of BM that were either unexposed (A), exposed to 75μM (B) or 150μM (C) SM or exposed to 1% ethanol (D). Untreated cultures generated a well-stratified epithelium that adhered to the underlying connective tissue. Tissues treated with 75μM SM demonstrated an intact epithelium that was well-attached to the underlying connective tissue (B). However, these tissues demonstrated a significant degree of altered tissue organization (B) that was similar to that seen for ethanol-exposed cultures (D). In contrast, cultures exposed to 150μM SM demonstrated complete dermal-epidermal separation (C) and an overall thinning of the epithelium. These preliminary findings showed that a 150μm dose of SM for 7 min could mimic the vesicating damaged induced by SM *in vivo*.

To assess the degree of apoptotic cell death in exposed tissues, M30 staining for Rafts exposed to different doses of SM and ethanol was performed from frozen sections. A four-fold increase in apoptotic cells was observed at a dose of 150μM of SM when compared to controls and twice as many apoptotic cells were seen with cultures treated with 75μM of SM (Fig. 23). We next determined if higher SM doses could increase SM-mediated tissue damage in Raft cultures by performing experiments using 150μM and 300μM of SM doses in comparison to 1 and 2% ethanol controls (Fig 24, 25). Low power magnification of H&E stained sections after treatment with 300μM SM showed a significant degree of tissue damage including complete separation of tissue from the BM zone as well as necrosis of keratinocytes and fibroblasts. Less damage was seen in tissues exposed to 150μM SM and there was no separation at the BM interface (Fig.25) To confirm these findings, frozen sections were stained using the M30 antibody. Numbers of apoptotic cells were greatest in tissues exposed to 300μM SM while ethanol-treated tissues showed a very minimal number of apoptotic cells. ***These findings established that doses similar to those found to induce SM damage in 2-D cultures of kerationcytes were also able to induce tissue damage in 3-D organotypic cultures. These tissue alterations included separation of the epithelium at the BM zone in a pattern similar to those found in our in vivo studies (REPORT Year 2).***

TASK 8 : Dose-time response to establish the role of basement membrane components to SM in 3-D, organotypic cultures

2. Establishing the role of basement membrane in human skin response to sulfur mustard - In light of these findings, we next studied the effects of SM on organotypic cultures grown in the presence and absence of pre-existing BM components. This would allow comparison to MTT assays carried out on different BM components in 2-D cultures described above. Keratinocytes were seeded on AlloDerm, the de-epidermalized, acellular cadaver dermis derived from human skin that forms intact BM at its dermal-epidermal interface. In this way, it would be possible to determine if BM can protect skin-like tissues from SM-induced damage when compared to tissues grown without BM components. To accomplish this, tissues were grown on AlloDerm, collagen Rafts or on polycarbonate membranes coated with either Type I Collagen, Type IV Collage, Fibronectin or control plastic. After 7 days in culture tissues were exposed to SM (150μM) and compared to tissues exposed to 1% ethanol. Fig. 27 represents the low power view of H&E stained tissue sections after SM exposure and Fig. 28 represents the higher magnification view. SM at a dose of 150μM induced separation at the BM zone when both collagen Raft (Fig. 27 B, Fig. 28 C) and plastic, non-coated inserts (Fig. 27 D, Fig. 28 B) were compared to the ethanol control (Fig. 27 D, E, Fig. 28 B, D). In contrast, tissues grown on AlloDerm showed that the BM interface was intact (Fig. 27 C, Fig. 28 E) as seen in ethanol-exposed controls (Fig. 27 F, Fib. 28F). Similarly, SM induced separation at the BM zone for tissues grown on different substrates (Type I Collagen, Type IV Collagen, Fibronectin) when compared to ethanol controls (Fig. 29 and Fig. 30).

To confirm these findings a dose of 150μM SM was used and compared to 1% ethanol and untreated controls to compare the effect of SM on organotypic cultures on which keratinocytes were grown on Rafts and AlloDerm (Fig. 31 and 32). Tissues treated with 150μM SM demonstrated intact tissues (Fig. 31 B) with minimal numbers of damaged, eosinophilic cells in the supra-basal layer (Fig. 32 B arrows) while untreated tissues showed a well-stratified epithelium that was similar to ethanol controls. In contrast, SM-treated Rafts showed a significantly higher number of damaged keratinocytes that displayed nuclear condensation and eosinophilic cytoplasm proving that SM could induce more severe damage to cells grown on Rafts than those grown on AlloDerm. To confirm these findings, we performed

immunofluorescent staining using the M30 antibody to assess numbers of apoptotic cells in exposed tissues (Fig. 33 & 34). Rafts treated with SM showed a 10-fold increase in number of apoptotic cells when compared to AlloDerm (Fig. 34), which displayed number of apoptotic cells that were similar to non-treated and ethanol controls. To determine if the induction of apoptosis demonstrated a dose-dependency, we performed experiments on AlloDerm using two different doses of SM along and compared them to controls. AlloDerms exposed to doses of 75μM and 150μM of SM were similar to untreated and ethanol controls in both tissue morphology (Fig. 35, 36) and upon M30 staining and numbers of apoptotic cells after M30 staining when compared to controls (Fig. 37).

In light of these findings, we next determined the minimal SM dose required for the induction of tissue damage in AlloDerm cultures. We selected 5 different SM doses (75, 150, 300, 600, 1200 μM) and compared these to ethanol controls (0.5, 1, 2, 4, 8 %) (Fig. 38 and 39). We found that the epithelium remained intact at SM doses of 75 and 150μM as induction of SM-mediated damage started at a dose of 300μM. At elevated doses of 600 and 1200μM SM tissue alterations were more prominent and were characterized by separation of the BM zone. Ethanol treated cultures showed little tissue damage even at elevated levels of ethanol exposure. M30 staining of these cultures showed a gradual increase in the number of apoptotic cells with increasing doses of SM from 75 to 300μM SM (Fig. 41). An SM dose of 75μM showed 3.8% of apoptotic cells compared to 57.2% observed for 1200μM while the maximum percentage of apoptotic cells observed for the highest dose of ethanol (8%) was only 3.6%. This gradual increase in numbers of apoptotic cells showed that AlloDerm tissues were susceptible to SM, but only above a threshold level of SM (600μM). ***These findings showed that only tissues with an intact BM could resist SM-induced damage, thus demonstrating that BM structure was protective upon SM exposure. This protective effect was only seen at doses of SM below 600 uM.***

TASK 5: Dose-time response to establish the response of JEB tissue constructs which were reverted to a normal phenotype by retroviral gene transfer to SM
TASK 6: Assay the response of JEB and normal organotypic cultures to high, vesicating doses of SM
TASK 7: Assay the response of JEB keratinocytes expressing mutated forms of the gamma- chain of laminin 5

3. Establishing the role of laminin 5-mediated adhesion in the response of 3-D tissues to sulfur mustard – the response of JEB mutants to sulfur mustard in 3-D tissues - Since it appeared that BM could protect tissues exposed to SM, we performed a final experiment to determine if JEB cells grown on AlloDerm demonstrated a differential susceptibility to 150μM SM (Fig. 42 and 43). All JEB cells showed a degree of epithelial separation at the BM zone when compared to ethanol-exposed control cultures. Normal cells grown on AlloDerm showed protection from SM damage but AlloDerm did not protect JEB cells, (FGAL, Delta BC, Pfu, Delta C115 and Gamma2wt) against the SM induced damage. This was confirmed by M30 staining of these tissues where we observed the induction of apoptosis due to SM compared to ethanol controls (Fig. 45). Paradoxically, FGAL and Gamma 2 WT cells showed the greater number of apoptotic cells among all different JEB cell types. ***This suggests that restoration at laminin 5-mediated adhesion did not protect tissues from SM-induced damage when tissues were exposed to 150μM SM and that restoration of laminin 5 alone was not sufficient to provide protection from the effects of SM.***

KEY RESEARCH ACCOMPLISHMENTS:

1 - We established dose/time responses of normal keratinocytes following exposure to SM and ethanol vehicle in tissue culture media (150uM) that induced biologically-meaningful changes in cell apoptosis and cell viability in 2-D cultures.

2 - We established dose/time responses of JEB keratinocytes following exposure to SM and ethanol vehicle in tissue culture media (150uM) that induced biologically-meaningful changes in cell apoptosis and cell viability in 2-D cultures.

3 - We have that established cells grown on the BM component Type IV Collagen demonstrated the greatest sensitivity of cells to SM-induced damage in 2-D cultures. These findings demonstrated that individual ECM or BM components were not able to provide protection from SM damage in 2-D cultures.

4 – We have found that restoration of laminin 5 function could provide protection from SM damage only if the SM dose was lower than a threshold amount (150 μM in 2-D) culture. Above this dose, even cells with intact laminin 5-mediated adhesion could not withstand SM-induced damage (300μM).

5 – We determined that doses similar to those found to induce SM damage in 2-D cultures of kerationcytes were also able to induce tissue damage in 3-D organotypic cultures. These tissue

6 – We have found that showed that only tissues with an intact BM could resist SM-induced damage, thus demonstrating that BM structure was protective upon SM exposure. This protective effect was only seen at doses of SM below 600 uM.

7 - We found that restoration at laminin 5-mediated adhesion did not protect tissues from SM-induced damage when tissues were exposed to 150μM SM and that restoration of laminin 5 alone was not sufficient to provide protection from the effects of SM..

REPORTABLE OUTCOMES

PAPERS

1. Andriani, F., Margulis, A., Lin, N., Griffey, S., and Garlick, J.A. Analysis of microenvironmental factors contributing to basement membrane assembly and normalized epidermal phenotype, J. INVEST. DERMATOL. 120:923-931, 2003.

2. Greenberg, S., Prabhu, P., Garfield, J., Hamilton, T., Petrali, J. and Garlick, J.A., Characterization of the initial response of bioengineered human skin to sulfur mustard. (submitted to J. INVEST. DERMATOL.)

ABSTRACTS PRESENTED

1. Prabhu, P., Greenberg, S., Lin, N., Garfield, J., Hamilton, T., Petrali, J and Garlick, J.A. Characterization of the Initial Response of Engineered Human Skin to Sulfur Mustard (Society for Investigative Dermatology, 2004)

2. Kamath, P., Greenberg, S., Petrali, J., Hamilton, T., Garfield, J., Pommeret, O., Meneguzzi, G., and Garlick, J.A. Characterization of the Initial Response of Bioengineered Human Skin to Sulfur Mustard: The Role of Basement Membrane (U.S. Army Medical Defense Review Bioscience, 2004).

CONCLUSIONS

A major goal of our research studies was to determine the initiating site of SM induced damage that leads to vesicating injury in human skin. YEAR 1 of our research allowed us to generate optimized *in vitro* and *in vivo* human tissue models harboring basement membrane that have made many of the discoveries in this report possible. YEAR 2 of this research focused on characterization of the *in vivo* response of bioengineered human skin to prevesicating and vesicating doses of SM.

During this year of our research, we received approval for the use of an in-house facility for SM exposures. This laboratory was constructed during YEARS 1 and 2 of our research and final approval for its use was obtained one year ago. This facility greatly facilitated the progress of our work as it allowed all studies with SM to be performed in our laboratory. YEAR 3 of our research has allowed us to establish that intact basement membrane significantly reduces the vulnerability of 3-D, human skin-like tissues to vesicating injury. The finding of an increased susceptibility of human skin-like tissues without structured basement membrane to SM-induced vesication indicates that this structure is a critical site for the initiation of SM injury in human skin. Studies in 2-D cultures demonstrated that the presence of proteins found in the cutaneous basement membrane zone were not able to reduce the sensitivity to SM damage. In fact, quite the opposite was true, as we determined that cell viability (MTT assay) was lowered and apoptosis was increased (M30 assay) when cells were grown in 2-D culture on the basement membrane component Type IV Collagen and exposed to 150μM of SM. Since it is known that human epidermal keratinocytes have elevated growth on Type IV Collagen, it is possible that this increased proliferation was associated with the elevation of cell damage. Similarly, even in 3-D cultures, the presence of basement membrane proteins that were not organized into structured basement membrane were not sufficient to protect keratinocytes from SM damage. We concluded that it was critical to have well-structured basement membrane in 3-D (AlloDerm) cultures in order to prevent SM damage leading to vesication. To further establish the role of the basement membrane as a mediator of SM-induced vulnerability, we focused on the role of laminin 5. By using JEB cells restored with a variety of γ2 chain retroviral constructs, we concluded that restoration of adhesive function mediated by laminin 5 could decrease susceptibility to SM injury. These findings directly implicate laminin 5 and it's role in structured basement membrane that mediate adhesive interactions that can prevent SM-induced vesication and can directly modulate SM injury in human skin.

Chart 1:Colony forming efficiency test for diff. Doses of Ethanol.

Plate 1			Plate 2			Plate 3		
Obj.#	Area	Diameter (mean)	Obj.#	Area	Diameter (mean)	Obj.#	Area	Diameter (
1	303	19.01095	1	723	29.23695	1	368	21.00228
3	431	22.4343	2	981	35.07506	2	1452	42.55793
4	297	18.57384	3	274	17.98097	5	1369	40.98646
5	655	27.72862	4	497	23.99	6	635	27.42119
6	719	29.17088	5	271	17.63542	7	190	14.83235
7	981	34.67185	6	1158	38.17083	12	788	30.52805
8	966	32.08782	7	201	15.18621	13	620	26.82806
9	100	10.25018	8	1484	42.61647	14	561	25.79769
10	218	15.93938	10	784	31.45005	15	1358	41.23758
11	248	17.03653	12	753	30.25857	16	354	20.27196
12	421	22.1994	13	1594	44.31307	17	1117	36.77989
14	341	19.97868	14	327	19.86307	18	223	16.18283
15	108	11.67423	15	705	28.99963	19	848	31.66589
16	575	25.96036	16	213	14.60063	20	557	25.61567
17	257	17.30348	17	560	25.71567	21	397	21.52352
19	466	23.09092	18	885	32.77757	22	564	25.59877
22	340	20.34564	19	302	18.4119	23	1003	36.18402
23	252	17.48212	20	1359	40.73583	25	524	24.80816
24	749	31.67792	21	731	29.84407	26	414	21.91118
26	295	18.8583	23	314	19.1414	27	800	30.98713
27	417	21.10617	24	567	25.63724	28	838	31.67329
28	500	24.01897	25	1278	39.90689	29	263	17.29511
29	908	33.62228	27	230	16.0985	30	1027	36.47375
33	190	15.03517	28	847	33.12015	31	735	29.40827
34	131	14.35246	29	256	17.58948	32	1570	43.80937
39	379	21.48697	30	1730	45.71595	33	1128	37.05792
41	599	26.66582	32	196	15.62357	35	395	21.51804
43	495	24.06542	33	813	31.70016	36	436	22.78733
46	338	19.79765	34	982	35.82237	37	502	24.43275
47	204	15.55703	36	826	33.93631	39	364	20.66486
50	153	12.24627	38	246	16.62804	40	385	21.19656
53	196	14.63457	40	908	32.95882	41	336	20.19264
56	799	31.08588	41	1714	45.46995	42	480	23.92561
57	486	23.7671	42	985	34.64849	43	302	18.93908
61	756	29.99797	43	915	33.03319	44	779	31.15737
64	370	20.51874	44	1123	36.98126	45	1301	39.77202
65	1285	40.55771	45	343	20.56274	47	929	33.56456
69	270	17.70592	47	736	29.52664	48	246	16.91179
73	147	12.24352	48	1019	35.03419	49	326	19.43613
78	196	14.86915	49	487	23.96436	52	774	30.40629
79	254	16.86913	50	634	27.07093	53	935	33.47803
82	604	26.59736	51	1322	41.54865	54	285	18.11605
85	531	25.03112	52	1726	45.68951	57	238	16.54171
86	658	27.99984	53	441	22.72913	58	420	21.98574
90	281	17.53221	Stats	Area	Diameter (mean)	59	1082	37.68928
94	232	16.66273	Min	196	14.60063	Stats	Area	Diameter (
95	524	24.8019	(Obj.#)	32	16	Min	190	14.83235
96	576	25.94113	Max	1730	45.71595	(Obj.#)	7	7
102	298	18.77829	(Obj.#)	30	30	Max	1570	43.80937
108	229	16.27969	Range	1534	31.11533	(Obj.#)	32	32
Stats	Area	Diameter (mean)	Mean	782.7273	29.47727	Range	1380	28.97702
Min	100	10.25018	Std.Dev	447.8669	9.309393	Mean	671.5111	27.35898
(Obj.#)	9	9	Sum	34440	1297	Std.Dev	369.8065	8.007271
Max	1285	40.55771	Samples	44	44	Sum	30218	1231.154
(Obj.#)	65	65				Samples	45	45
Range	1185	30.30754						
Mean	434.56	21.70607						
Std.Dev	256.4732	6.597242						
Sum	21728	1085.304						

Plate 4			Plate 5			Plate 6		
Obj.#	Area	Diameter (mean)	Obj.#	Area	Diameter (mean)	Obj.#	Area	Diameter (mean)
1	693	28.66456	2	333	19.88689	1	685	28.4904
2	606	26.8391	3	457	23.60689	2	369	20.75996
3	633	27.27014	4	572	25.84705	3	1981	49.6653
4	898	32.7391	10	705	28.69458	4	240	16.68826
5	685	28.54366	13	1663	45.83457	5	252	17.42439
6	299	18.61875	14	587	26.44698	6	616	27.25112
7	922	34.17847	15	1606	44.38457	7	356	20.58161
8	666	28.09636	16	260	18.25182	8	365	20.79862
9	1131	38.86394	17	1606	44.10838	9	949	35.24616
10	230	16.5682	18	420	22.20976	10	351	20.38016
11	329	19.83361	19	1511	42.74728	11	333	19.79145
12	651	27.7603	20	1141	37.76366	12	603	26.66379
13	773	31.61734	21	996	34.7277	13	1556	43.41113
14	778	30.46585	22	378	21.82349	14	679	28.46158
15	245	16.73562	24	278	18.55956	20	957	31.19653
16	848	32.20823	28	330	19.70147	24	203	15.02552
17	447	23.38809	29	385	20.99992	25	657	28.20578
18	1079	36.99848	30	256	17.35729	26	617	26.88225
19	917	34.32692	31	653	27.54719	27	965	34.37101
20	570	26.36699	33	1090	36.01027	29	1465	42.81949
21	888	34.27879	36	639	27.4251	30	257	17.93176
22	429	22.59546	37	1852	47.57377	32	1405	40.98995
23	1645	44.49541	38	472	23.53242	33	2525	54.89707
24	266	18.10159	39	1373	40.96551	34	308	19.23189
26	434	22.32742	40	551	25.44096	35	234	16.08917
30	316	19.36658	41	574	26.1926	36	345	19.85205
31	483	23.76301	42	1032	35.2921	37	729	29.34691
34	641	27.40071	44	496	24.02659	38	475	23.76461
35	693	28.70903	45	2182	54.34765	39	341	19.80422
36	497	23.99812	46	349	20.1659	40	885	33.29909
39	923	33.45653	48	680	28.37125	41	361	20.52434
40	515	24.64205	51	287	18.14533	42	410	21.87765
41	906	33.00581	53	551	25.46806	43	228	16.20058
42	506	24.66411	55	371	21.15667	44	1404	41.41729
43	529	24.95889	56	417	21.87907	45	301	19.06744
45	397	21.63952	58	498	23.98555	47	926	33.60464
46	304	19.0132	63	805	31.01447	48	362	20.48055
47	541	25.22305	64	332	19.79741	49	435	22.32147
48	823	31.3452	Stats	Area	Diameter (mean)	50	232	16.60924
49	802	30.86987	Min	256	17.35729	51	323	19.33572
51	727	29.21968	(Obj.#)	30	30	Stats	Area	Diameter (mean)
52	765	29.94201	Max	2182	54.34765	Min	203	15.02552
Stats	Area	Diameter (mean)	(Obj.#)	45	45	(Obj.#)	24	24
Min	230	16.5682	Range	1926	36.99036	Max	2525	54.89707
(Obj.#)	10	10	Mean	754.9474	28.71815	(Obj.#)	33	33
Max	1645	44.49541	Std.Dev	504.5143	9.617395	Range	2322	39.87155
(Obj.#)	23	23	Sum	28688	1091.29	Mean	667.125	26.519
Range	1415	27.9272	Samples	38	38	Std.Dev	519.721	9.810958
Mean	653.0952	27.45476				Sum	26685	1060.76
Std.Dev	277.2394	6.139822				Samples	40	40
Sum	27430	1153.1						
Samples	42	42						

Chart 1:Colony forming efficiency test for diff. Doses of Ethanol.

Plate 7				Plate 8		
Obj.#	Area	Diameter (mean)		Obj.#	Area	Diameter (
1	311	18.84619		1	981	34.25568
2	318	19.13212		2	664	27.40764
3	1861	47.4571		3	627	29.62269
4	319	19.42469		4	867	32.62684
6	338	20.03454		5	1857	47.70511
7	2393	53.89959		6	724	29.20603
8	319	19.38202		7	1074	37.28857
9	2921	60.42813		8	1434	41.99668
10	1095	36.68781		9	526	24.80192
12	668	28.04055		10	671	28.0817
13	377	20.92064		11	956	34.29499
15	2657	56.46736		12	977	34.44915
18	314	19.39491		13	564	25.91216
21	1229	38.13656		14	208	15.60507
22	1235	38.62394		15	1547	44.14896
23	470	23.73361		16	452	23.18513
24	1179	39.52578		17	378	20.97375
25	564	25.93602		19	1376	41.49363
27	637	27.13687		20	612	26.79121
29	499	24.28621		21	284	18.60869
30	2715	57.31591		22	2120	50.5307
31	521	24.75276		23	874	32.32846
32	808	30.94194		24	2446	54.7328
35	320	19.49257		25	790	30.42181
36	243	16.84583		26	1243	39.00727
38	591	27.60254		27	1324	41.81233
39	350	20.67114		29	489	23.73582
41	404	21.85555		30	805	30.57047
43	410	21.99871		32	266	18.03897
44	278	17.76215		34	398	21.72645
45	620	27.06714		37	904	34.10687
46	3746	68.06725		38	1326	40.3833
47	981	34.38712		39	891	33.26693
48	757	29.96356		Stats	Area	Diameter (
49	2014	49.61019		Min	208	15.60507
50	1735	46.23339		(Obj.#)	14	14
Stats	Area	Diameter (mean)		Max	2446	54.7328
Min	243	16.84583		(Obj.#)	24	24
(Obj.#)	36	36		Range	2238	39.12773
Max	3746	68.06725		Mean	928.9394	32.39751
(Obj.#)	46	46		Std.Dev	520.7398	9.362057
Range	3503	51.22141		Sum	30655	1069.118
Mean	1005.472	32.00173		Samples	33	33
Std.Dev	893.8641	13.99589				
Sum	36197	1152.062				
Samples	36	36				

Fig. 1: Colony forming efficiency test for diff. Doses of Ethanol.

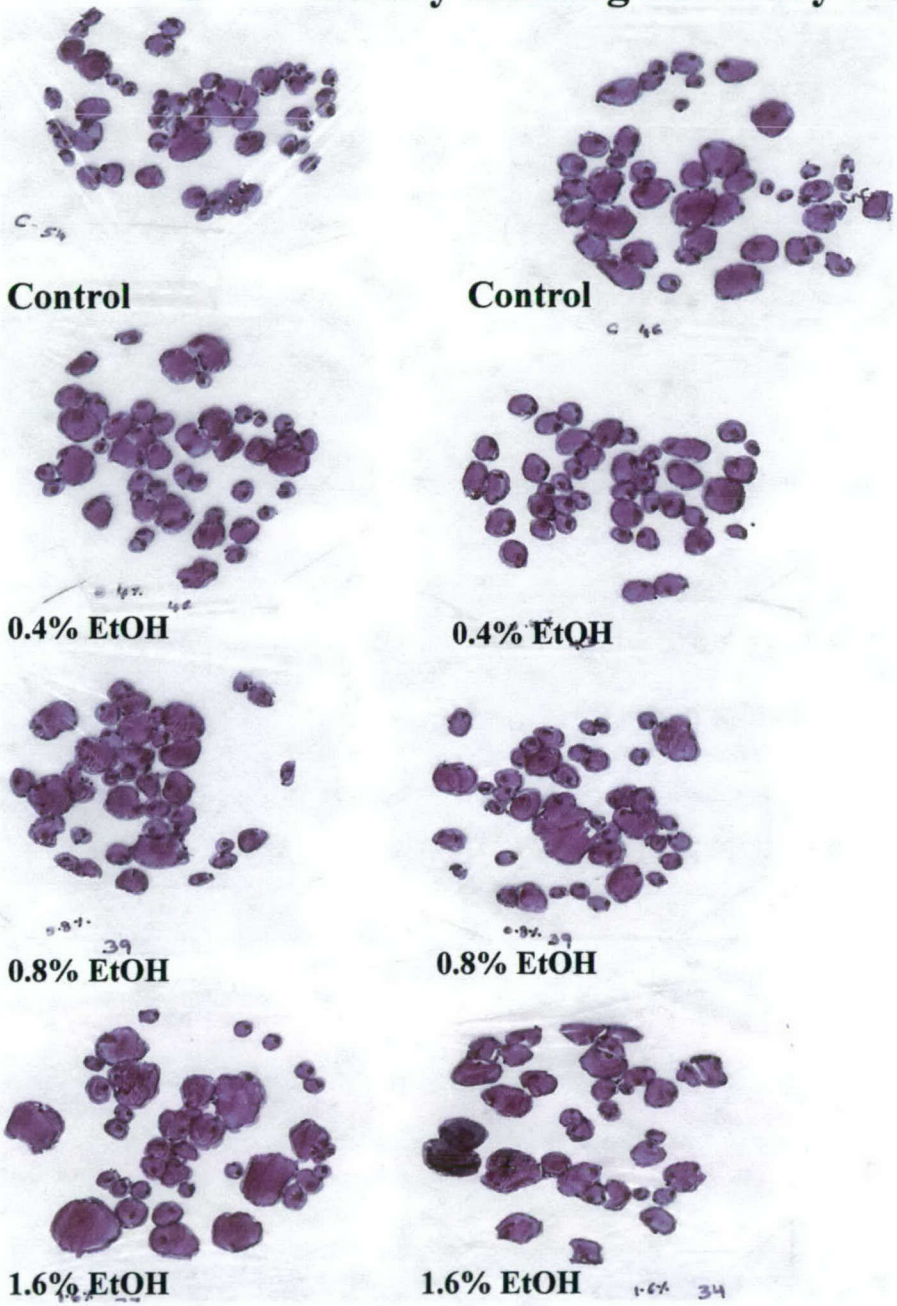

Fig. 1: Colonies shown by the Keratinocytes after the exposure to different doses of ethanol (0.4%, 0.8%, 1.6%) along with untreated control

Fig.2: Graphical representation of colony forming efficiency of keratinocytes exposed to diff.doses of ethanol.

Table:

Chemicals	Ave. no. of colonies.
Control	50
0.4%EtOH	45
0.8%EtOH	39
1.6%EtOH	35

Graph:

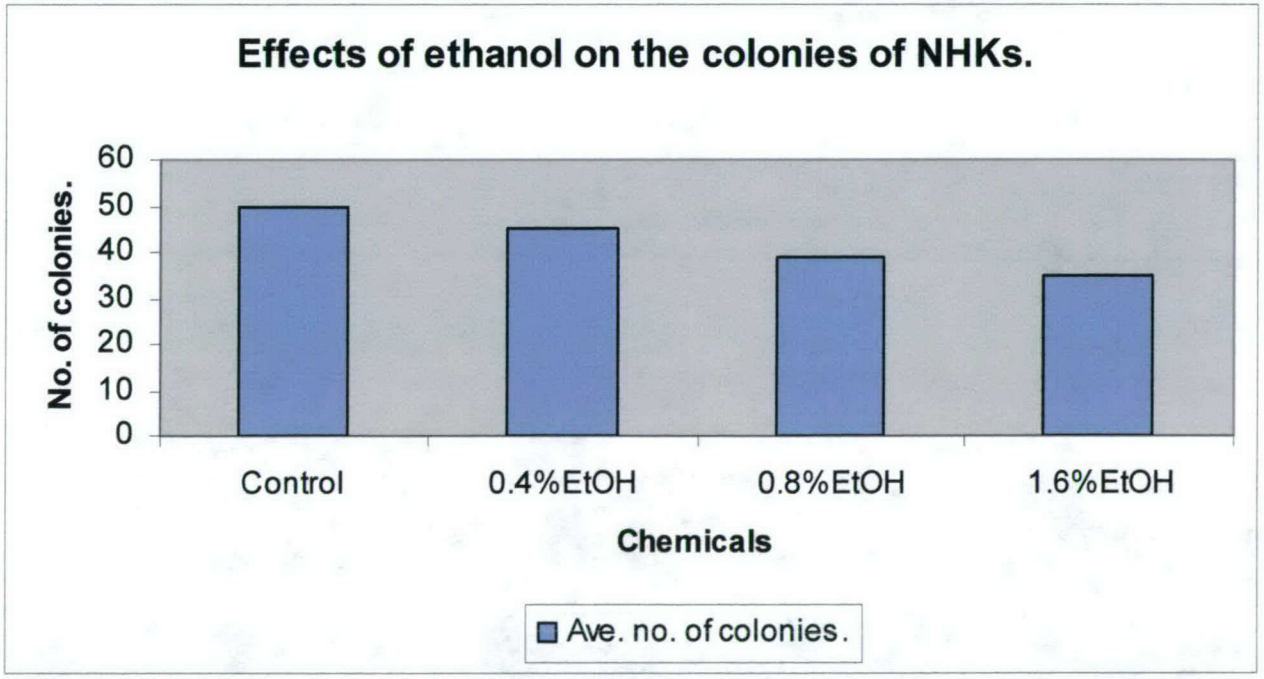

Fig. 3: Immunofluorescent staining for Apoptotic cells induced by diff. Doses of SM, Ethanol and control.

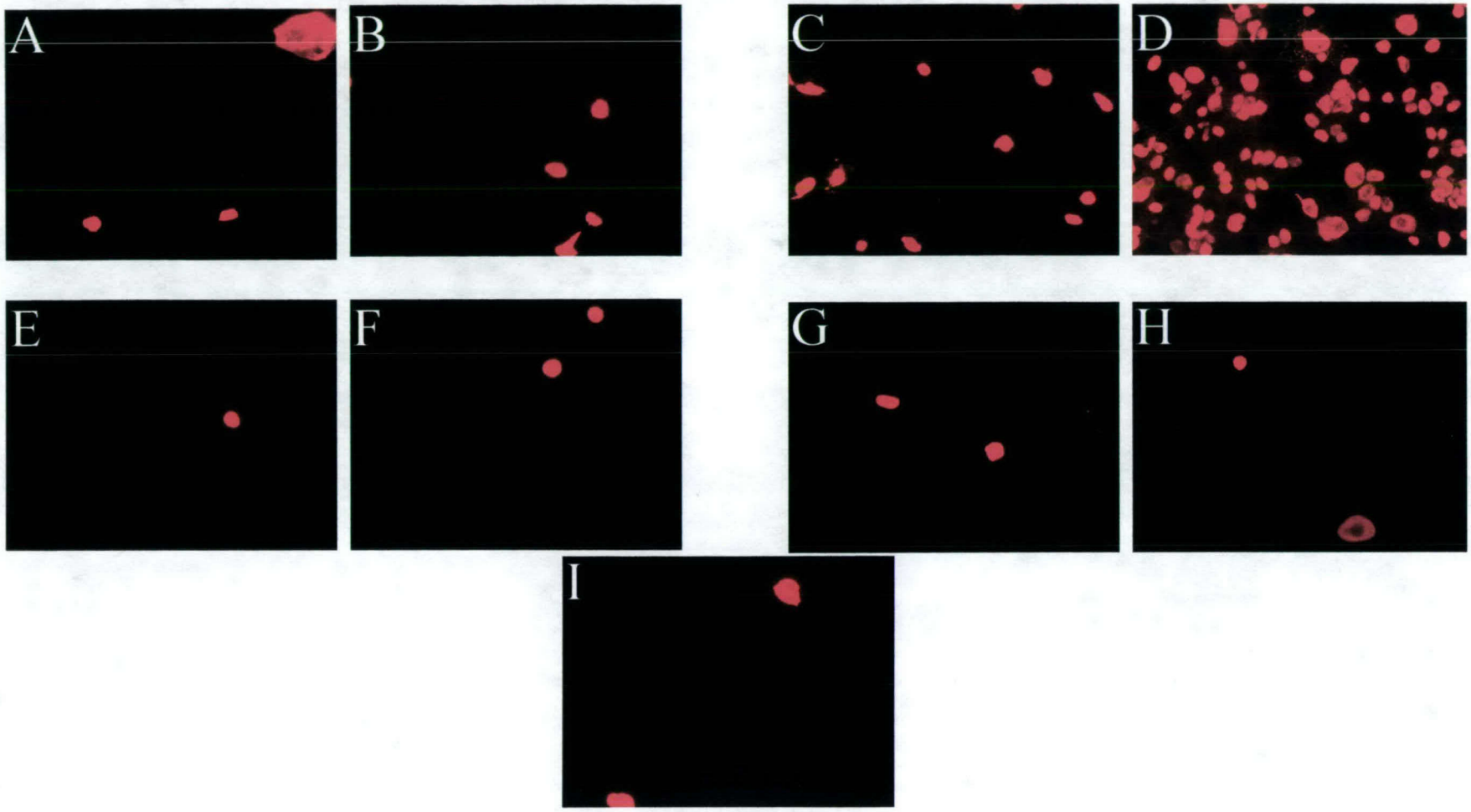

A-D -Varying doses of SM (37.5, 75, 150, 300*u*m)

E-H – Varying doses of concurrent Ethanol controls (0.25, 0.5, 1, 2%)

I – Untreated control.

Fig. 4: M30 Cytodeath staining for Keratinocytes exposed SM and Ethanol at diff. Sample intervals.

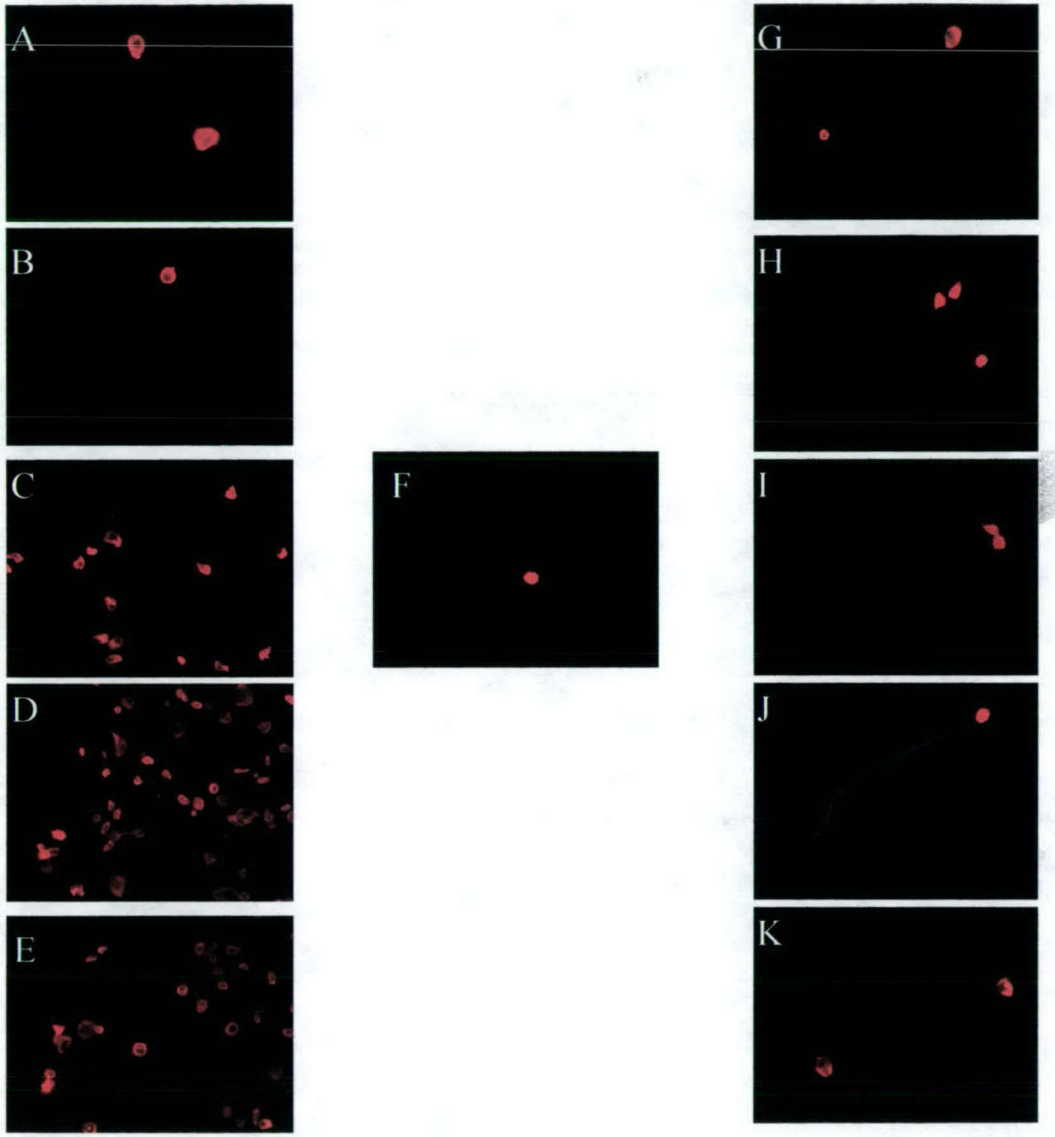

A-E– 1, 3, 7, 14, 28 min. of 150um of SM; **G-K** – 1, 3, 7, 14, 28 min of 1% Ethanol;

F– Untreated control.

Fig. 5: Apoptotic cell counts (NHK)

Table:

Chemicals	1min.	3.5min.	7min.	14min.	28min.
Control	4	4	4	4	4
SM (150ug)	18	69	795	4015	6783
1%EtOH	6	13	15	18	221

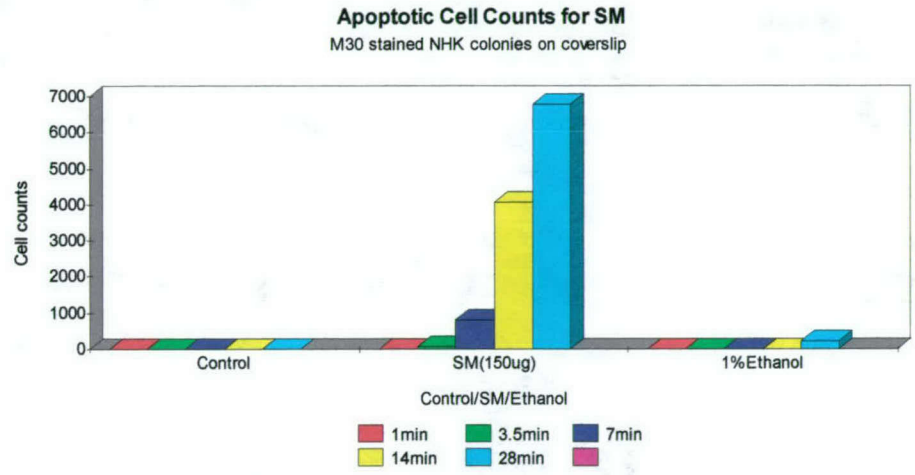

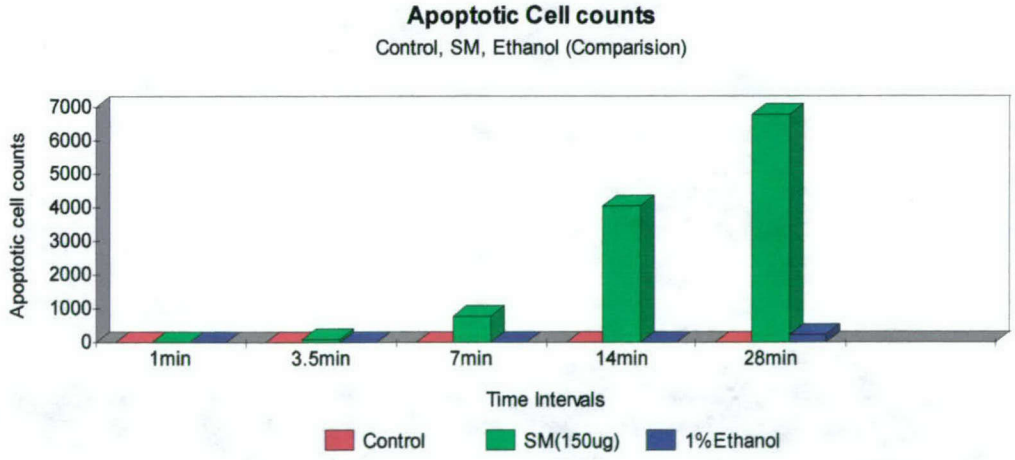

Fig. 6: M30 Cytodeath staining for 150*u*m SM and 1% Ethanol at two different intervals.

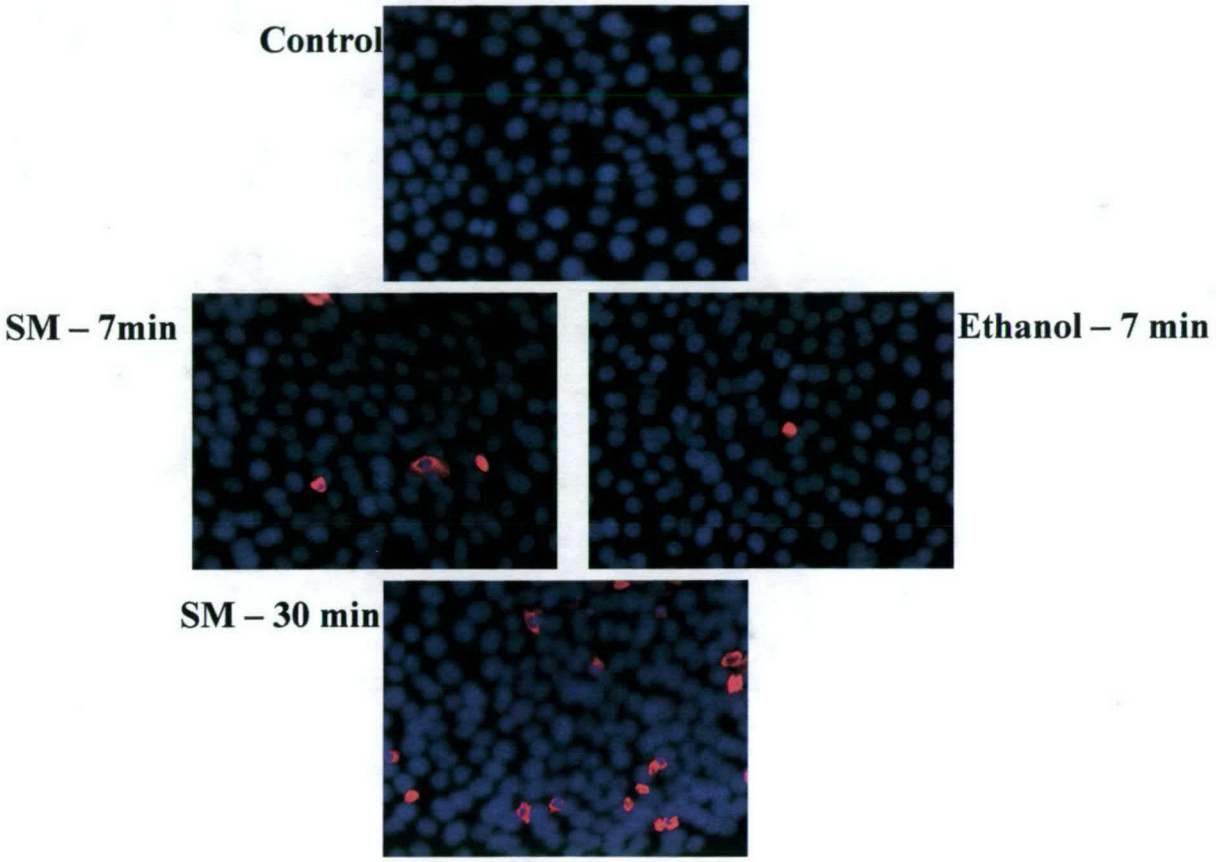

Fig.7: MTT Assay for NHK's on Plastic plates at diff. Cell density.

Plastic

Chemica	50000	25000	10000	1000
SM	**0.605**	0.153	0.302	0.029
Ethanol	**0.828**	0.449	0.289	0.013

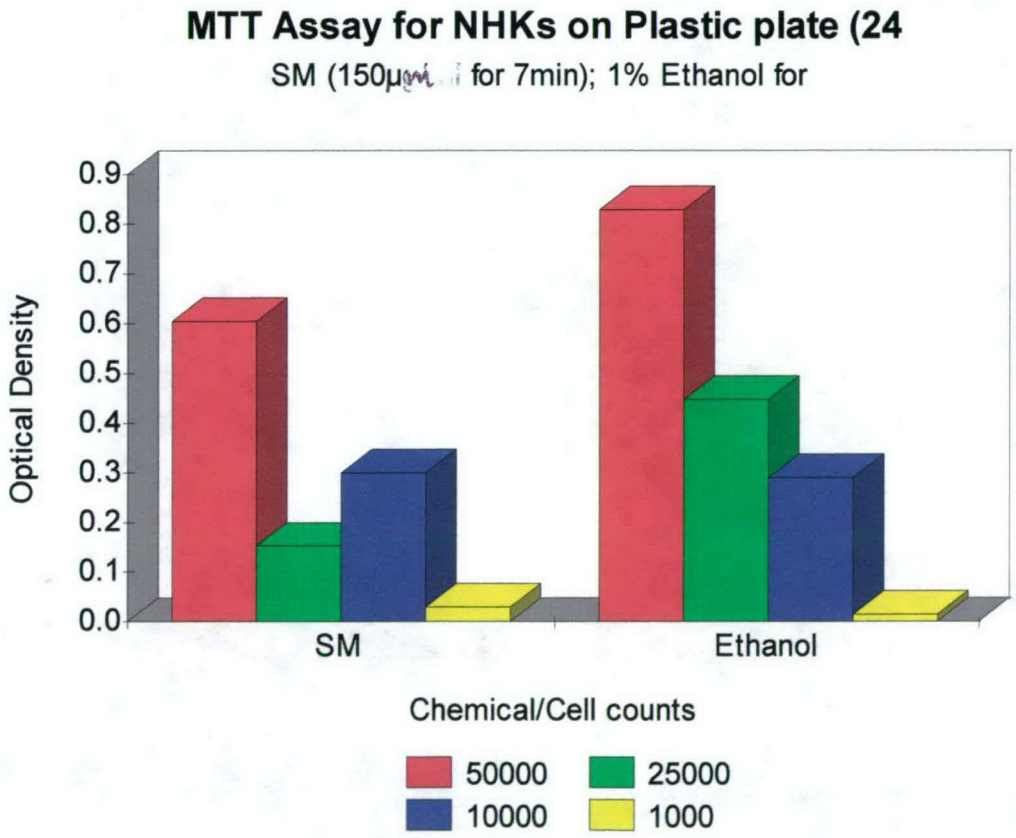

Fig. 8: MTT Assay for NHK's at varied Cell density on Type IVCollagen plates.

Chemica	50000	25000	10000	1000
SM	0.564	0.133	0.332	0.047
Ethanol	0.807	0.287	0.307	0.0413

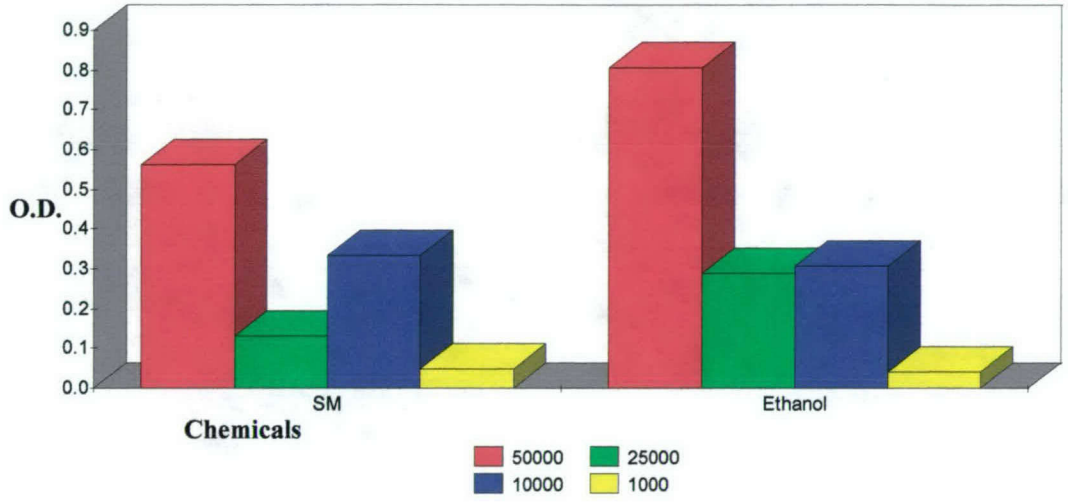

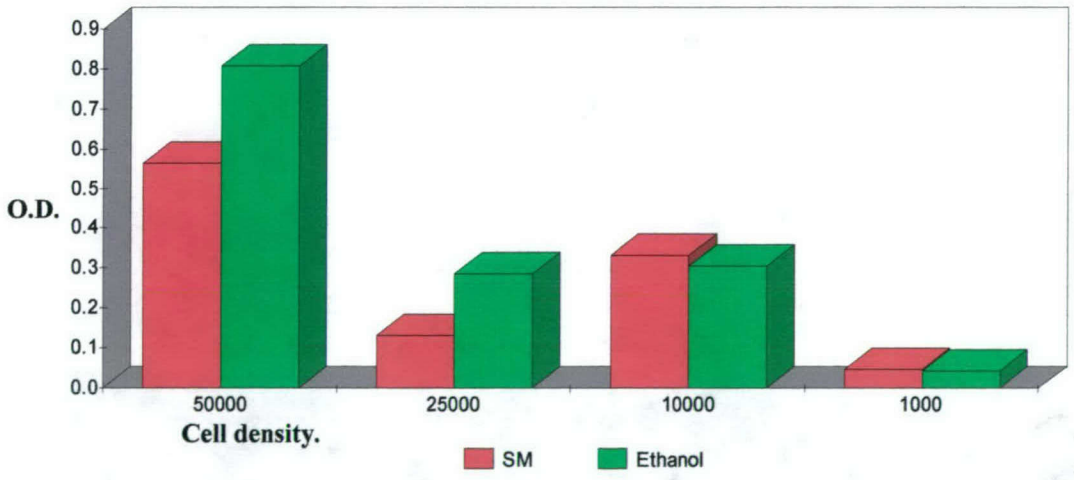

Fig. 9: MTT Assay at two different cell densities of NHK's on Col I

Chemica	50000	25000
SM	0.491	0.272
Ethanol	0.657	0.369

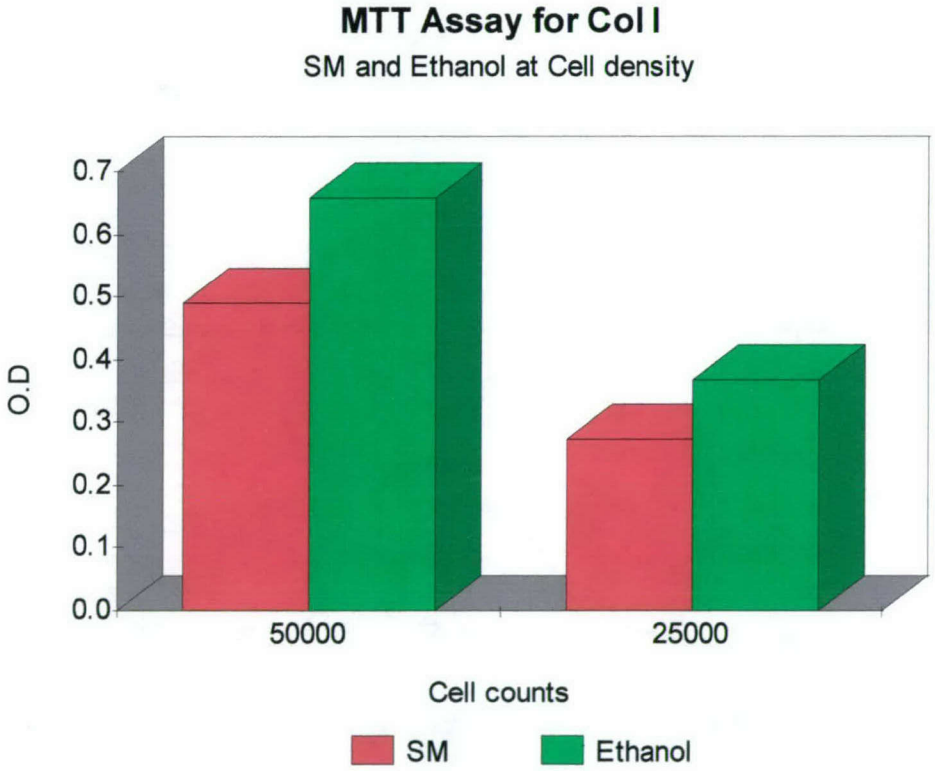

Fig.10: MTT Assay for 50000NHKs on diff. Plates.

Table:

	Plastic	Col I	col IV	FBN	Laminin	Poly-D
SM	**0.27**	0.261	0.226	0.165	0.189	0.096
Ethanol	**0.317**	0.349	0.436	0.301	0.285	0.107

Graph:

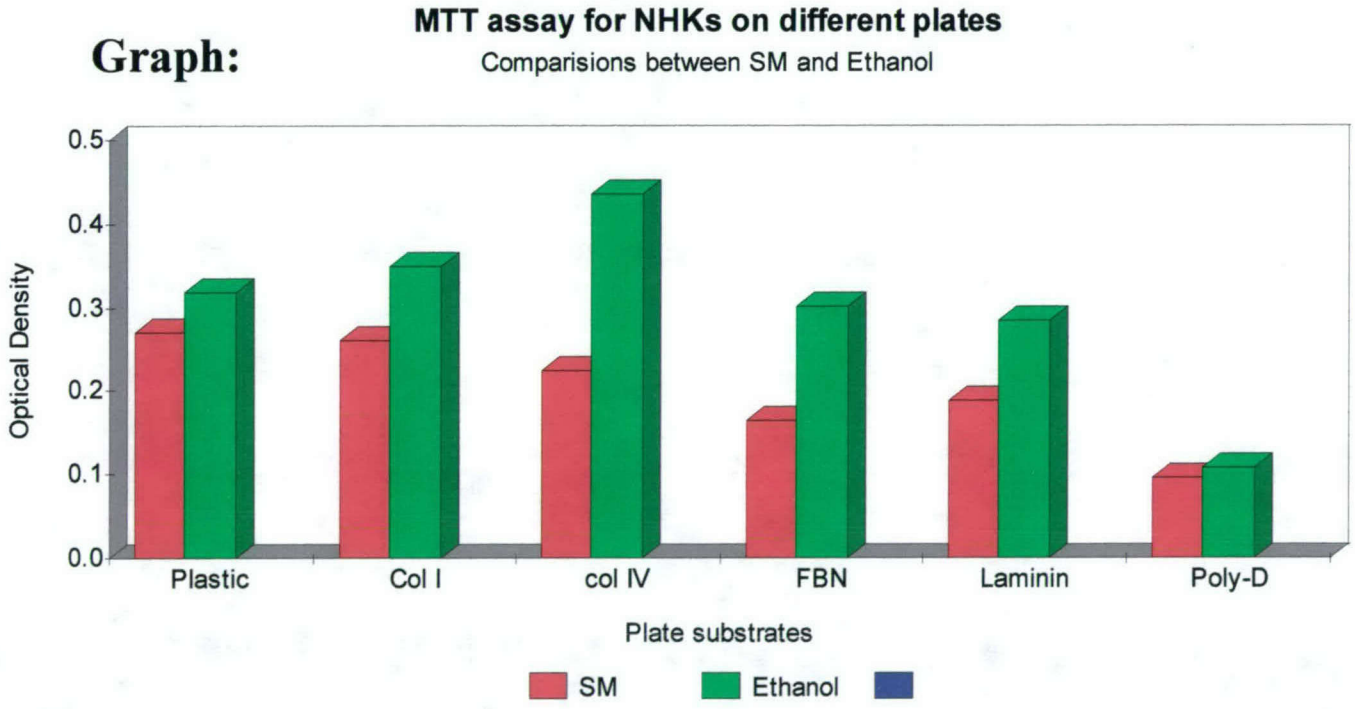

Fig. 11: MTT Assay for different doses of SM and ethanol on diff. substrates.

Table:

Doses/coating	Plastic	Col I	Col IV	FBN	Laminin
37.5u SM	0.942	1.002	0.886	1.005	1.277
75u SM	0.98	1.225	0.95	1.032	1.133
150u SM	0.768	0.822	0.795	0.85	0.873
300u SM	0.701	0.769	0.679	0.71	0.786
0.25% EtOH	0.991	1.059	1.067	1.038	1.044
0.5% EtOH	0.957	0.951	1.103	1.06	1.083
1% EtOH	0.992	1.178	1.096	1.155	1.173
2% EtOH	0.996	1.123	1.228	1.048	1.068

Graphs:

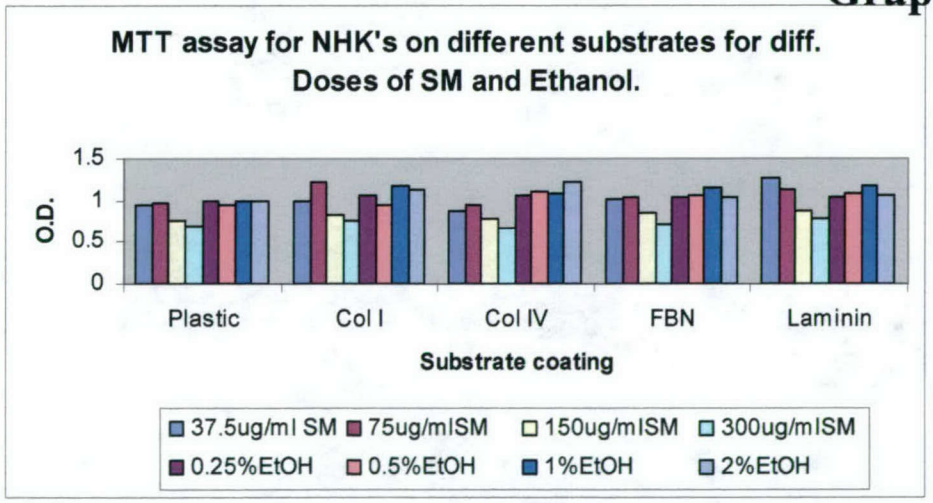

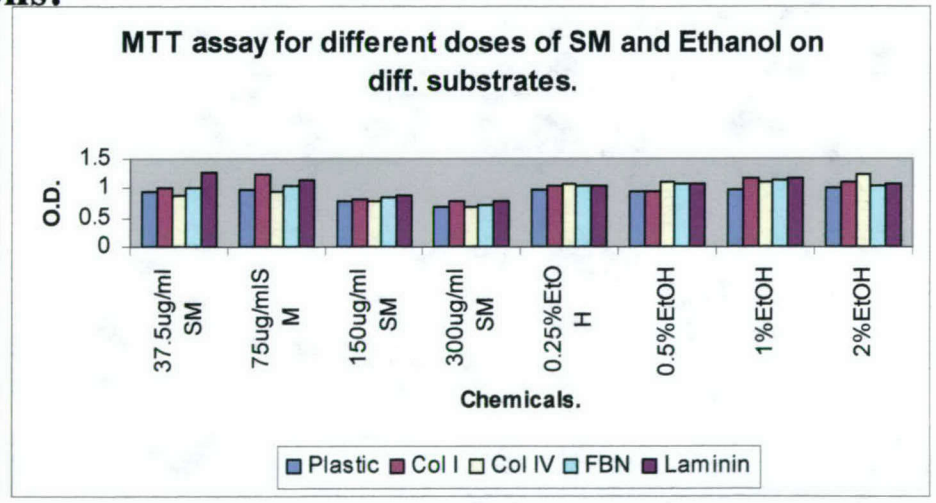

Fig. 12: MTT assay for JEB Cells on diff. Substrates. (150um SM and 1% ethanol)

Table:

Chemical/Substrates.		Delta bc	Pfu	Gamma2wt.	Delta C 115	Fgal.	NHK
Plastic							
	SM	0.649	0.572	1.03	1.396	1.152	0.842
	1%Ethanol	0.868	0.638	1.601	1.3	1.191	1.512
Coll							
	SM	0.749	0.836	1.673	1.74	1.674	0.931
	1%Ethanol	1.153	0.797	1.823	1.724	1.408	1.327
Col IV							
	SM	0.996	0.75	1.645	1.73	1.416	0.687
	1%Ethanol	1.253	0.765	1.676	1.639	1.531	1.268
Fibronectin							
	SM	0.97	0.842	1.497	1.599	1.318	0.973
	1% Ethanol	1.143	0.757	1.707	1.595	1.402	1.149
Laminin							
	SM	0.526	0.418	1.141	1.198	0.766	0.658
	1% Ethanol	0.494	0.475	0.954	0.852	0.833	1.499

Graphs:

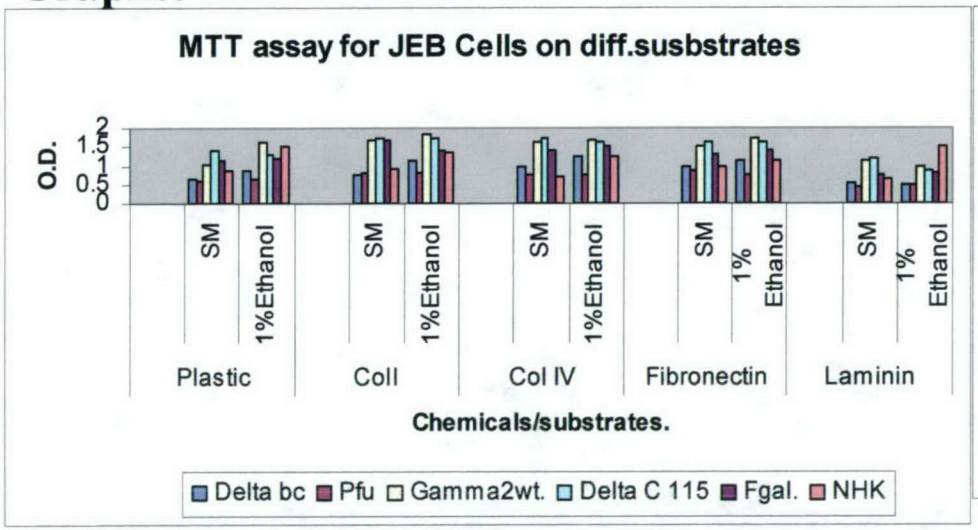

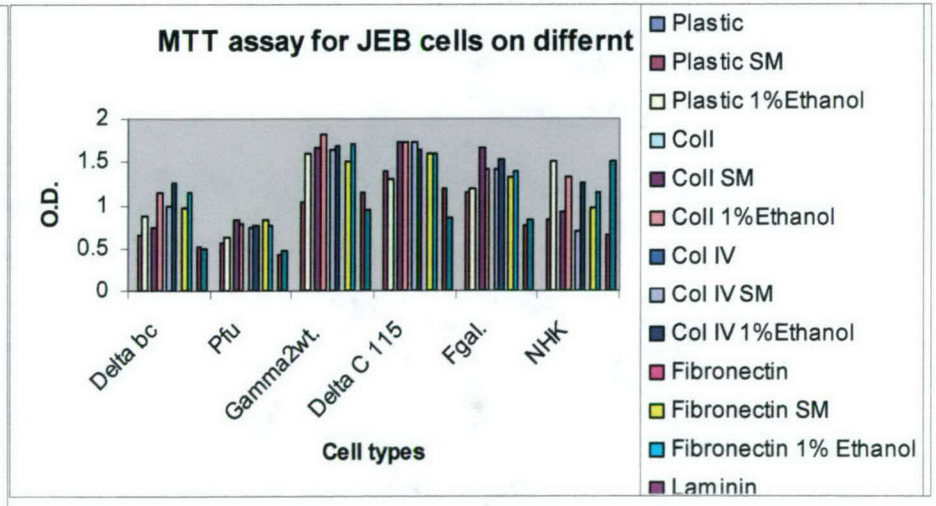

Fig. 13: MTT Assay for diff. Cell types on diff. Substrates.(300*u*m SM & 2% Ethanol.

Table:

		Del bc	Pfu	Gam2wt	Del C115	fgal	NHK
Plastic							
	SM	0.804	0.489	0.744	0.682	1.008	0.875
	Ethanol	0.875	0.447	0.885	0.63	1.151	1.187
Col I							
	SM	0.838	0.82	1.064	1.196	1.034	0.751
	Ethanol	0.956	0.968	1.219	1.224	1.429	1.263
Col IV							
	SM	0.316	0.291	0.373	0.441	0.369	0.328
	Ethanol	0.356	0.373	0.419	0.469	0.465	0.369
FBN							
	SM	0.677	0.78	0.885	0.971	1.162	0.944
	Ethanol	0.78	0.924	1.03	1.138	1.433	1.347
Laminin							
	SM	0.606	0.359	0.658	0.738	0.823	0.935
	Ethanol	0.474	0.285	0.697	0.479	0.831	1.114

Graph:

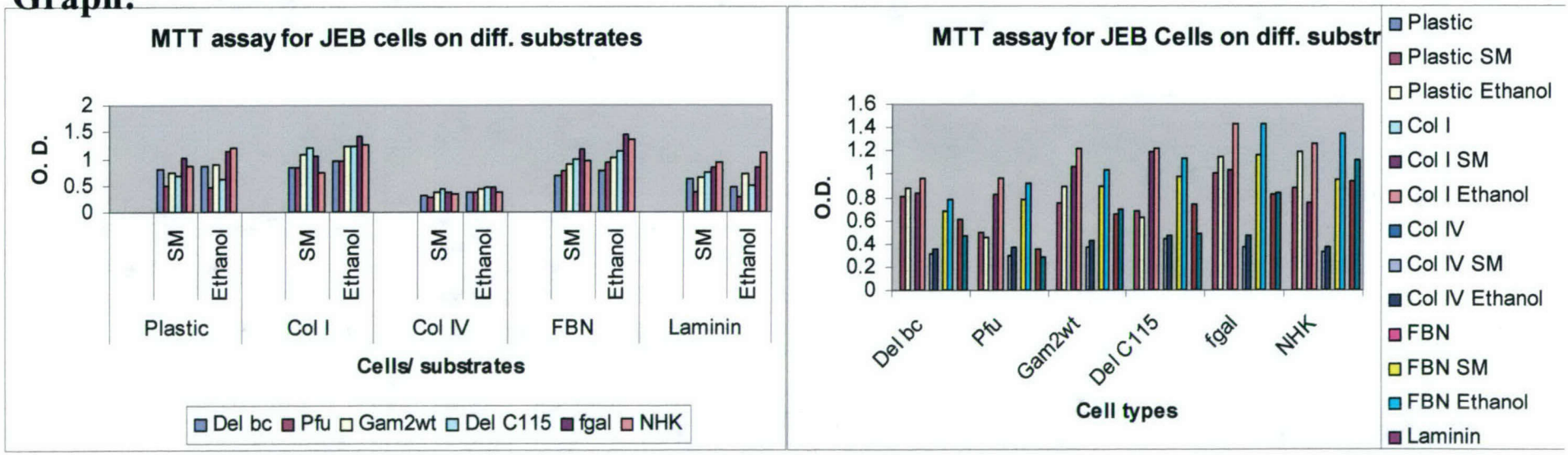

Fig. 14: MTT assay for 75*u*m SM on diff. Substrates.

Table:

Substrates	Chemicals	Delta bc	Pfu	Gam. Wt	Delta C115	Fgal	NHK
Col I	SM(75um)	1.433	1.219	2.021	1.376	1.421	1.265
	0.5% EtOH	1.549	1.216	2.064	1.474	1.664	1.527
Col IV	SM(75um)	1.372	0.992	1.851	1.414	1.459	1.392
	0.5%EtOH	1.33	1.039	1.99	1.318	1.448	1.512
FBN	SM(75um)	0.979	0.828	1.606	1.089	1.257	0.968
	0.5%EtOH	1.201	0.997	1.898	1.184	1.306	1.193

Graph:

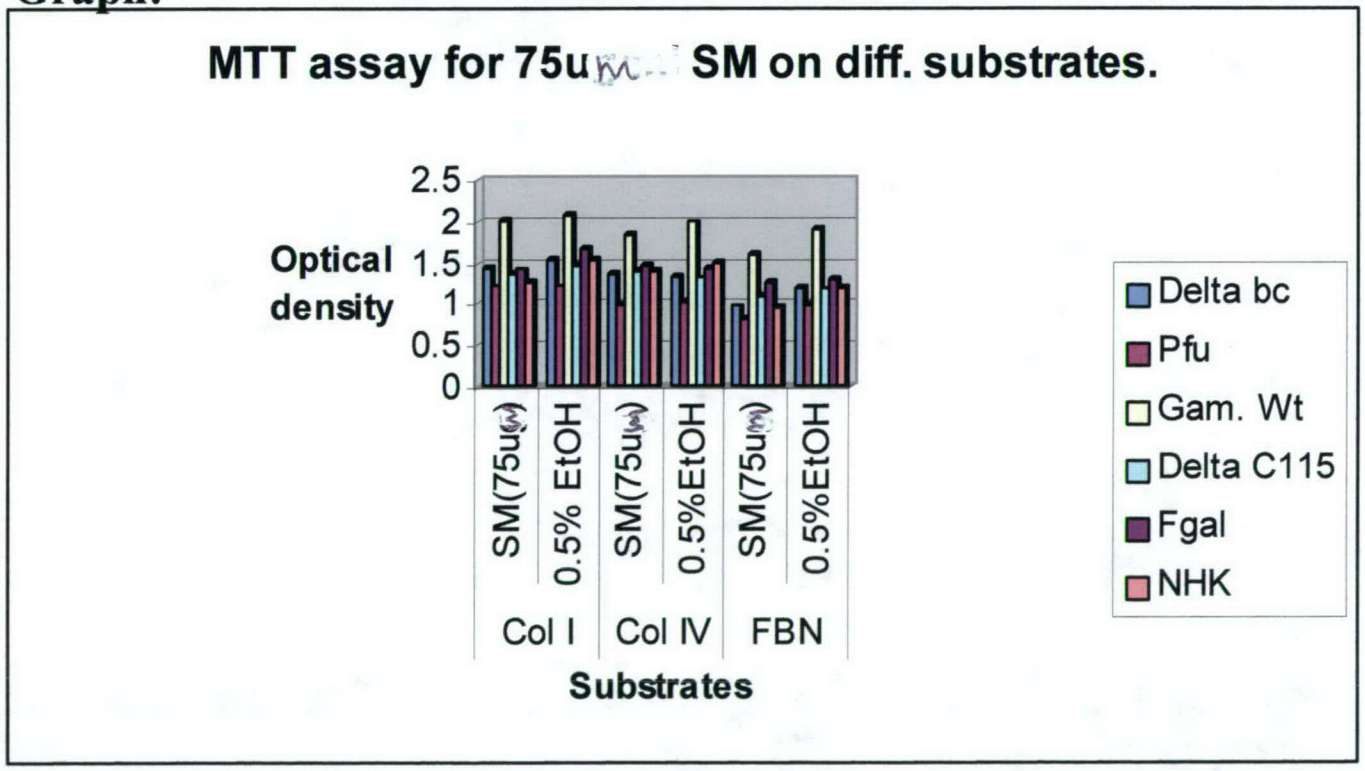

Fig. 15: MTT assay for 150*u*m SM on diff. Substrates.

Table:

Substrates	Chem.	Delta bc	Pfu	Gam. Wt	Delta C115	Fgal	NHK
Coll	SM (150um	1.192	0.954	1.633	1.349	1.115	1.116
	1% EtOH	1.288	1.156	2.095	1.315	1.455	1.309
Col IV	SM (150um	1.126	1.094	1.59	1.134	1.258	1.446
	1%EtOH	1.145	0.98	1.836	1.238	1.264	1.568
FBN	SM (150um	0.907	0.739	1.627	1.158	1.068	1.03
	1% EtOH	1.169	0.985	1.816	1.074	1.041	1.189

Graph:

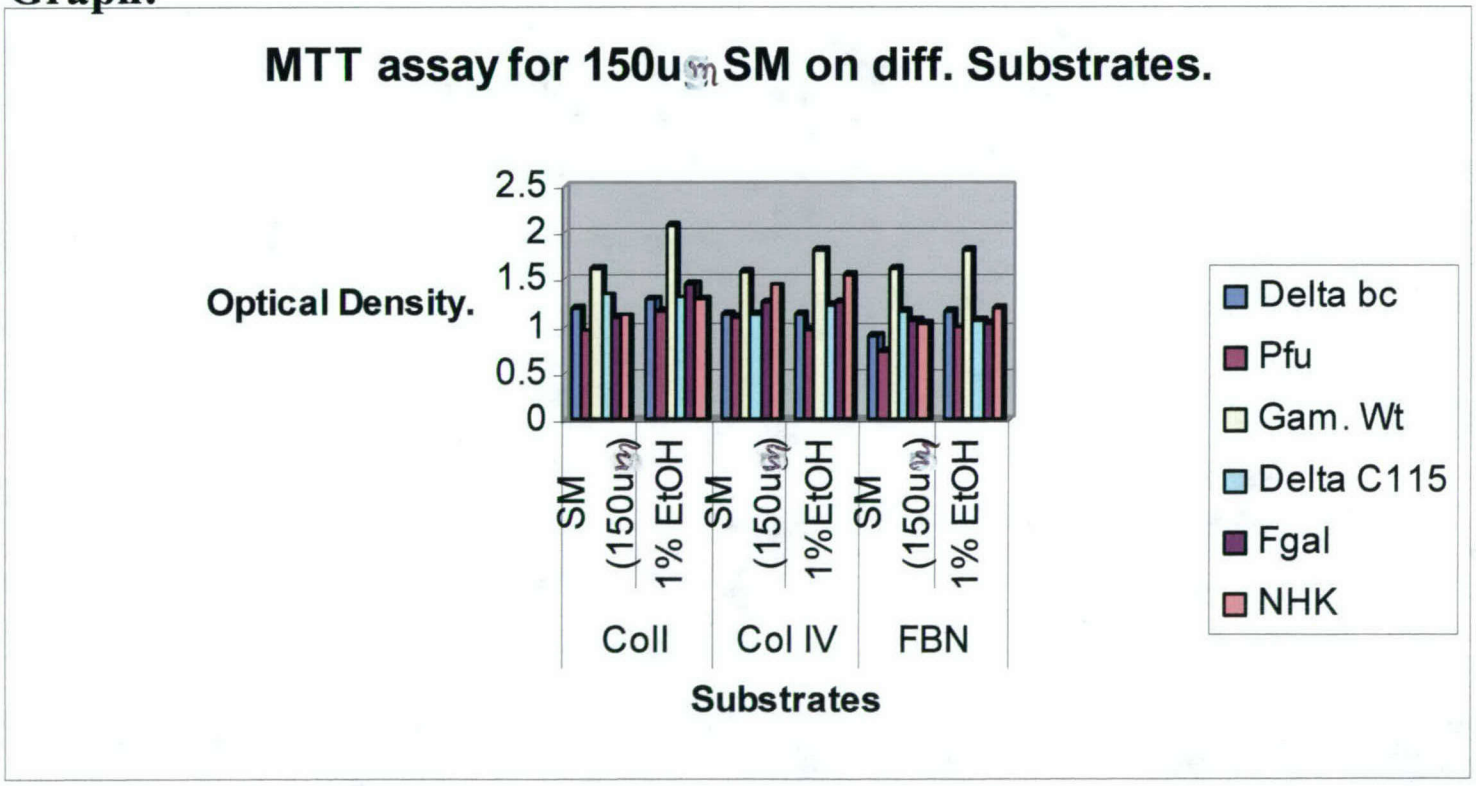

Fig. 16: MTT Assay for 300*u*m SM on diff. Substrates.

Table:

Sustrates	Chemicals	Delta BC	Pfu	Gamm Wt	Delta C115	Fgal	NHK
Coll	SM (300u	2.115	1.943	1.666	1.038	1.594	1.122
	2% EtOH	2.277	0.828	2.178	1.514	1.433	1.637
Col IV	SM (300u	0.998	0.933	1.833	1.317	1.141	1.03
	2%EtOH	1.478	1.112	2.002	1.273	1.295	1.326
FBN	SM (300u	0.876	0.594	1.538	0.892	1.007	0.846
	2% EtOH	1.103	0.912	1.64	1.003	1.176	1.341

Graph:

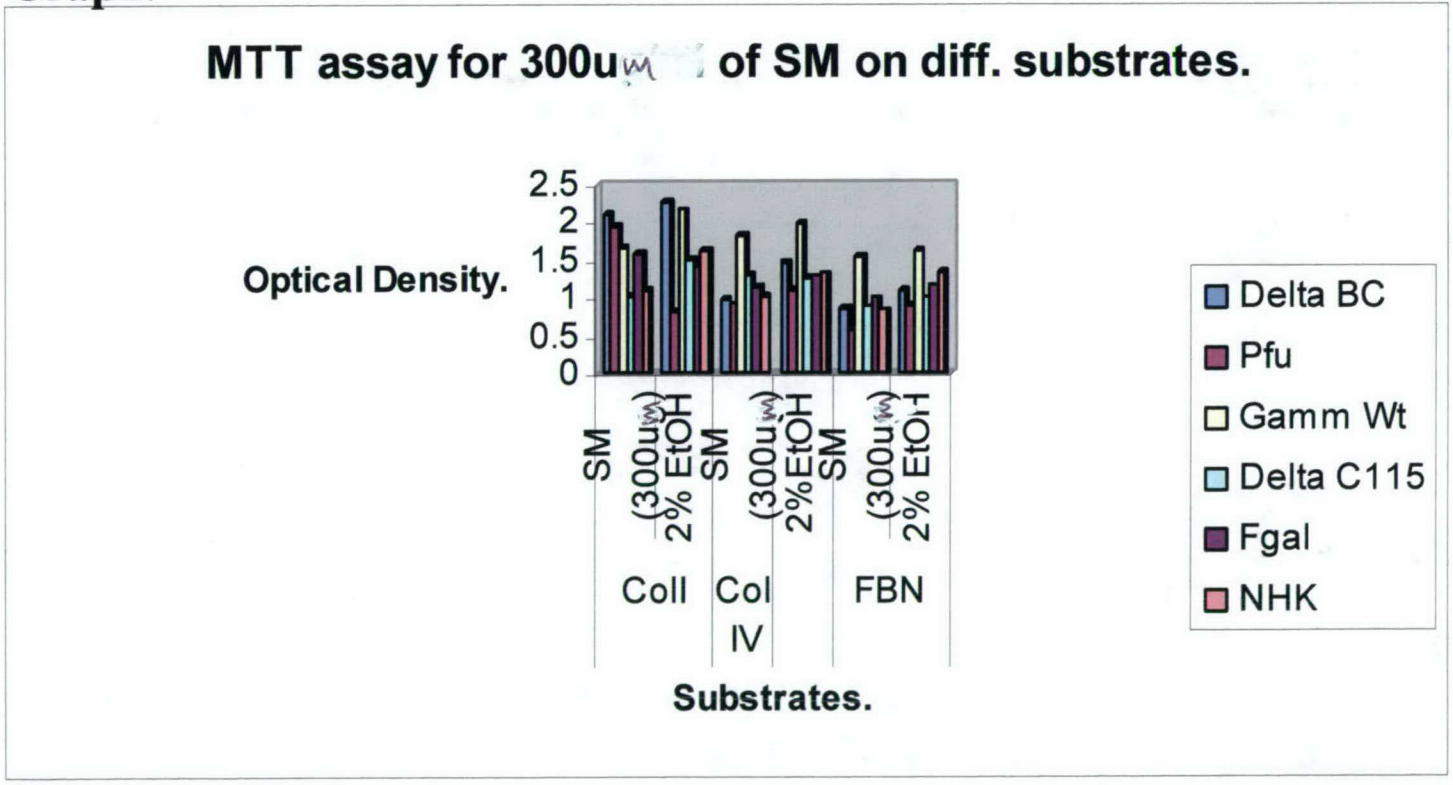

Fig. 17: MTT Assay for Delta bc Cells on Col I Plate.

Table:

Chemicals	O.D
75u SM	1.745
0.5% EtOH	1.491
150u SM	1.433
1% EtOH	1.592
300u SM	1.119
2% EtOH	1.978
450u SM	1.01
3% EtOH	1.28
600u SM	0.82
4% EtOH	1.352
750u SM	0.801
5% EtOH	1.399
900u SM	0.767
6% EtOH	1.394
1200u SM	0.593
8% EtOH	1.428

Graph:

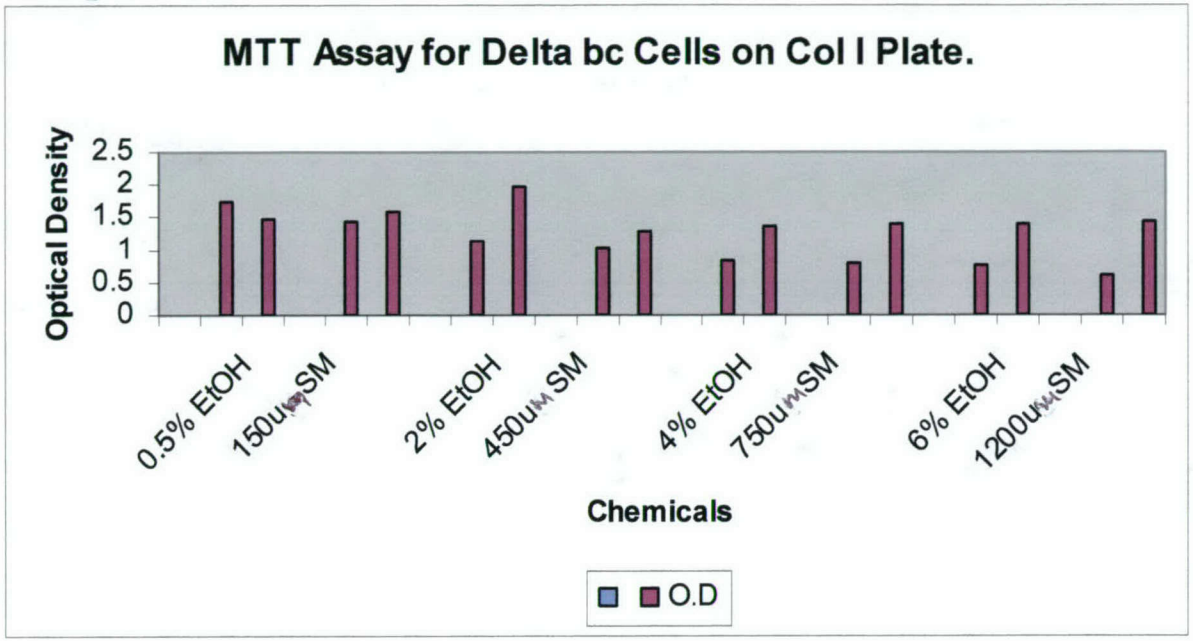

Fig. 18: MTT Assay for Delta bc Cells on Col IV Plate.

Table:

Chemicals	O.D
75uM SM	1.292
0.5% EtOH	1.628
150uM SM	1.32
1% EtOH	1.539
300uM SM	1.103
2% EtOH	1.168
450uM SM	1.112
3% EtOH	1.124
600uM SM	0.909
4% EtOH	1.234
750uM SM	0.729
5% EtOH	1.193
900uM SM	0.743
6% EtOH	1.267
1200uM SM	0.701
8% EtOH	1.01

Graph:

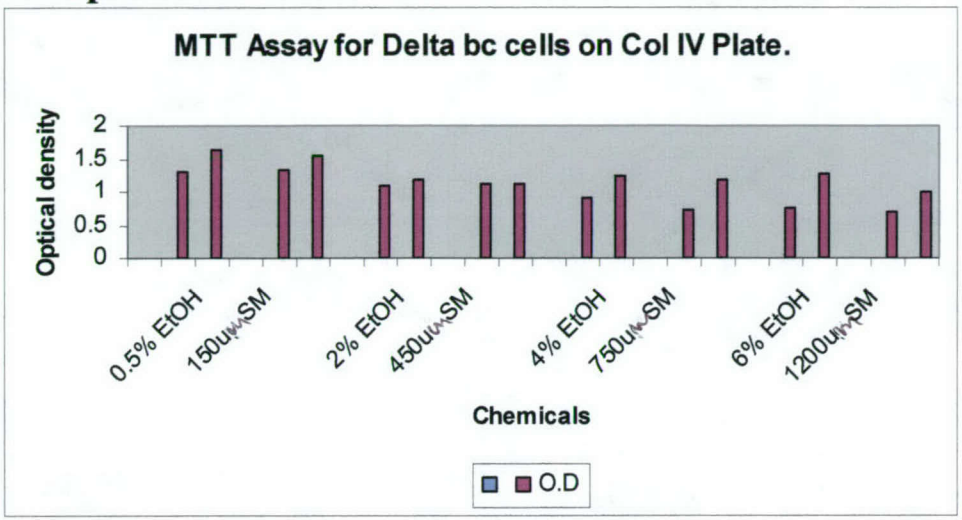

Fig.19: MTT Assay for Fgal Cells on Col I Plate.

Table:

Chemicals	O.D
75uM SM	1.49
0.5% EtOH	1.427
150uM SM	1.317
1% EtOH	1.521
300uM SM	1.202
2% EtOH	1.164
450uM SM	0.979
3% EtOH	1.472
600uM SM	1.078
4% EtOH	1.334
750uM SM	0.884
5% EtOH	1.228
900uM SM	1.003
6% EtOH	1.284
1200uM SM	0.82
8% EtOH	1.436

Graph:

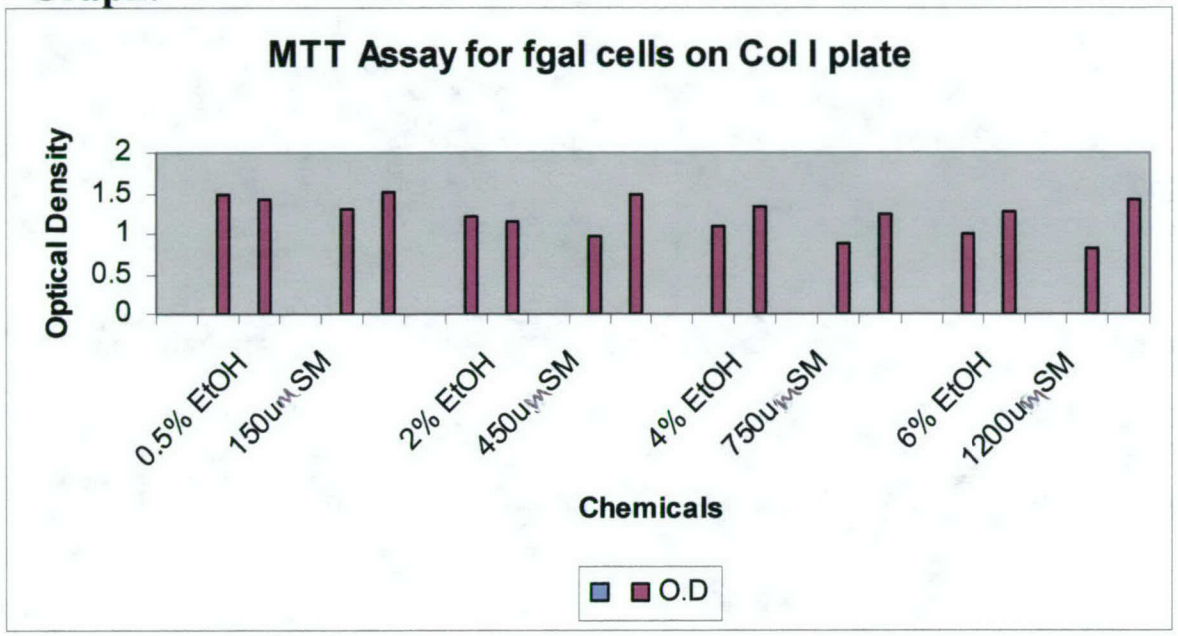

Fig. 20: MTT Assay for Fgal cells on Col IV Plate.

Table:

Chemicals	O.D.
75uM SM	1.468
0.5% EtOH	1.417
150uM SM	1.27
1% EtOH	1.377
300uM SM	0.841
2% EtOH	1.396
450uM SM	0.894
3% EtOH	1.318
600uM SM	0.818
4% EtOH	1.267
750uM SM	0.742
5% EtOH	1.218
900uM SM	0.596
6% EtOH	1.291
1200uM SM	0.544
8% EtOH	1.377

Graph:

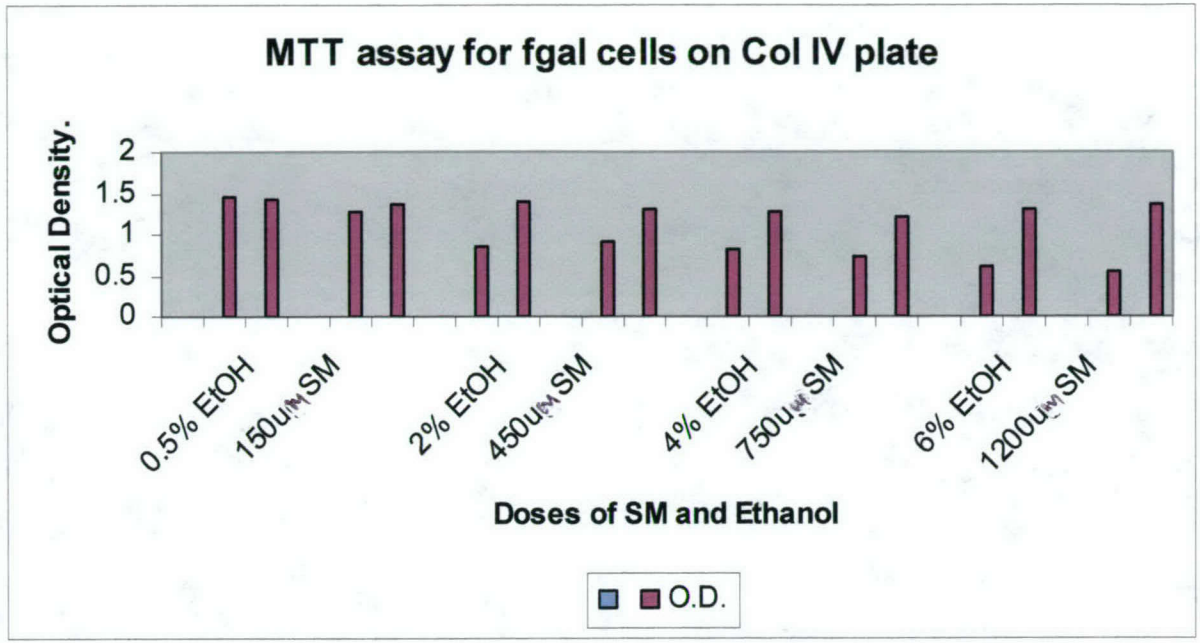

Fig. 21: H & E Staining for Rafts exposed to SM and Ethanol.

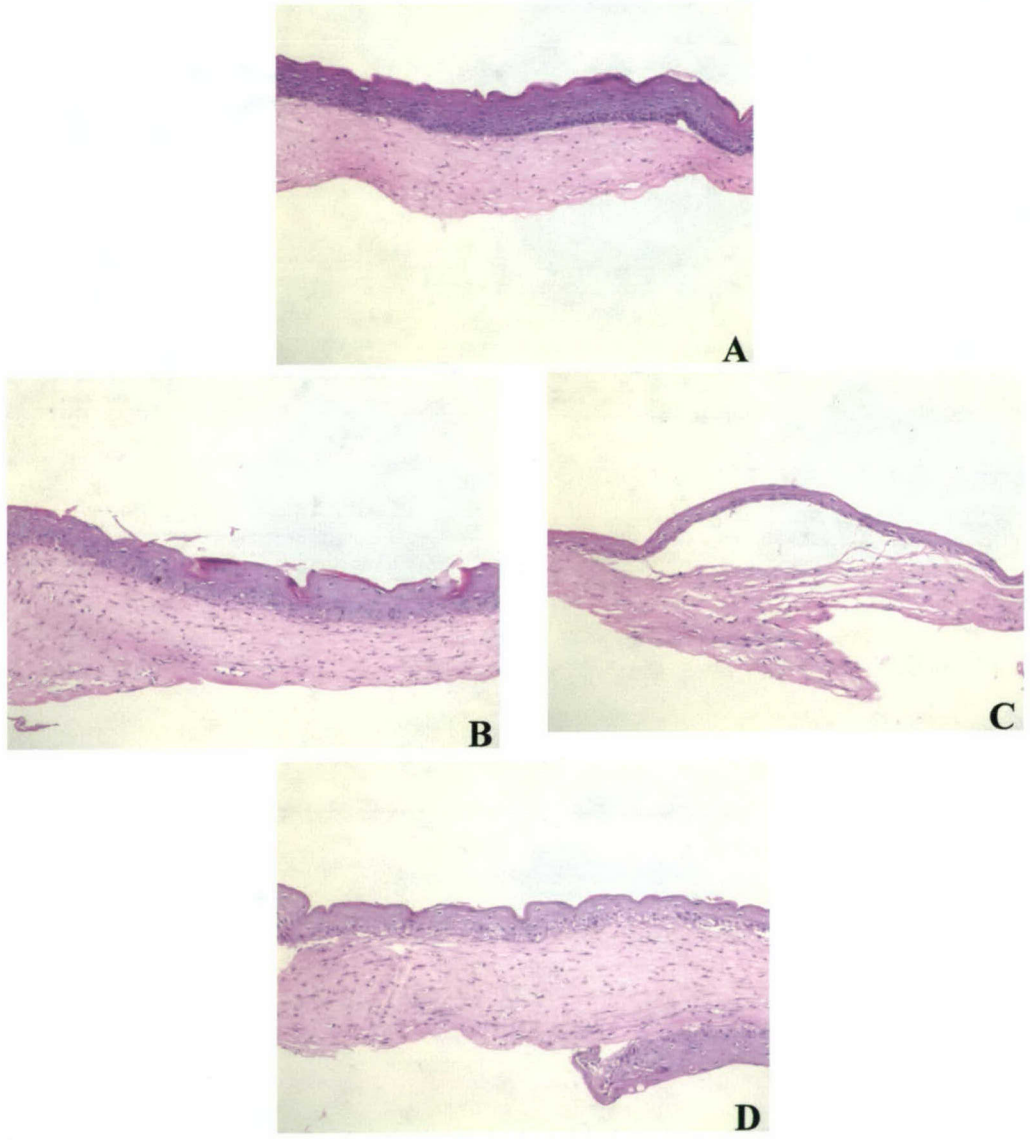

Fig: A- Control; B & C – 75 & 150*u*m SM; D- 1% Ethanol.

Fig. 22: H&E Staining for Rafts exposed to diff. Doses of SM along with Controls

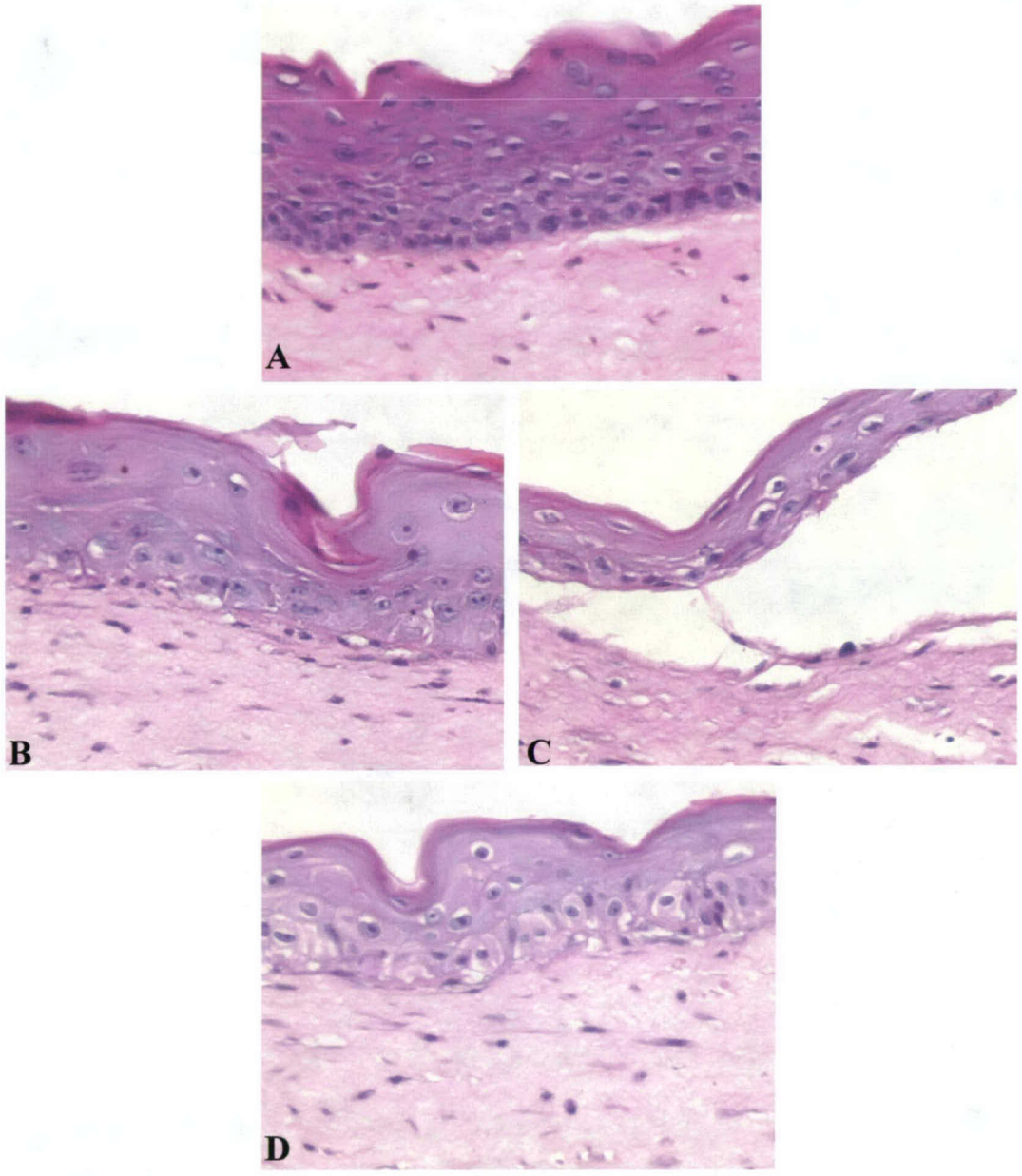

Fig: A - Control; B & C – 75 & 150 *u*m SM; D - 1% Ethanol.

Fig. 23: M30 Staining for Rafts exposed to SM and Ethanol.

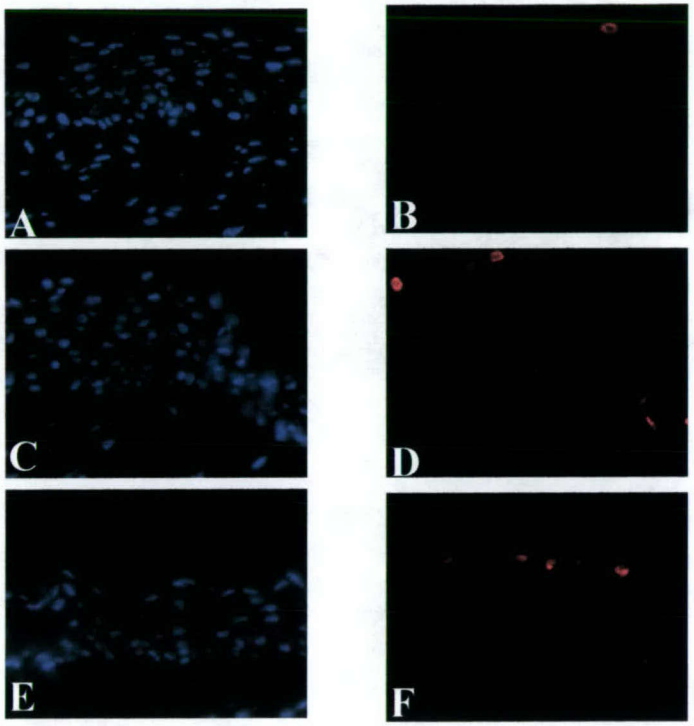

Fig: A& B - Raft exposed to 1% Ethanol; C&D - Raft exposed to *75um* SM; E& F - Raft exposed to 150*u*m SM.

A

Fig. 24: H&E Staining for diff. doses of SM and Ethanol controls.

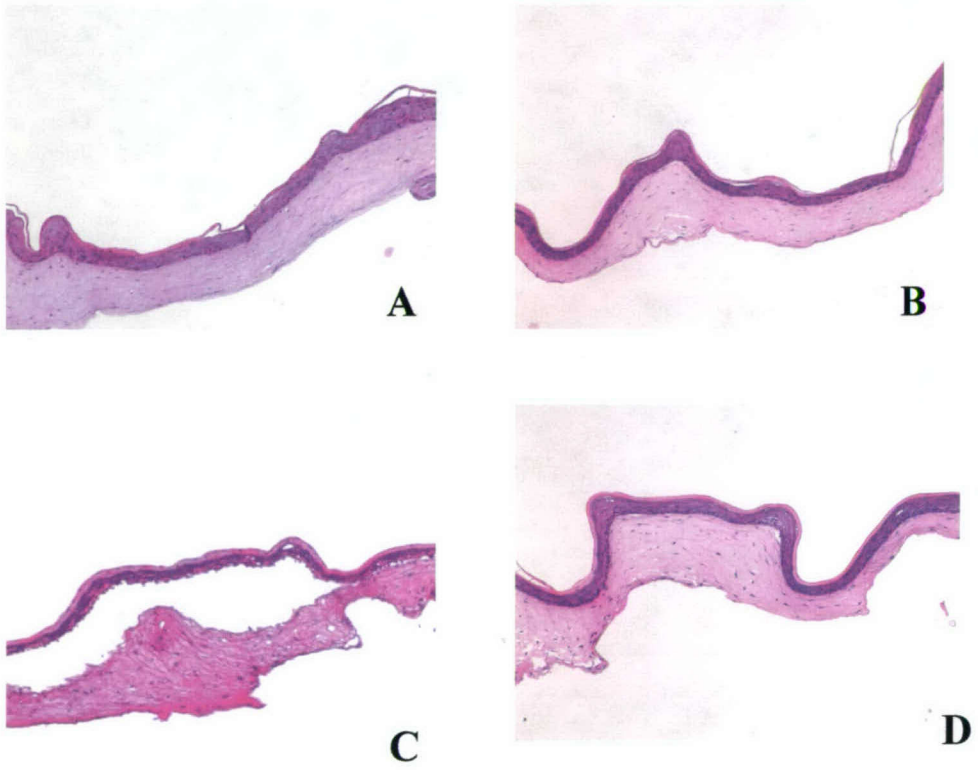

Fig : A & C – 150 &300*u*m of Sulfur Mustard.

B & D – 1 & 2 % Concurrent Ethanol controls.

Fig. 25: H & E Staining for diff. Doses of SM and Ethanol.

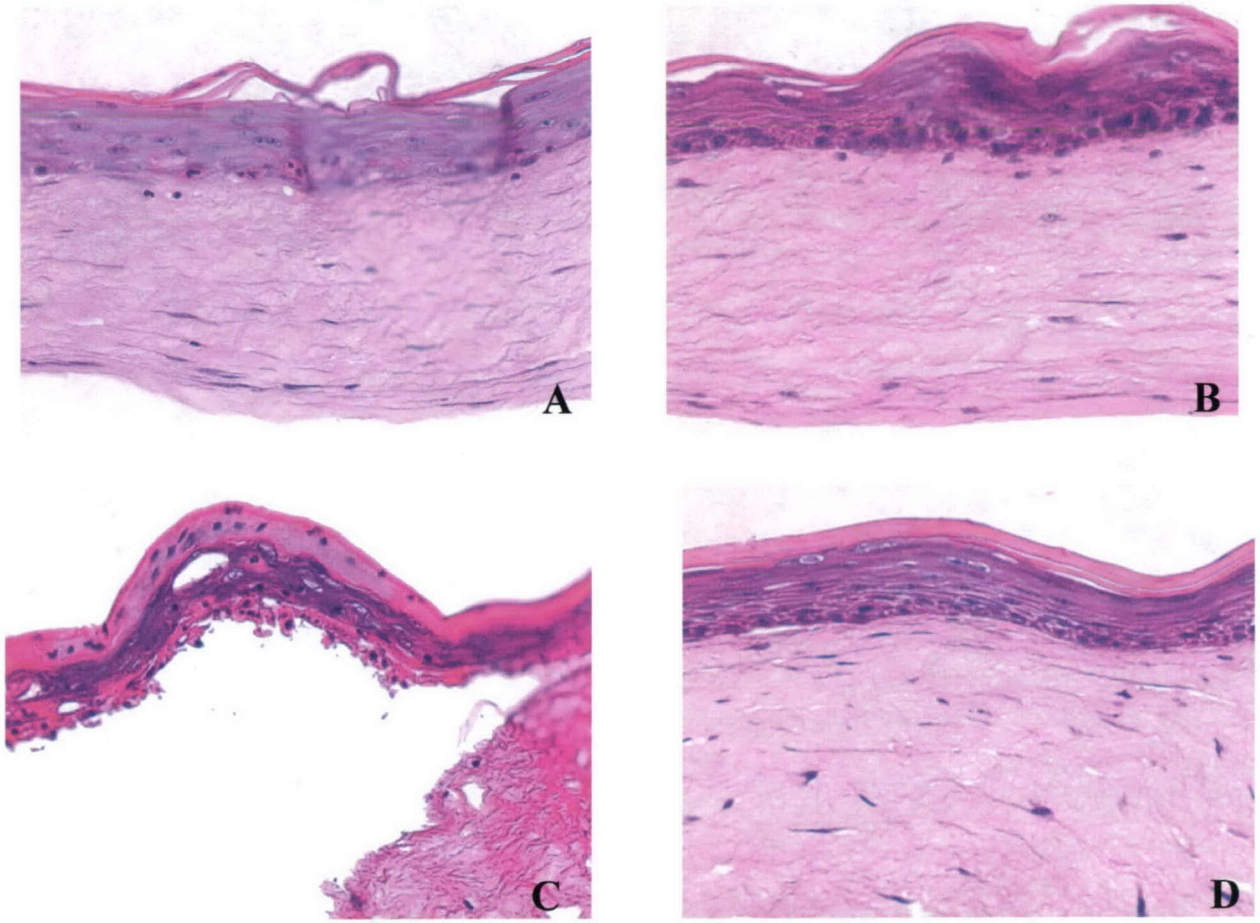

Fig: A & C – 150 and 300*u*m of SM;

B & C – 1 and 2 % Ethanol controls.

Fig. 26: M30 Staining for the rafts exposed to diff . doses of SM and Ethanol

SM– 150um/7min.

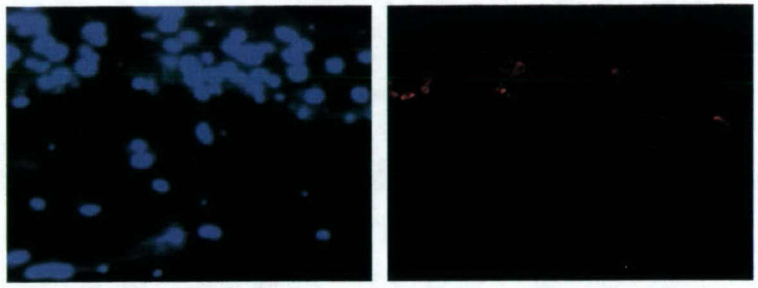

1% Ethanol/7min.

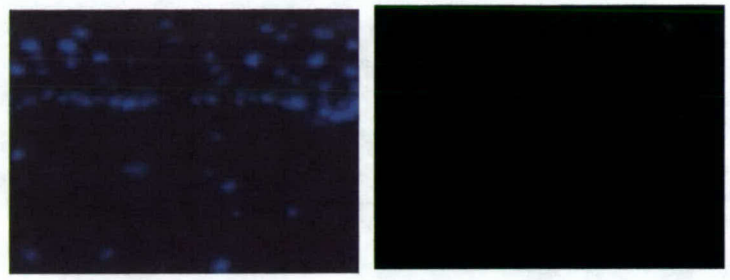

SM—300um/7min.

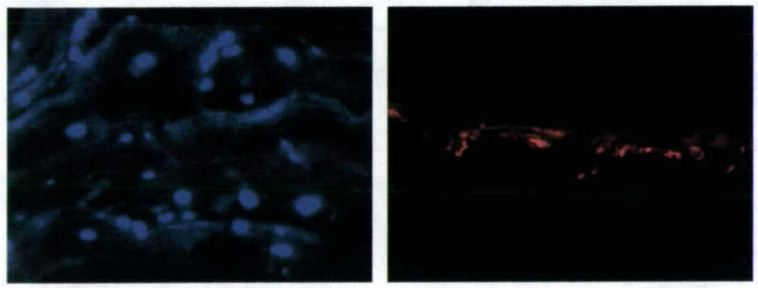

2% Ethanol/ 7min.

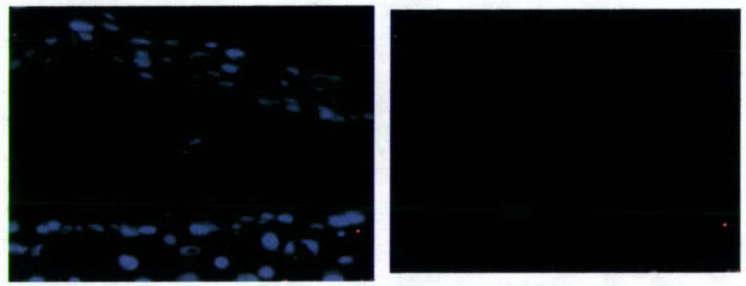

Fig. 27: H&E Staining for NHK's on different substrates (3-D culture)

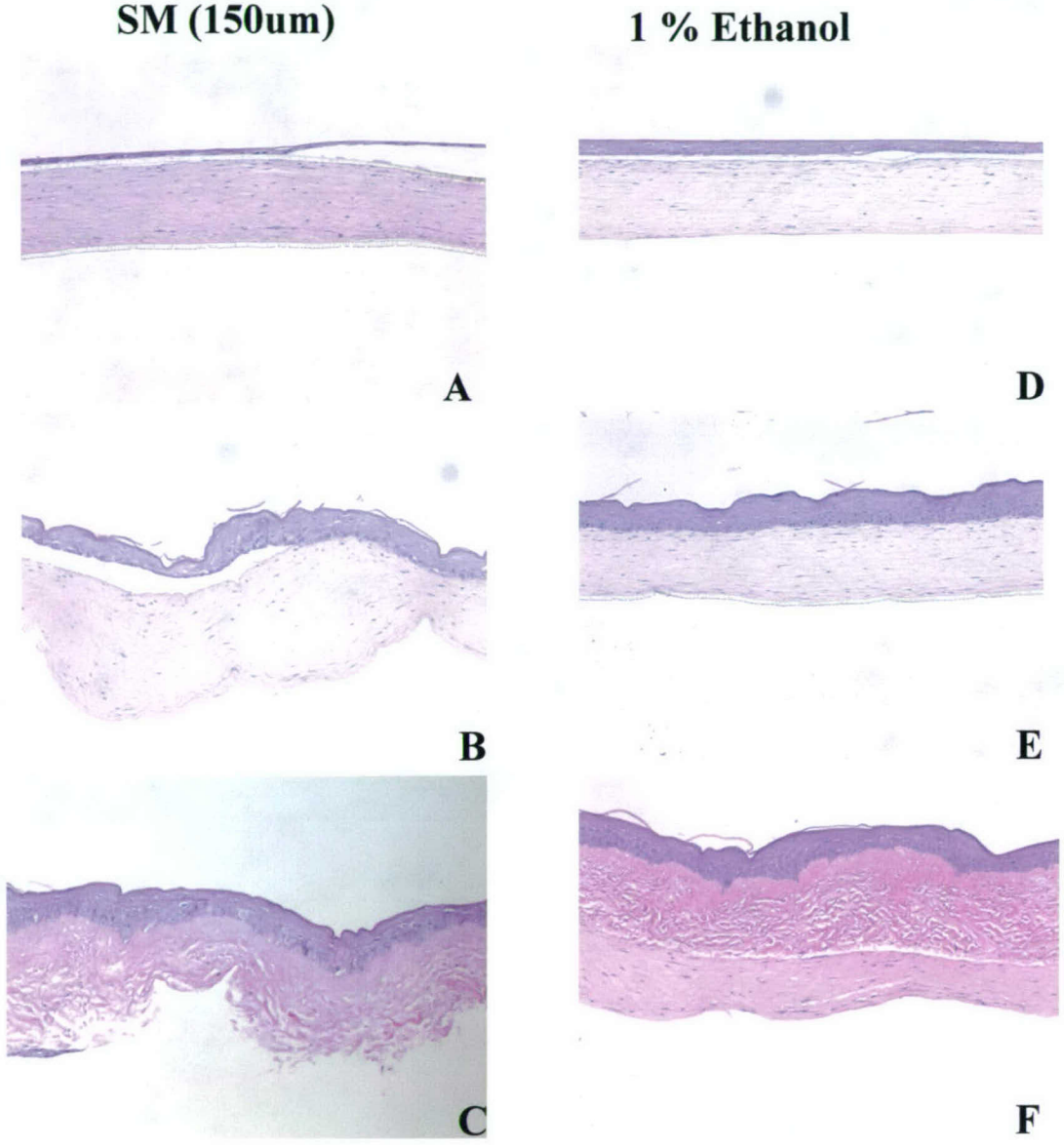

Fig: A&D- Plastic; B&E- Raft; C&F- Alloderm.

Fig. 28: H & E Staining for NHK's on diff. substrates.

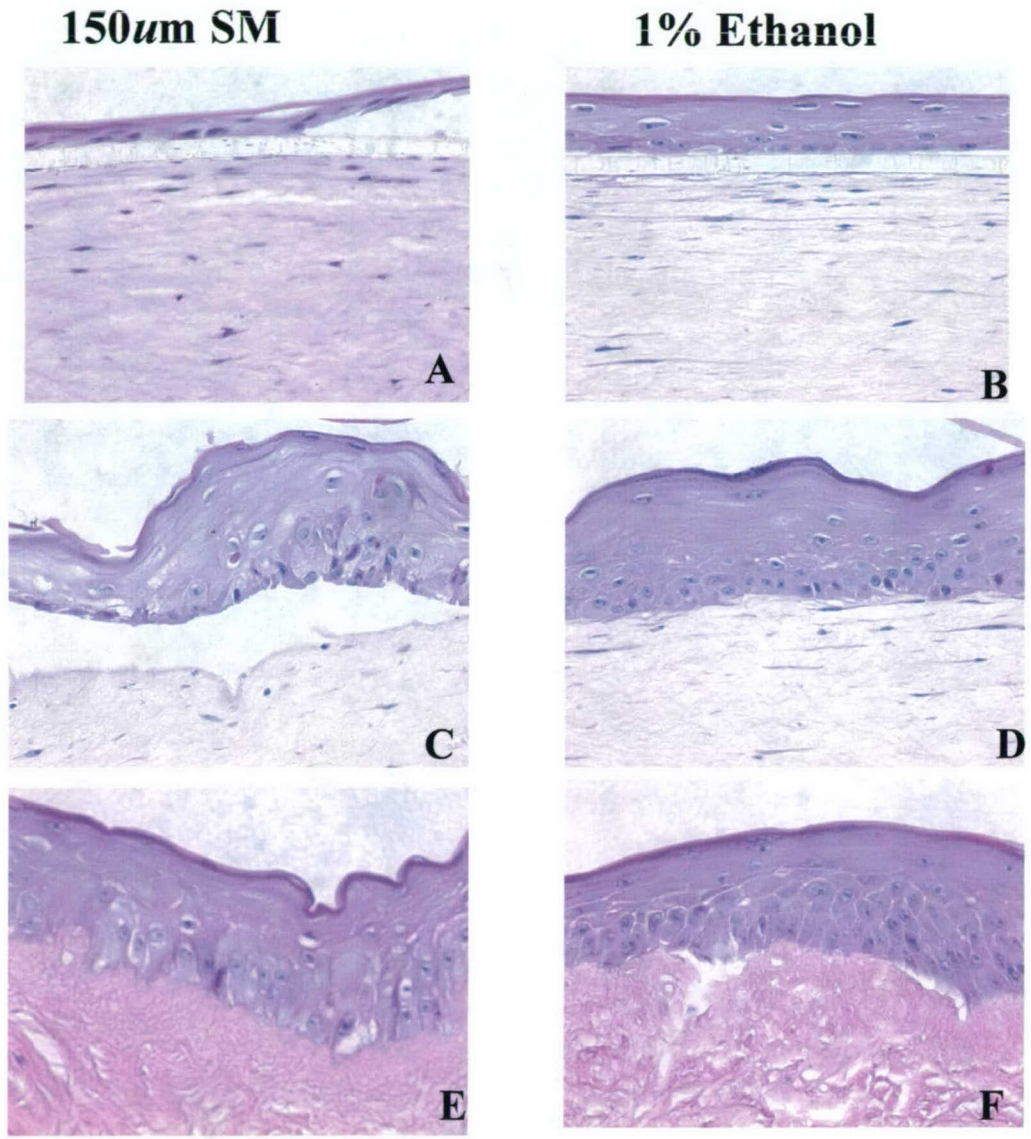

Fig: A&B – Plastic; C&D – Raft; E&F - Alloderm.

Fig. 29: H & E Staining for NHK's on diff. Substrates (3- D cultures)

SM (150*um*) **1% Ethanol**

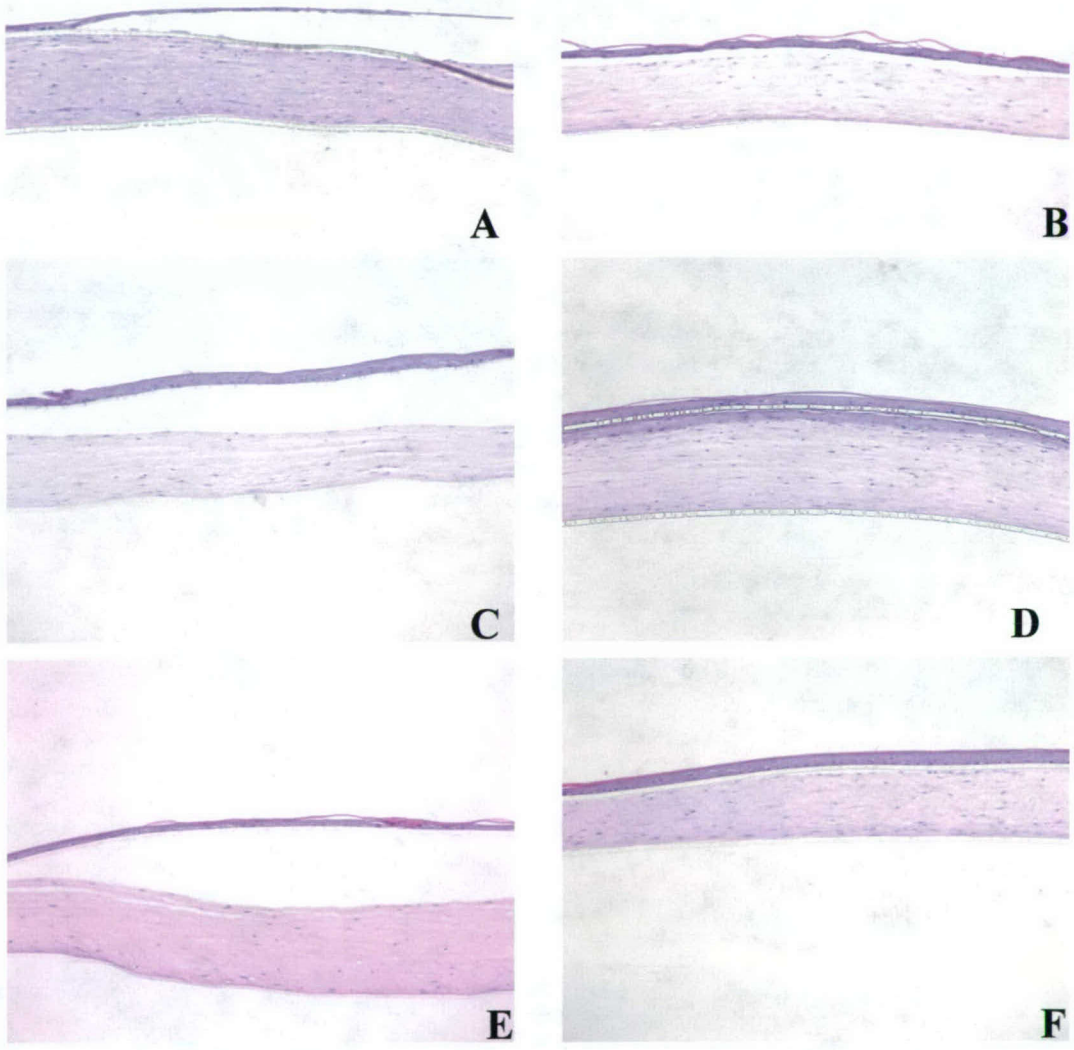

Fig: A&B- Col I; C&D- Col IV; E& F- Fibronectin.

Fig. 30: Effects of SM and Ethanol on NHK's on diff. Substrates (3-D)

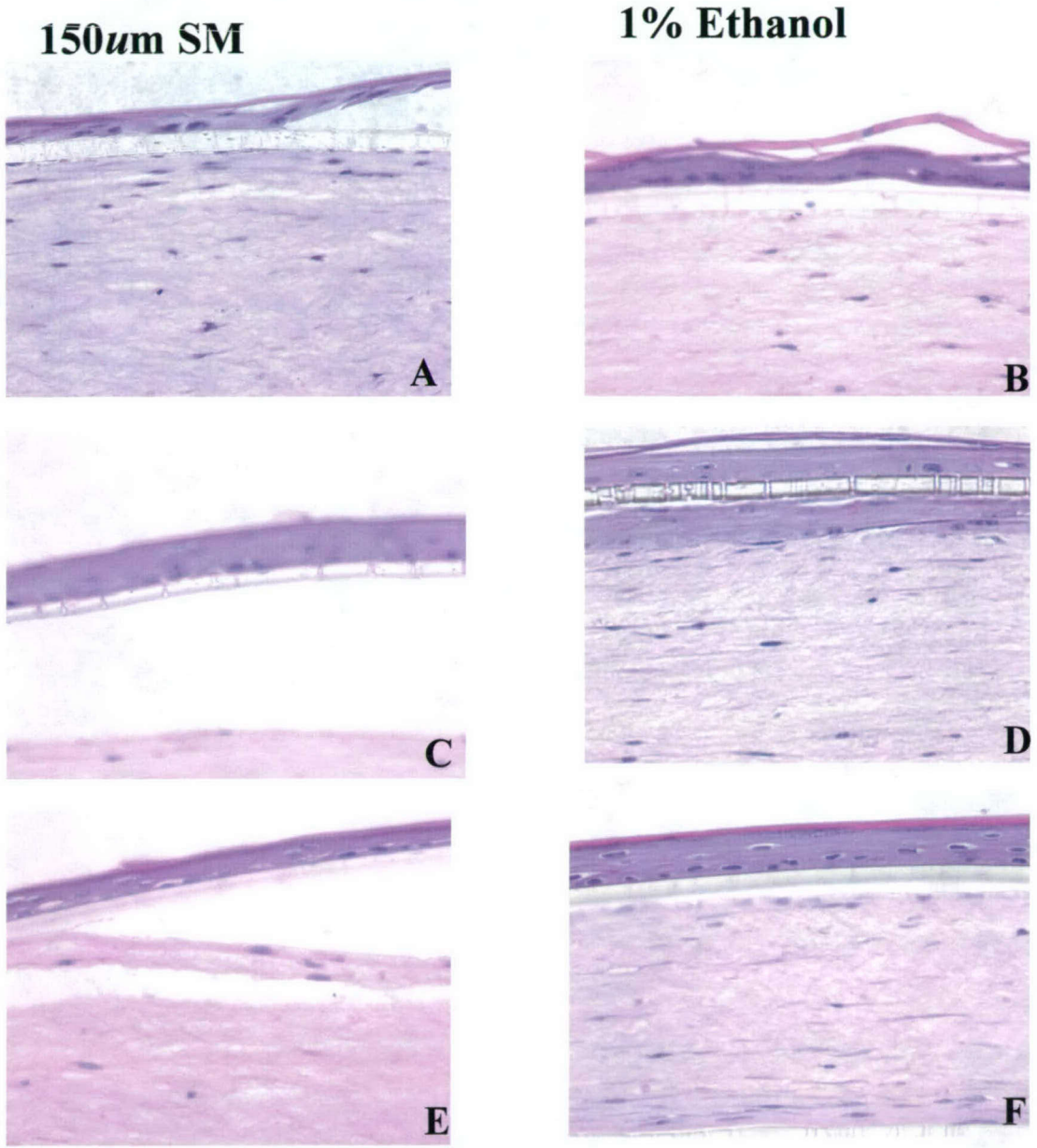

Fig: A&B – Col I; C&D – Col IV; E&F – Fibronectin.

Fig. 31: Effects of SM on Alloderm and Raft along with controls.

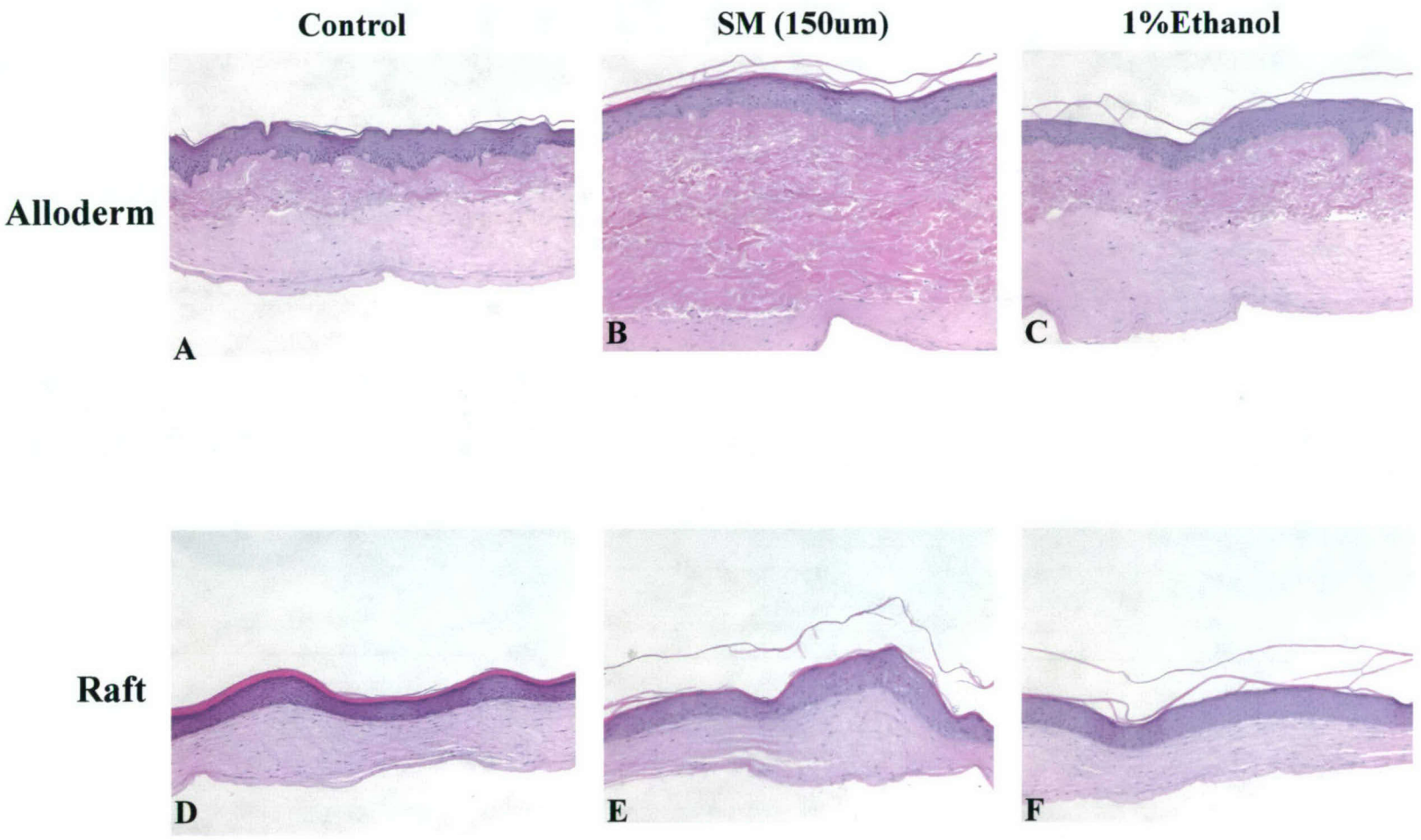

Fig: A& D – Control; B& E – 150*u*m SM; C&F – 1% Ethanol.

Fig. 32: Effects of SM on Alloderm and Rafts along with controls.

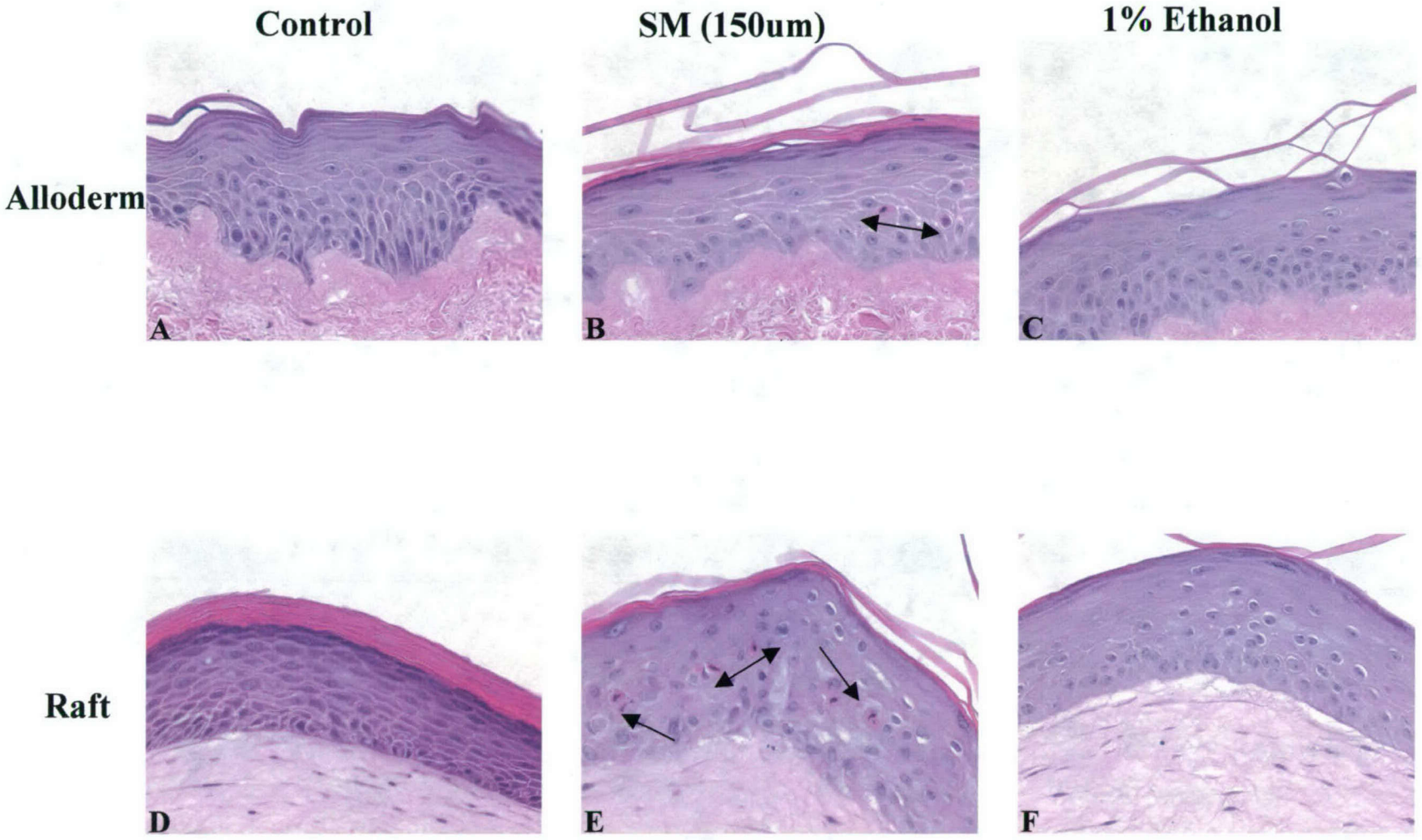

Fig: A&D – Controls; B&E - 150um of SM; C&F – 1% Ethanol.

Fig.33: M30 Staining for Alloderms and Rafts exposed to SM and Controls.

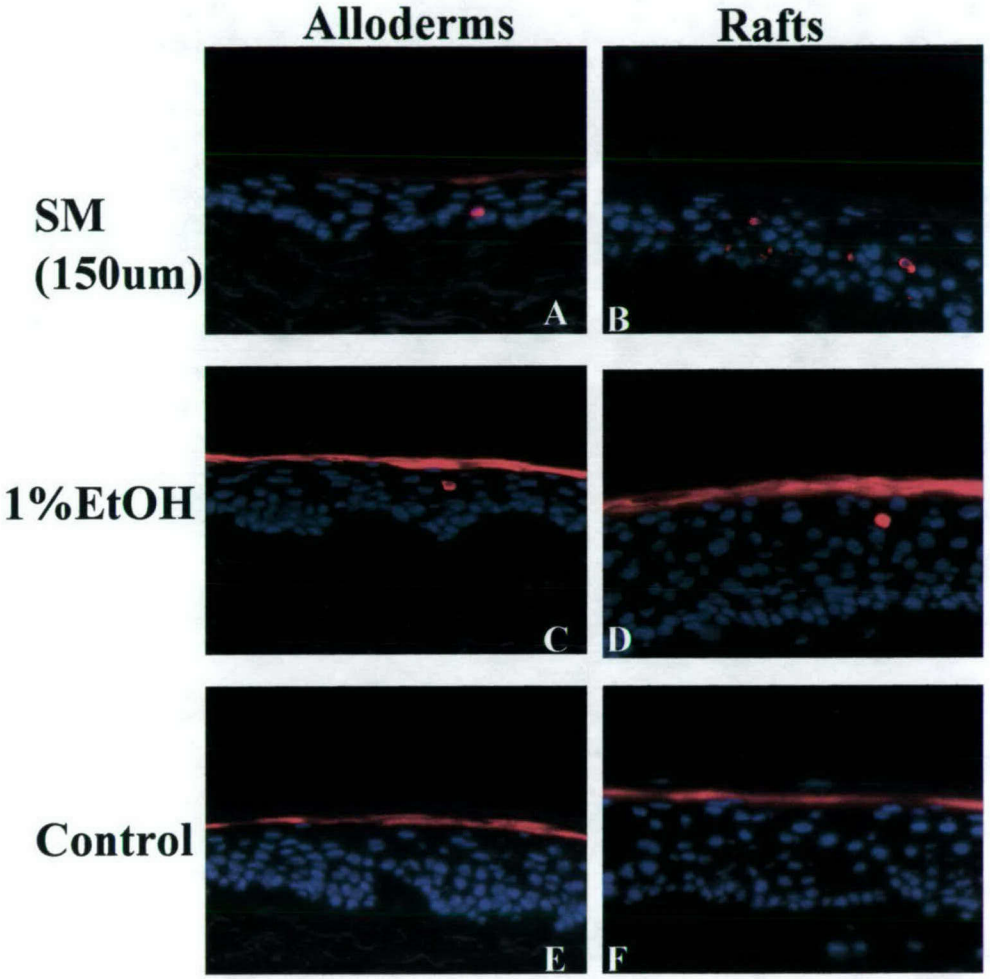

A,C, E –Alloderms; B, D, F- Rafts.

Fig. 34: Apoptotic cell counts for keratinocytes on rafts and alloderms.

Table:

Chemicals	No. of apoptotic cells on alloderm	No. of apoptotic cells on raft.
Control	0	3
1% Ethanol	6	9
SM (150um)	22	265

Graph:

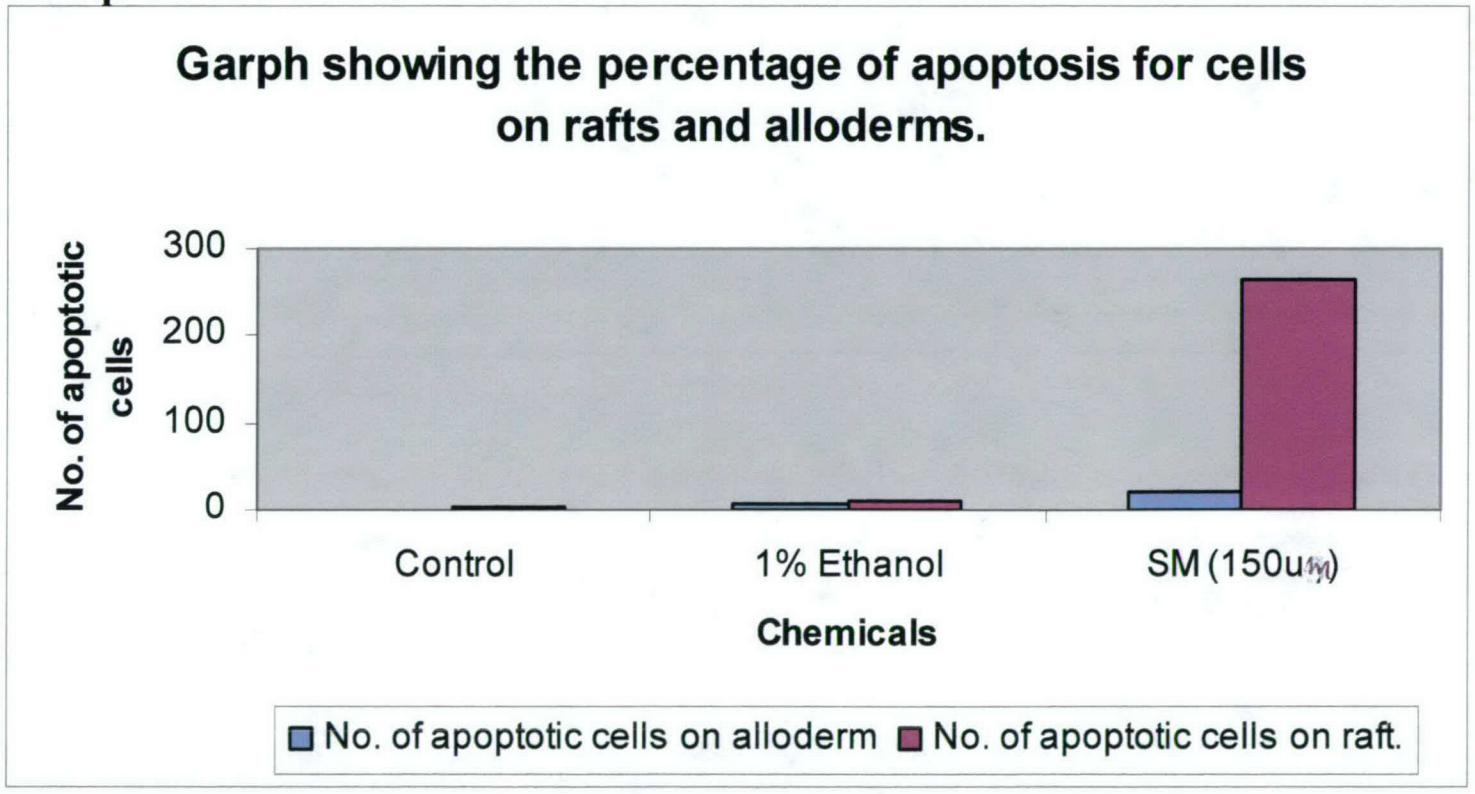

Fig. 35: Alloderm exposed to diff.doses of SM and Controls.

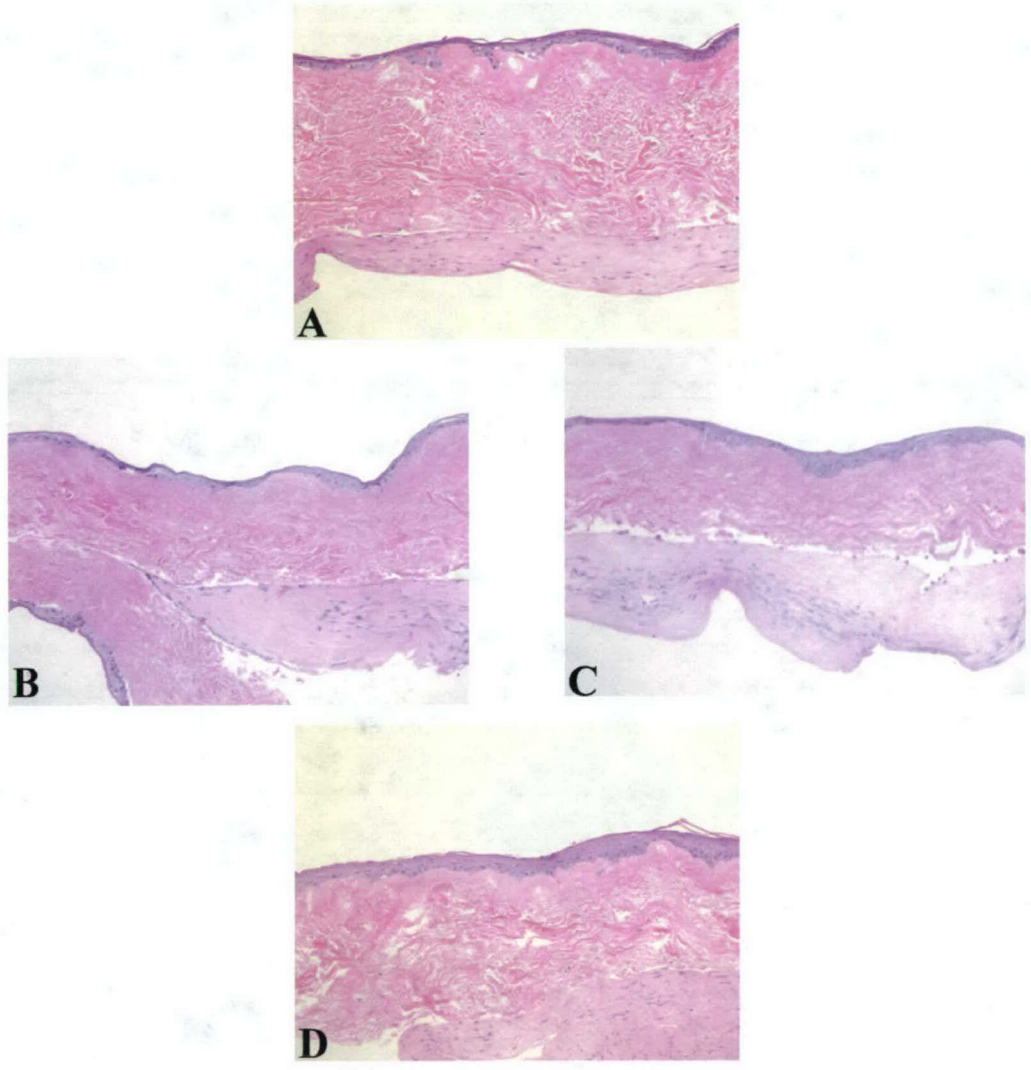

Fig: A-Control; B&C- 75& 150um SM; D- 1% Ethanol.

Fig. 36: Alloderm exposed to diff. Doses of SM and Controls

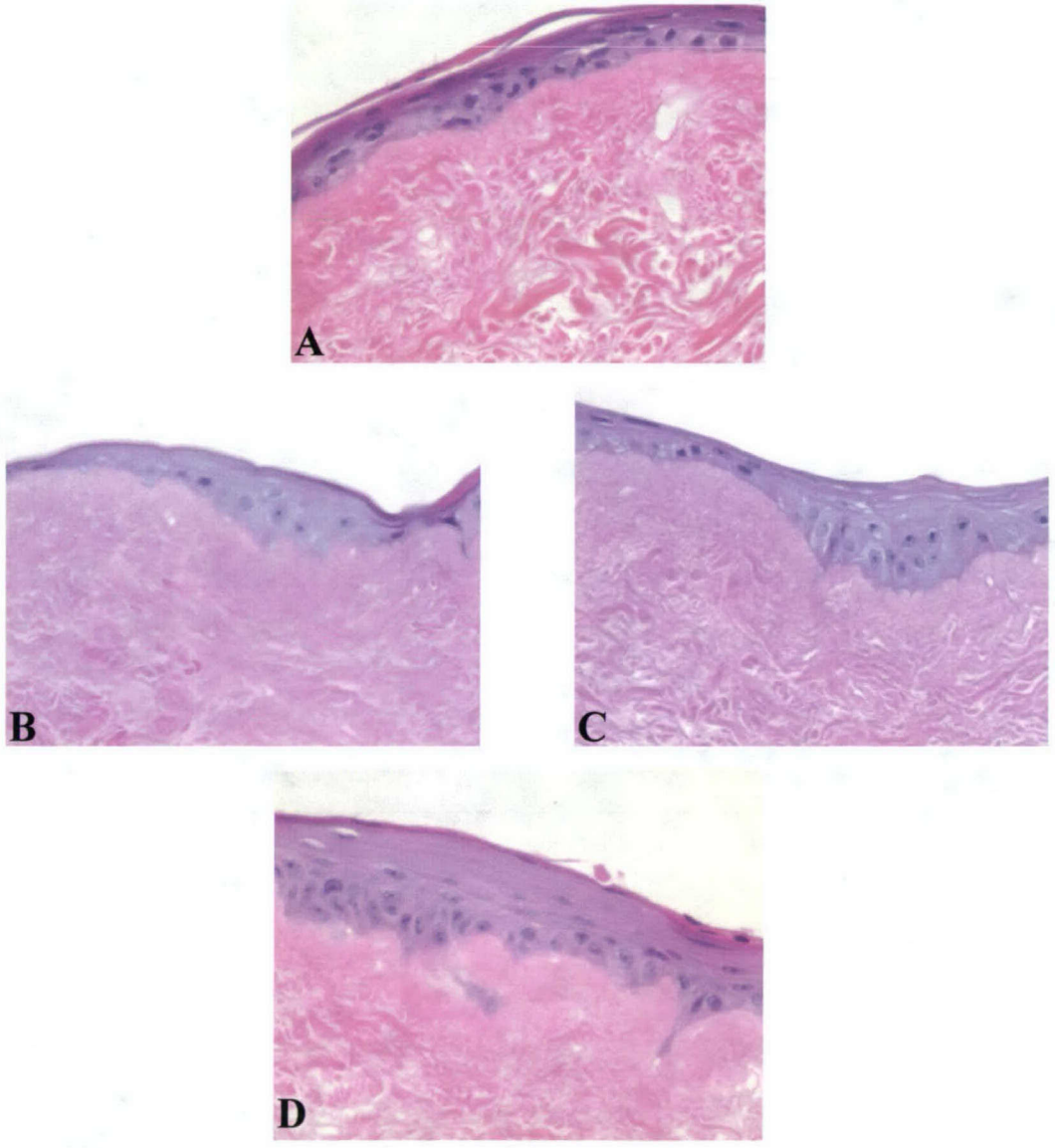

Fig: A- Control; B& C – 75 & 150um SM; D- 1% Ethanol.

Fig. 37: M 30 Staining for Alloderm exposed to SM and Controls.

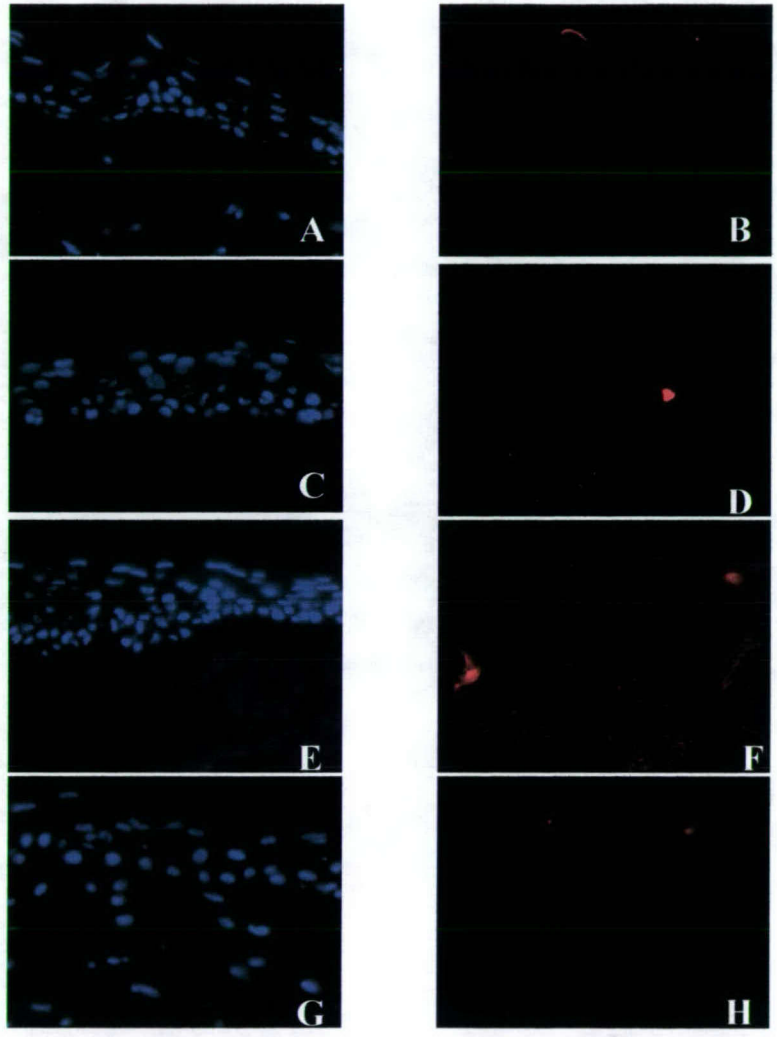

Fig: A, B- Control; C, D- 75 um SM; E, F-150um SM; G, H- 1% Ethanol.

Fig. 38: Dose Response to SM shown by NHK's on Allos along with controls

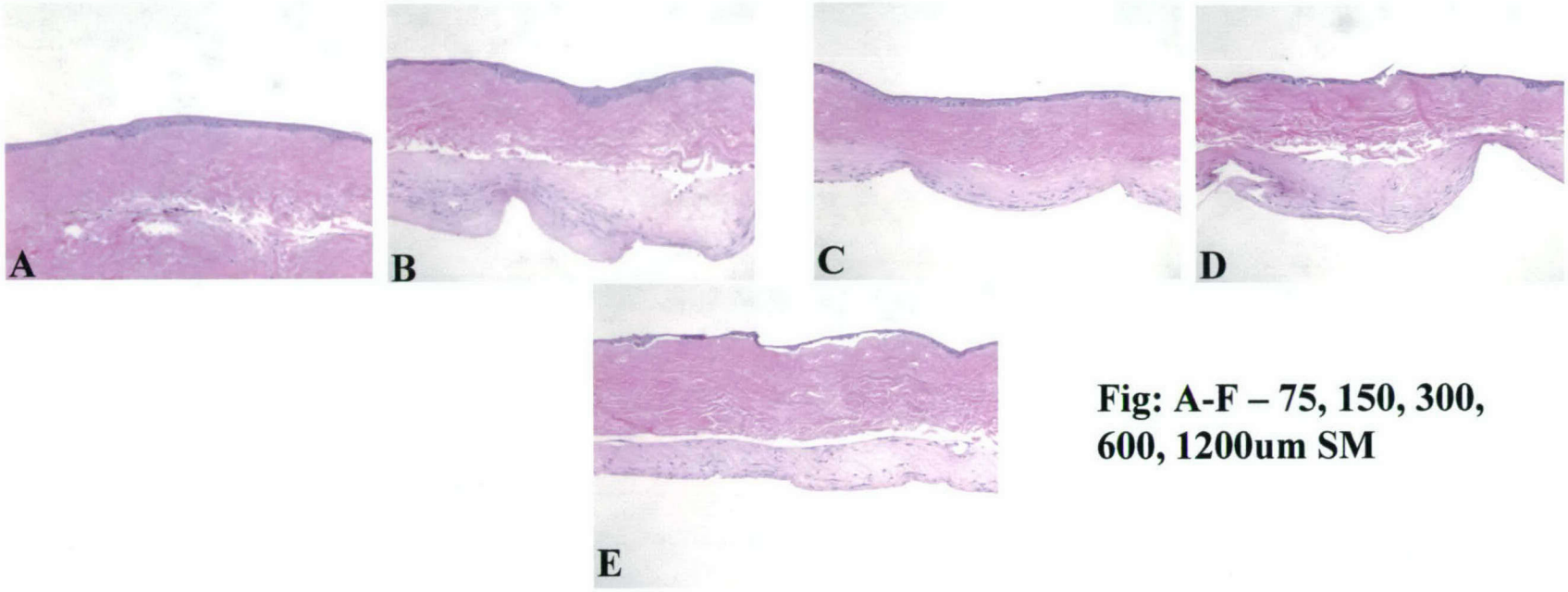

Fig: A-F – 75, 150, 300, 600, 1200um SM

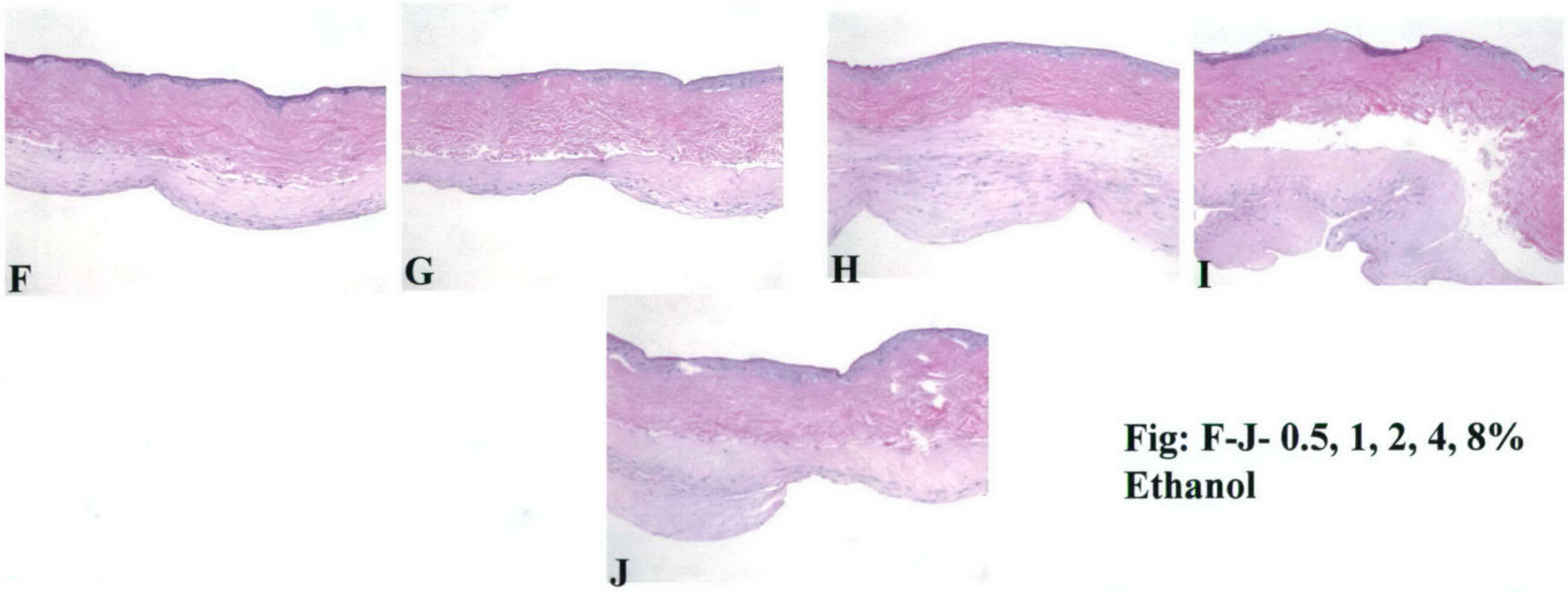

Fig: F-J- 0.5, 1, 2, 4, 8% Ethanol

Fig.39: Dose Response to SM shown by NHK's on Alloderm along with controls

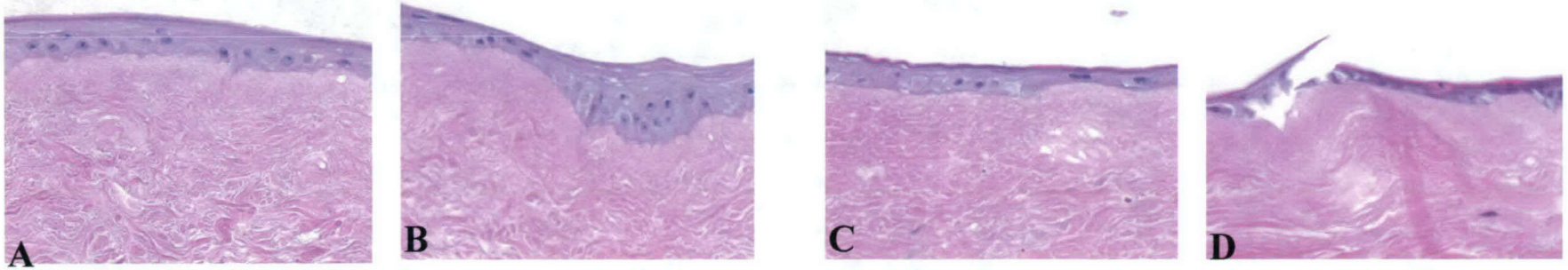

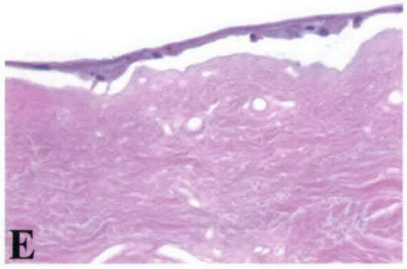

Fig: A-E – 75, 150, 300, 600, 1200um SM

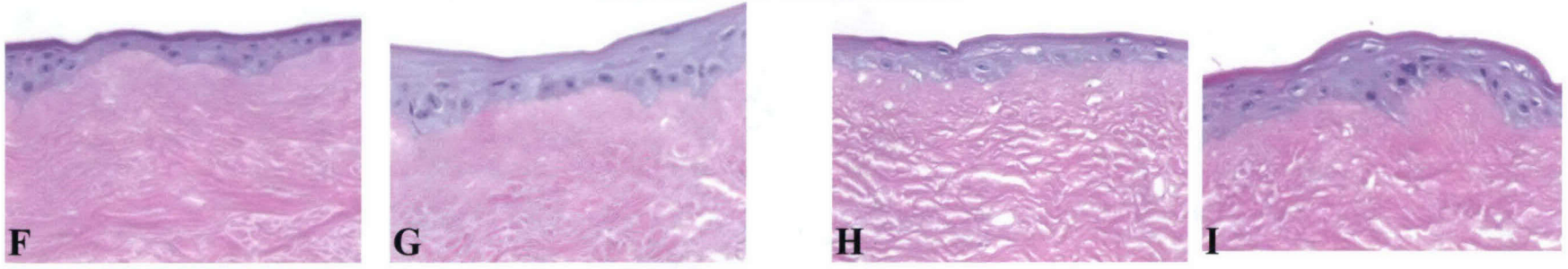

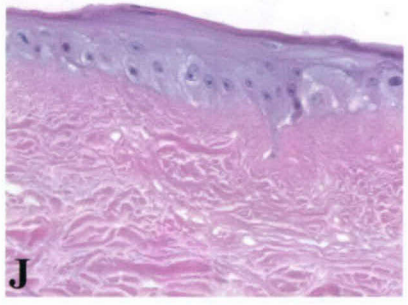

Fig: F-J – 0.5, 1, 2, 4, 8% Ethanol

Fig. 40: M30 Staining for dose-response shown by NHKs on Alloderm

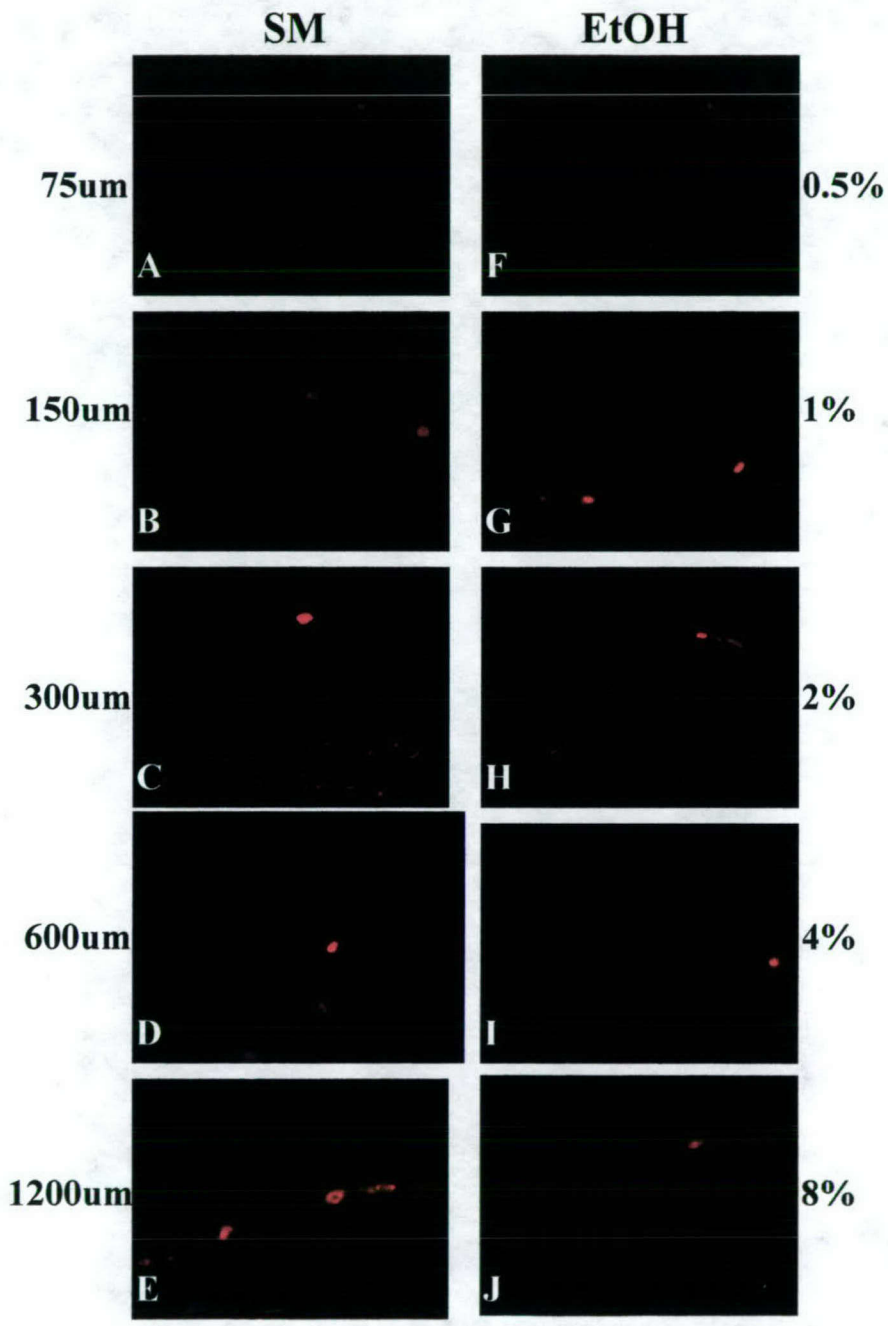

Fig: A-E – Diff. Doses of SM: F-J – Concurrent Ethanol controls.

Fig. 41: Apoptotic Counts Alloderm Exposed to diff. Doses of SM along with concurrent controls

Table:

Chemical	Apoptotic counts.
75uM SM	19
0.5% EOH	0
150uM SM	24
1% EtOH	5
300uM SM	61
2%EtOH	6
600uM SM	102
4%EtOH	17
1200uM SM	286
8%EtOH	18

Graph:

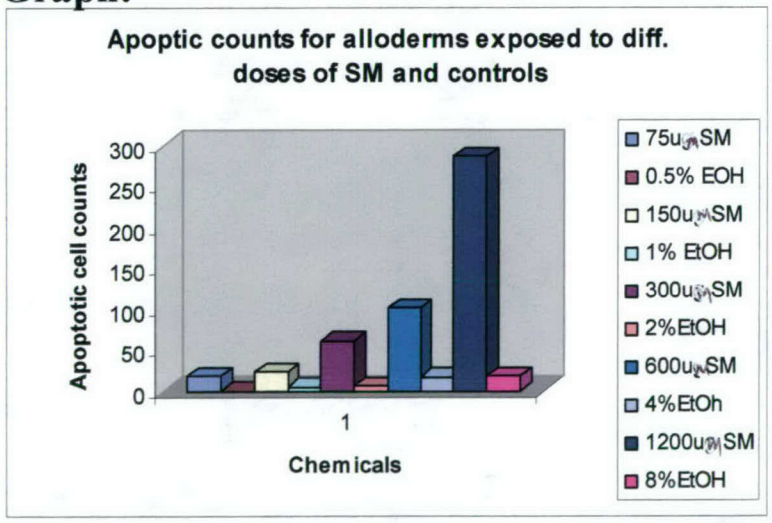

Fig. 42: Effects of SM on diff. Cell types seeded on alloderm along with controls.

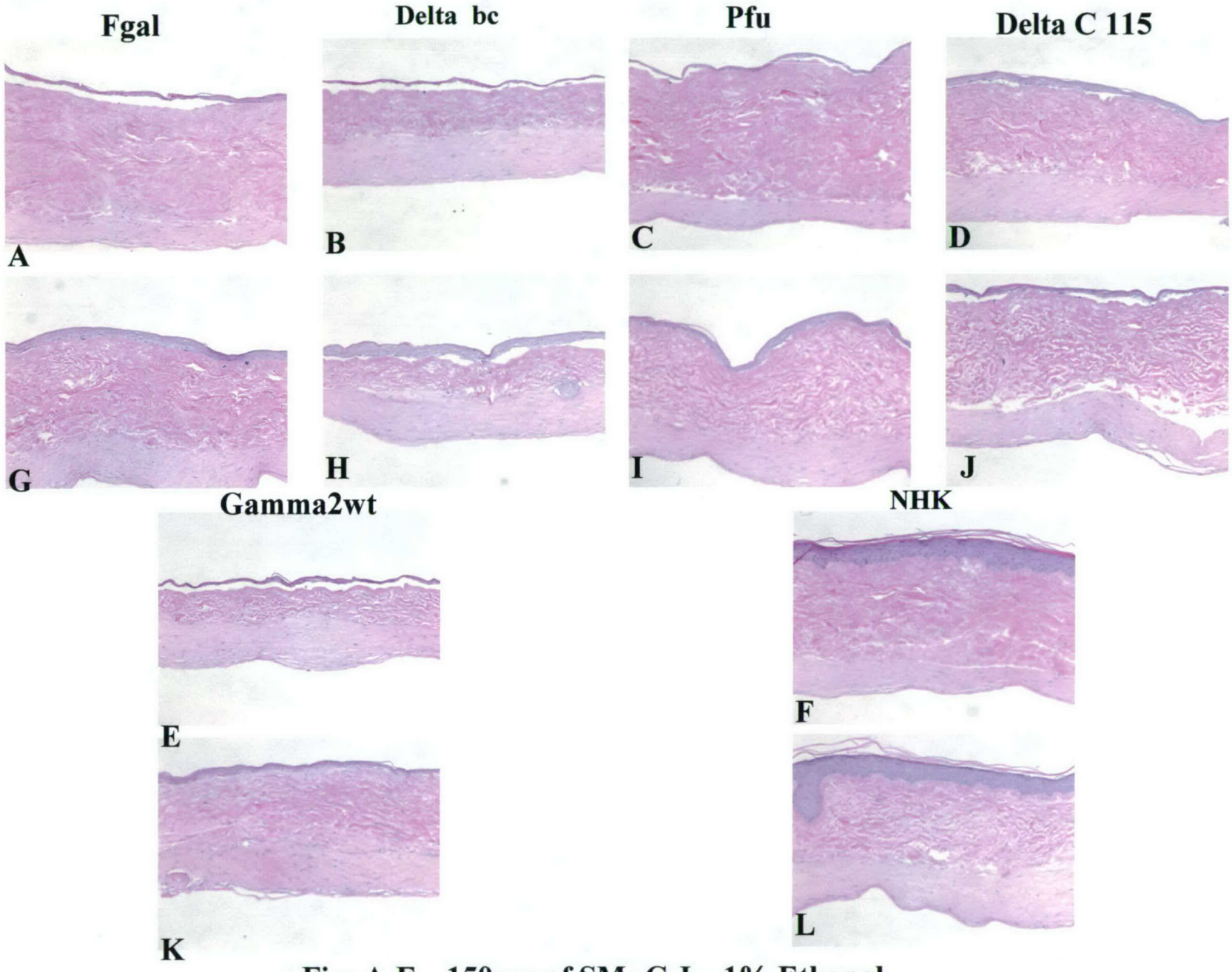

Fig: A-F – 150um of SM: G-I – 1% Ethanol.

Fig. 43: Effects of SM on diff. Cell types on alloderm along with controls.

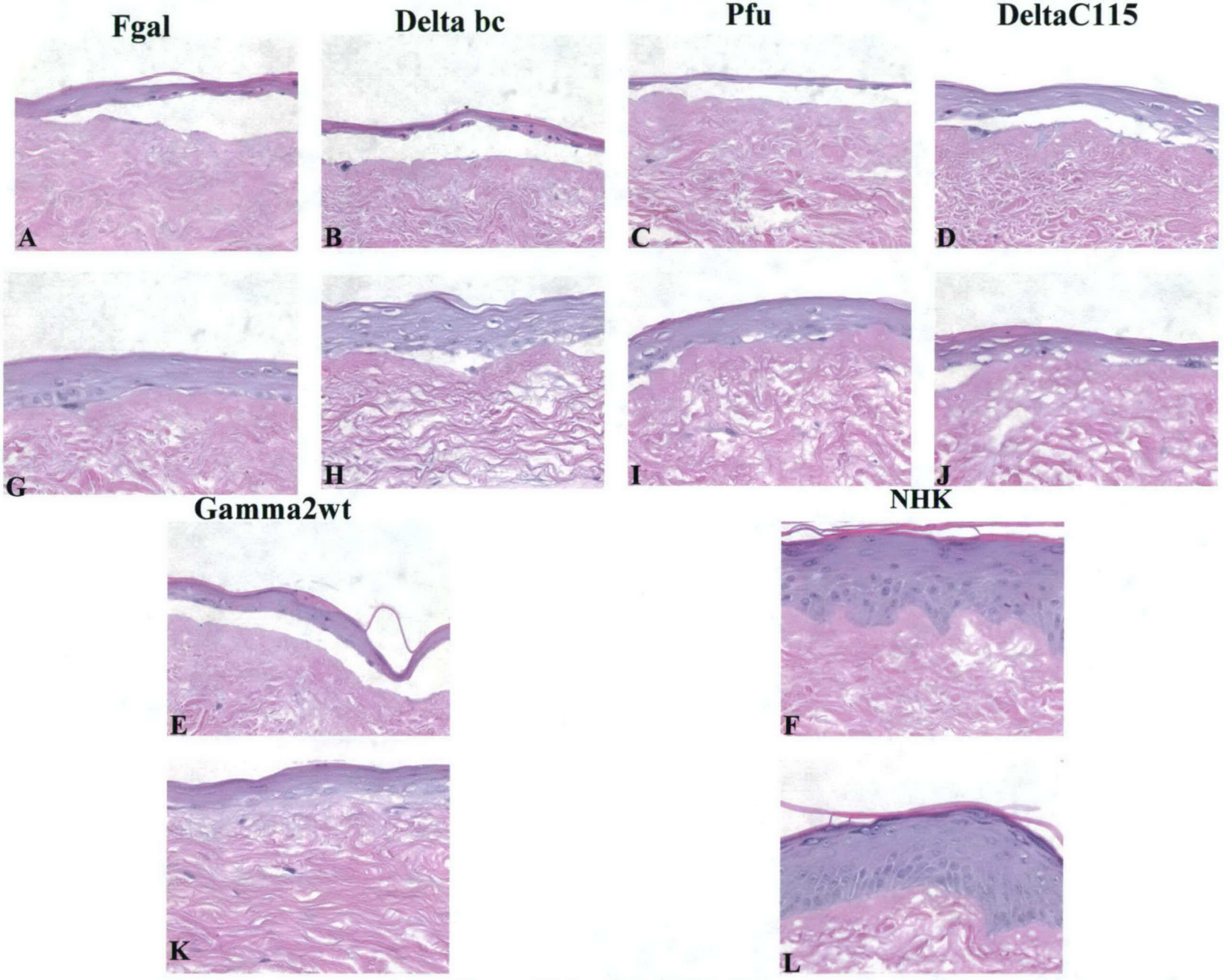

Fig: A-F – 150um SM; G-L- 1% Ethanol.

Fig. 44: M30Staining for diff.cell types on alloderm exposed to SM and Ethanol.

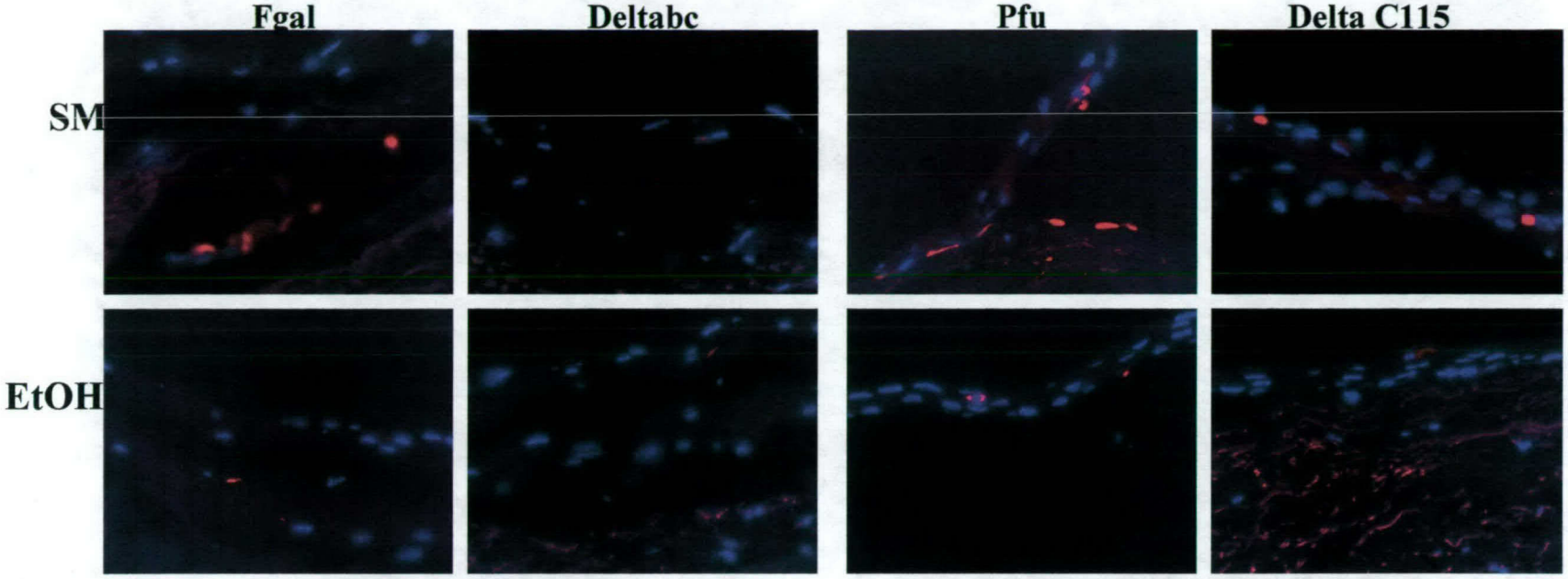

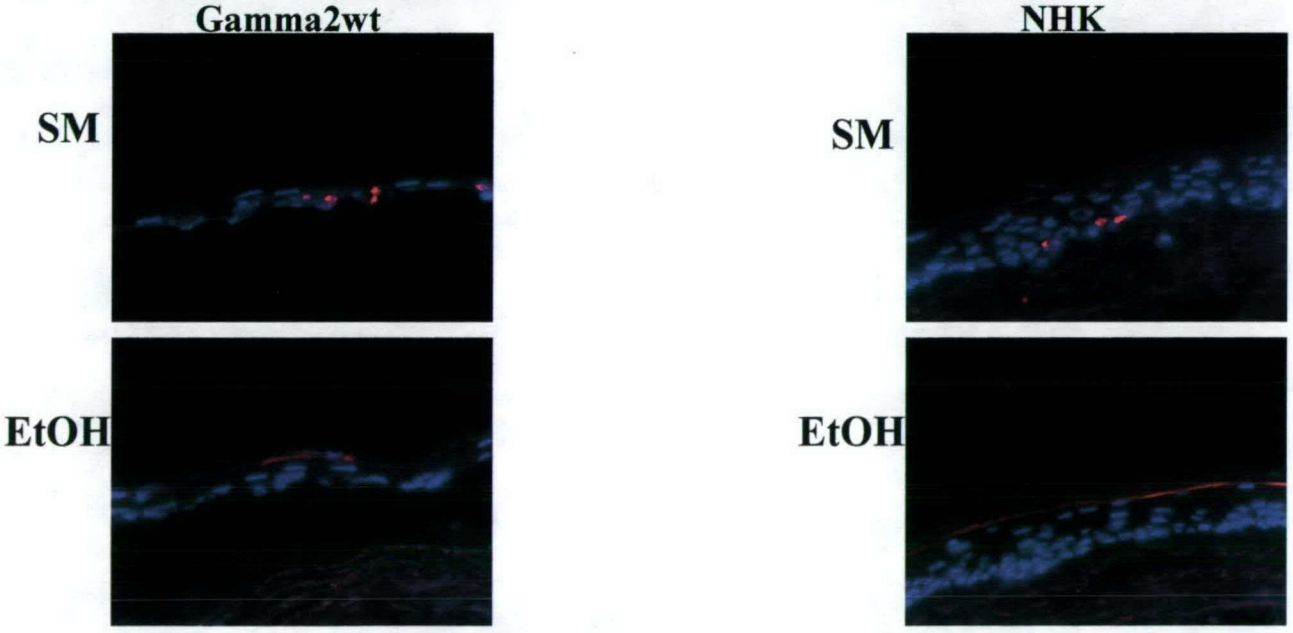

SM—150um; EtOH– 1%

Fig. 45: Apoptosis for diff. Cells on alloderm exposed to SM and Ethanol

Table: Percentage of apoptosis for diff.cell types on alloderm

Chemicals	fgal	Deltabc	pfu	DeltaC115	Gamma2wt	NHK
SM(150u)	20	4	17	7	19	5
1%EtOH	2	3	4	4	5	2

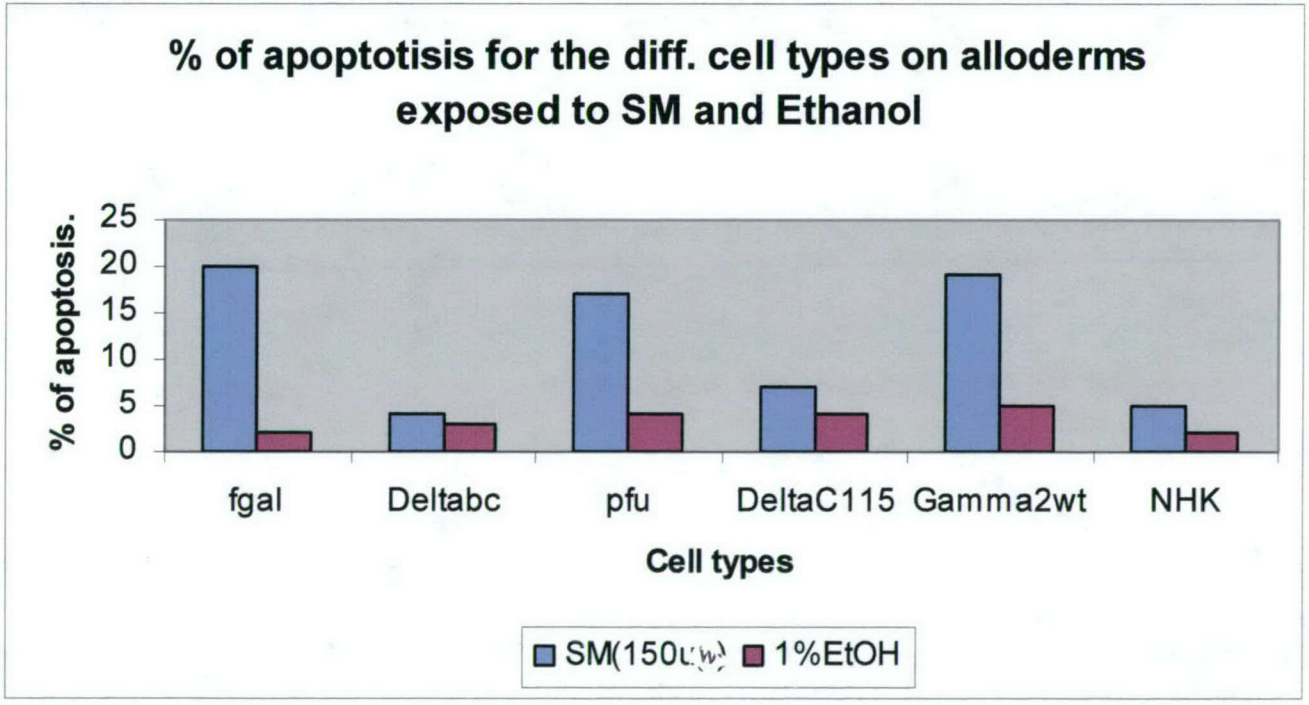

See related Commentary on page vii

Analysis of Microenvironmental Factors Contributing to Basement Membrane Assembly and Normalized Epidermal Phenotype

Frank Andriani,* Alexander Margulis,* Ning Lin,* Sy Griffey,‡ and Jonathan A. Garlick*†

*Department of Oral Biology & Pathology, School of Dental Medicine, SUNY at Stony Brook, Stony Brook, New York, USA;
†Department of Dermatology, School of Medicine, SUNY at Stony Brook, Stony Brook, New York, USA;
‡LifeCell Corporation, One Millenium Way, Branchburg, New Jersey, USA

To understand further the role of the dynamic interplay between keratinocytes and stromal components in the regulation of the growth, differentiation, morphogenesis, and basement membrane assembly of human stratified squamous epithelium, we have generated novel, three-dimensional organotypic cultures in which skin keratinocytes were grown in the absence or presence of pre-existing basement membrane components and/or dermal fibroblasts. We found that keratinocytes cultured in the presence of pre-existing basement membrane components and dermal fibroblasts for 9 d showed rapid assembly of basement membrane, as seen by a nearly complete lamina densa, hemidesmosomes, and the polarized, linear distribution of laminin 5 and a6 integrin subunit. Basement membrane assembly was somewhat delayed in the absence of dermal fibroblasts, but did occur at discrete nucleation sites when pre-existing basement membrane components were present. No basement membrane developed in the absence of pre-existing basement membrane components, even in the presence of dermal fibroblasts. Bromodeoxyuridine incorporation studies showed that early keratinocyte growth was independent of mesenchymal support, but by 14 d, both fibroblasts and assembled basement membrane were required to sustain growth. Normalization of keratinocyte differentiation was independent of both dermal fibroblasts and structured basement membrane. These results indicated that epithelial and mesenchymal components play a coordinated role in the generation of structured basement membrane and in the regulation of normalized epithelial growth and tissue architecture in an *in vitro* model of human skin. ***Key words: basement membrane/epithelial-mesenchymal interactions/fibroblasts/laminin 5/organotypic culture. J Invest Dermatol 120:923–931, 2003***

Microenvironmental factors, such as the dynamic cross-talk between epithelium and connective tissue, are known to regulate epidermal morphogenesis and homeostasis. Diffusible factors produced by keratinocytes and mesenchymal cells are known to support epidermal growth and differentiation through the reciprocal modulation of paracrine-acting, growth-regulatory factors (Smola *et al*, 1993; Szabowski *et al*, 2000). Epithelial–mesenchymal interactions have also been shown to mediate the synthesis of basement membrane constituents and to contribute to basement membrane formation (Fleischmajer *et al*, 1998; Smola *et al*, 1998b). Interactions between keratinocytes and extracellular matrix proteins at the basement membrane zone maintain tissue integrity and modulate keratinocyte adhesion, proliferation, migration, and gene expression (Fusenig, 1994; Jones *et al*, 1995).

Manuscript received May 6, 2002; revised August 22, 2002; accepted for publication August 26, 2002

Reprint requests to: Dr Jonathan A. Garlick, Department of Oral Biology and Pathology, School of Dental Medicine, SUNY at Stony Brook, Stony Brook, New York 11794-8702, USA. Email: jgarlick@notes.cc.sunysb.edu

Abbreviations: BrdU, bromodeoxyuridine; LI, labeling index

Epithelial basement membranes are composed of an intricate network of extracellular matrix proteins that interact at the epithelial–stromal interface (Christiano and Uitto, 1996). Interactions between the major constituents of basement membrane, including types IV and VII collagens, several members of the laminin family (laminins 1, 5, 6, and 7) and nidogen, mediate basement membrane stability and adhesion through complex molecular interactions. For example, laminin 5 within anchoring filaments links a6ß4 integrin to type VII collagen to promote epithelial attachment mediated by hemidesmosomes (Rousselle *et al*, 1997), whereas laminin 5 complexed to laminins 6 and 7 interacts with a3ß1 to contribute to basement membrane assembly and stabilization (Champliaud *et al*, 1996; Dipersio *et al*, 1997). Interactions between type IV collagen and ß1 integrins (Fleischmajer *et al*, 1997), as well as those between these integrins and laminins (Fleischmajer *et al*, 1998), have been shown to provide an early scaffold for basement membrane organization. Deposition and assembly of basement membrane is thought to occur concurrently with the normalization of epithelial growth, morphogenesis, and differentiation (Bohnert *et al*, 1986; Marinkovich *et al*, 1993); however, mechanisms of basement membrane assembly that are mediated by epithelial and mesenchymal factors and the concomitant regulation of epidermal phenotype remain unclear.

The integrated events that occur during basement assembly need to be studied in biologic systems in which a high degree of

0022-202X/03/$15.00 ·

tissue complexity can be achieved. For example, whereas the synthesis of basement membrane components by keratinocytes and fibroblasts has most commonly been studied in monolayer cultures (Stanley *et al*, 1982; Bohnert *et al*, 1986; Woodley *et al*, 1988; Olsen *et al*, 1989), keratinocytes do not express their differentiated phenotype and signals from a structured extracellular matrix are not present in these cultures. To overcome this limitation, three-dimensional organotypic cultures, which mimic many of the *in vivo* features of human skin, have been used to investigate the role of epithelial–mesenchymal cross-talk in epidermal biology (Marinkovich *et al*, 1993; Zieske *et al*, 1994; Fleischmajer *et al*, 1998; Smola *et al*, 1998b; Hildebrand *et al*, 2002); however, the dynamics of basement membrane assembly have not been fully explored due to the failure of organotypic cultures to demonstrate morphologically identifiable basement membrane (Prunieras *et al*, 1983; Bohnert *et al*, 1986; Grinnell *et al*, 1986; O'Keefe *et al*, 1987; Contard *et al*, 1993; Ohji *et al*, 1994). As intact basement membrane is known to be a critical signal for the normal control of epidermal growth and differentiation (Stoker *et al*, 1990; Fleischmajer *et al*, 1993; Marinkovich *et al*, 1993), it is important to generate organotypic tissues that can develop normalized basement membrane structure.

In this study, we have optimized the growth and differentiation of skin-like, organotypic cultures by combining the two components thought to be critical in the normalization of epidermal homeostasis: dermal fibroblasts and basement membrane. These organotypic cultures allow us to ask how basement membrane components and/or dermal fibroblasts direct the assembly and organization of structured basement membrane and the concomitant normalization of epidermal phenotype. This was accomplished by growing keratinocytes on an acellular, human dermal substrate (AlloDerm) that was repopulated with human fibroblasts. We have found that organotypic cultures grown with dermal fibroblasts on pre-existing basement membrane components demonstrated a high degree of tissue normalization and formed a structured, mature basement membrane. In contrast, keratinocytes grown in the absence of pre-existing basement membrane components were well-stratified, but did not form structured basement membrane and showed aberrant tissue organization. In the absence of dermal fibroblasts, basement membrane assembly occurred at discrete initiation sites, as long as pre-existing basement membrane components were present. Maturation of well-structured basement membrane was found to be associated with the linear deposition of the receptor-ligand pair in hemidesmosomes, laminin 5 and α6 integrin. Furthermore, sustained keratinocyte growth required both intact basement membrane and dermal fibroblasts, whereas normalized tissue differentiation was independent of these components. This novel human tissue model recapitulates the morphology of the *in vivo* tissue to a large degree and has facilitated further clarification of the contributions made by basement membrane components and dermal fibroblasts to normal epidermal morphogenesis.

MATERIALS AND METHODS

Monolayer cell culture Normal human epidermal keratinocytes were cultured from newborn foreskin by the method of Rheinwald and Green (1975) in keratinocyte medium described by Wu *et al* (1982). Cultures were established through trypsinization of foreskin fragments and grown on irradiated 3T3 fibroblasts. 3T3 cells were maintained in Dulbecco's modified Eagle's medium containing 10% bovine calf serum. Human dermal fibroblasts were derived from foreskins and grown in media containing Dulbecco's modified Eagle's medium and 10% fetal calf serum. All animal experiments were approved by SUNY at Stony Brook's IACUC and were performed in compliance with stipulations of that body.

Organotypic culture Organotypic cultures grown in the absence of pre-existing basement membrane components ("collagen raft" cultures) were prepared as previously described (Vaccariello *et al*, 1999). Briefly, early passage human dermal fibroblasts were added to neutralized type I collagen (Organogenesis, Canton, Massachusetts) to a final concentration of 2.5×10^4 cells per mL. Three milliliters of this mixture was added to each 35 mm well insert of a six-well plate and incubated for 4–6 d in media containing Dulbecco's modified Eagle's medium and 10% fetal calf serum, until the collagen matrix showed no further shrinkage. At this time, a total of 5×10^5 normal human epidermal keratinocytes were seeded directly on the contracted collagen gel. Organotypic cultures were grown in the presence of pre-existing basement membrane components ("AlloDerm cultures") by seeding keratinocytes on AlloDerm, a de-epidermalized, acellular cadaver dermis derived from human skin, which was treated to remove the surface epithelium and stromal cells while still retaining basement membrane components on its surface (LifeCell Corp., Branchburg, New Jersey). This de-epidermalized dermis was layered on the contracted collagen gel described above with the basement membrane facing up, and fibroblasts migrated from the gel below into the AlloDerm. Cultures were prepared in the absence of fibroblasts by incubating contracted collagen gels with distilled water for 3 h. Cultures were maintained submerged in low calcium epidermal growth media for 2 d, submerged for 2 d in normal calcium epidermal growth media and raised to the air–liquid interface by feeding from below with normal calcium cornification medium for an additional 3–10 d (Vaccariello *et al*, 1999). Cultures were maintained for 2, 9, and 14 d and were performed in triplicate. For proliferation assays, bromodeoxyuridine (BrdU) (Sigma, St Louis, MO) was added to organotypic cultures 8 h prior to harvesting at a final concentration of 10 μM.

Immunofluorescence Specimens were frozen in embedding media (Triangle Biomedical, Durham, North Carolina) in liquid nitrogen vapors after being placed in 2 M sucrose for 2 h at 4°C. Tissues were serial sectioned at 6 μm and mounted on to gelatin-chrome alum-coated slides. Tissue sections were washed with phosphate-buffered saline and blocked with 10 μg goat IgG per mL, 0.05% goat serum, and 0.2% bovine serum albumin, vol/vol in phosphate-buffered saline without fixation. Sections were incubated with monoclonal antibodies to laminin 5 (GB-3, Gift of Dr G. Meneguzzi), α6 integrin subunit (G0H3) (Chemicon International Inc., Temecula, California), BrdU (Boehringer Mannheim, Indianapolis, Indiana) and filaggrin (Biomedical Technologies Inc., Stoughton, Massachusetts) and detected with Alexa 594™-conjugated goat anti-rat or anti-mouse IgG (Molecular Probes, Eugene, Oregon). Slides were coverslipped with Vectashield containing 1 μg per mL DAPI (Vector Laboratories, Burlingame, California). Fluorescence was visualized using a Nikon Eclipse 600 microscope and photomicroscopy was performed using a Texas Red filter. For routine light microscopy, tissues were fixed in 10% neutral buffered formalin, embedded in paraffin, and 4 μm sections were stained with hematoxylin and eosin.

Transmission electron microscopy Organotypic cultures were cut into small pieces of approximately 2×2 mm and fixed in 2% glutaraldehyde in 0.1 M cacodylate and 0.1 M sucrose at pH 7.2. The samples were then postfixed in 2% osmium tetroxide in 0.1 M cacodylate and 1% tannic acid in 0.1 M cacodylate. Following fixation the samples were dehydrated in graded ethanol, cleared with propylene oxide and infiltrated with Spurr's resin. Following polymerization of the resin, thick sections were produced using a Reichert Ultracut E microtome and sections were stained with toluidine blue to determine orientation. The blocks were then thin sectioned at approximately 90 nm and mounted on copper grids. Grids were stained with 5% uranyl acetate in deionized water and Reynold's lead citrate. Stained grids were examined at various magnifications using a Hitachi H-600 transmission electron microscope (Hitachi, Brisbane CA, USA).

RESULTS

Basement membrane components and dermal fibroblasts optimize epidermal morphogenesis The organotypic tissue model was fabricated by growing human keratinocytes on an acellular, human dermal substrate (AlloDerm) that was repopulated with human fibroblasts that migrated into the dermis from an underlying contracted collagen gel (**Fig 1*A***). Keratinocytes grown on AlloDerm generated an epithelium with an *in vivo*-like tissue architecture after 9 d (**Fig 1*B***). In the presence of fibroblasts. These cultures demonstrated an orthokeratinized epithelium with polarized, columnar basal cells nested in rete pegs and well-formed spinous and granular layers (**Fig 1*B***, layer A). The upper part of the connective tissue showed papillary dermis composed of a fine, collagenous network (**Fig 1*B***, layer B1) and the lower reticular dermis composed of denser collagen bundles (**Fig 1*B***, layer B2). Fibroblasts seeded

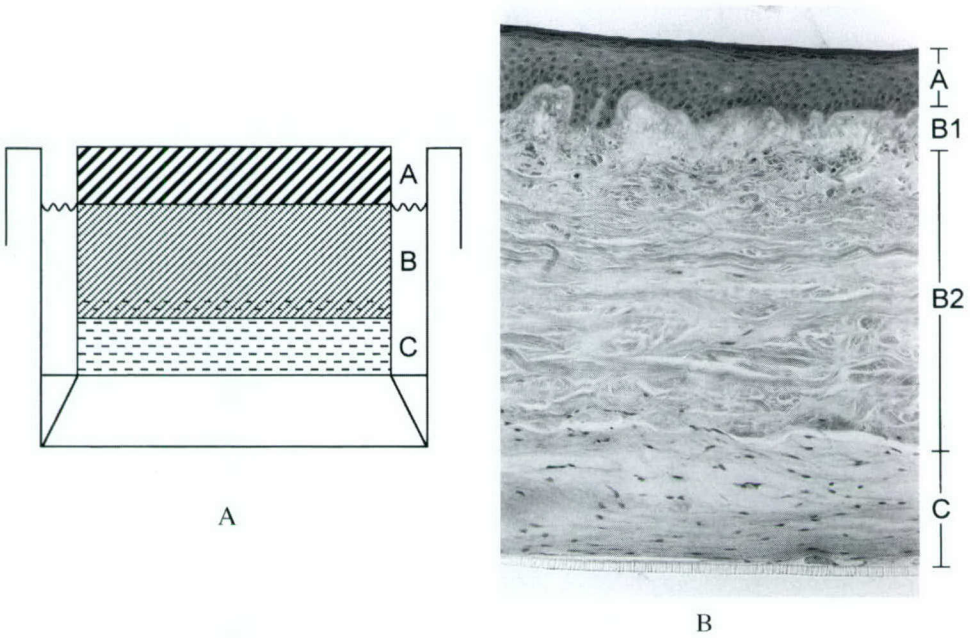

Figure 1. Schematic representation of the AlloDerm culture model and tissue morphology of AlloDerm cultures. As seen in (*A*), a type I collagen gel that contained dermal fibroblasts (*C*) was fabricated and allowed to contract for 7 d. AlloDerm, a de-epidermalized, acellular human dermis (*B*), was then laid on this gel to allow fibroblasts to migrate into the dermis. Twenty-four hours later, keratinocytes (*A*) were seeded on the pre-existing basement membrane components present on the surface of the AlloDerm. Cultures were submerged in media for 4 d and then grown at an air–liquid interface for either 3 or 10 additional days. "Collagen raft" cultures were grown directly on the collagen gel (*C*), without the intervening AlloDerm substrate. In (*B*), the morphologic components of the AlloDerm culture model are seen after 9 d in culture. An orthokeratinized stratified squamous epithelium is seen that shows polarized basal cells and rete pegs (*A*). Basal keratinocytes are resting on a papillary dermis composed of fine, collagen fibrils (*B1*) that is overlying a reticular dermis containing dense collagen bundles (*B2*). Beneath the dermis is the contracted, type I collagen gel, which was seeded with fibroblasts (*C*). Fibroblasts have migrated from the gel into the dermis. The polycarbonate membrane that supports these cultures is seen under the collagen gel.

into the contracted type I collagen gel (**Fig 1*B***, layer C) repopulated the AlloDerm by migrating into its lower surface. AlloDerm tissues have been found to retain the pre-existing basement membrane components types IV and VII collagen and laminin 1 on their upper surface (data not shown). In the absence of fibroblasts, keratinocytes cultured for 9 d in AlloDerm cultures, showed a thin epithelium that demonstrated all morphologic strata (**Fig 2*A***). In comparison, the incorporation of fibroblasts (**Fig 2*B***, *arrows*) into these cultures resulted in a fully stratified epithelium, which showed normal morphologic differentiation and tissue architecture (**Fig 2*B***). A considerably thinner epithelium demonstrating less prominent morphologic strata was seen when cultures were grown without fibroblasts and without pre-existing basement membrane components (collagen raft cultures) for 9 d (**Fig 2*C***). These cultures demonstrated altered tissue architecture that was characterized by flattened basal cells and a lack of clear transition between morphologic strata. In contrast, cultures grown without basement membrane components but with fibroblasts for 9 d showed a well-stratified epithelium (**Fig 2*D***). The lower layers of this epithelium showed altered tissue organization, however, suggesting that pre-existing basement membrane components present in the AlloDerm were needed to polarize basal keratinocytes and achieve optimal tissue architecture.

When grown on AlloDerm with fibroblasts for 14 d, the epithelium continued to mature and showed a well-polarized basal layer and surface hyperorthokeratosis (**Fig 2*F***). In contrast, the epithelium remained thin when AlloDerm cultures were grown without fibroblasts for 14 d (**Fig 2*E***), suggesting that little growth had occurred beyond day 9 in cultures grown without fibroblasts. Alterations in morphology were evident in 14 d cultures grown without fibroblasts or basement membrane components (**Fig 2*G***). In these cultures, basal cells were widely spaced and flattened, the surface layer was parakeratotic and no clear transition between morphologic strata could be identified. Tissue stratification improved when these cultures were grown in the presence of fibroblasts for 14 d but the tissue remained highly disorganized (**Fig 2*H***). A summary of the morphologic findings for all cultures is seen in **Table I**. These findings demonstrated that the presence of both pre-existing basement membrane components and dermal fibroblasts were required to generate an epithelium with optimal morphology and tissue organization. Dermal fibroblasts were needed to support full stratification, whereas basement membrane components were required to improve tissue architecture.

Pre-existing basement membrane components direct the assembly of structured basement membrane The ultrastructural appearance of the basement membrane zone in organotypic cultures grown with and without fibroblasts and/or pre-existing basement membrane components was studied by transmission electron microscopy (**Fig 3**). No lamina densa or basement membrane structure was seen when collagen rafts were grown with fibroblasts for 9 d (**Fig 3*A***). The dermal–epidermal interface of these cultures showed electron-dense condensations that did not display structural features of hemidesmosomes (**Fig 3*A***, *arrows*). In contrast, cultures grown for 9 d on AlloDerm with fibroblasts demonstrated extended stretches of lamina densa (**Fig 3*B***). Isolated areas showed hemidesmosomes, consisting of inner and outer plaques associated with keratin filaments intracellularly (**Fig 3*B***, *inset, white arrow*) and fine bridging structures representing anchoring filaments on their extracellular surface (**Fig 3*B***, *inset, black arrows*). When grown in the absence of fibroblasts for 9 d, however, AlloDerm cultures did not show a continuous lamina densa, but rather demonstrated evenly spaced hemidesmosomes (**Fig 3*C***). Under higher magnification, these regions showed focal areas of lamina densa and hemidesmosomes (**Fig 3*C***, inset), which were adjacent to keratin filament bundles intracellularly (**Fig 3*C***, *inset, white arrows*) and filamentous structures that spanned to the lamina densa (**Fig 3*C***, *inset, black arrow*). Further maturation of basement

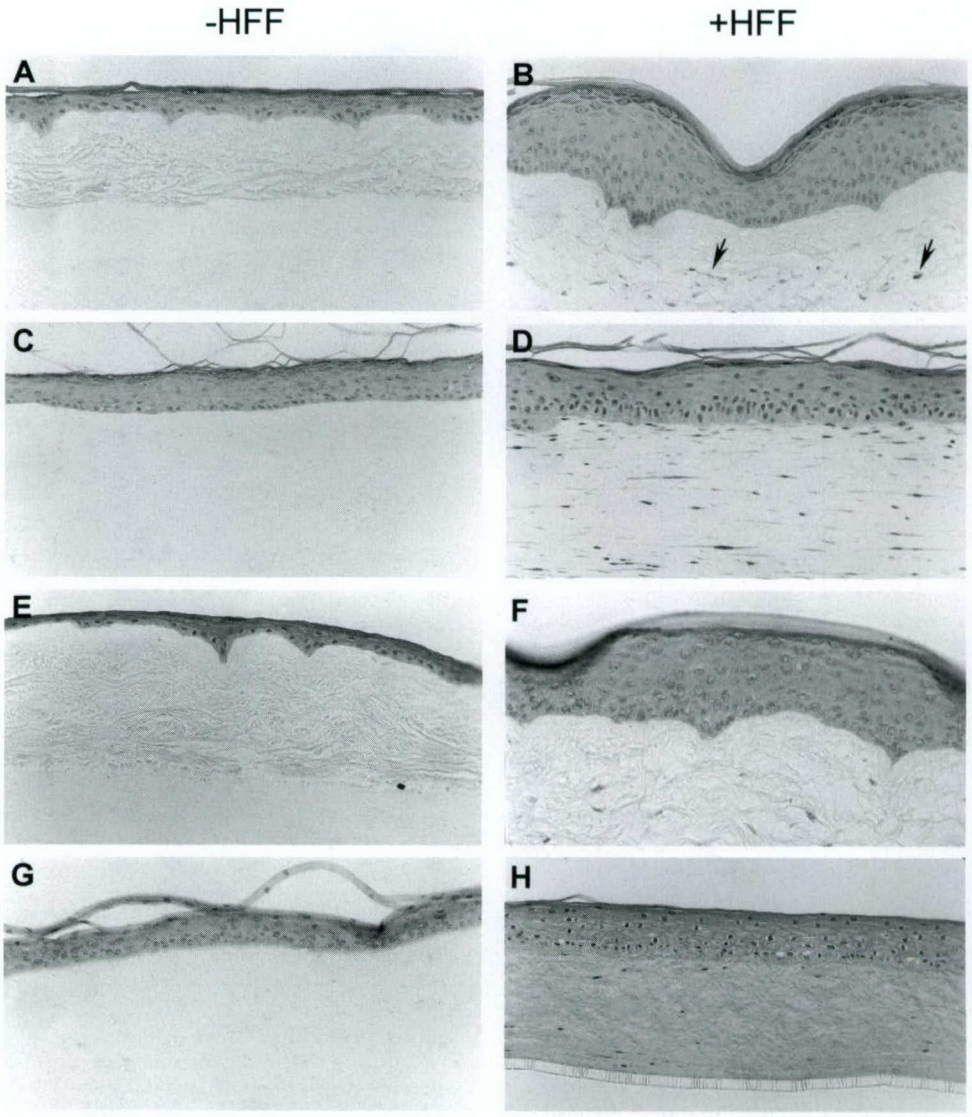

Figure 2. Morphogenesis of stratified squamous epithelium in the presence or absence of pre-existing basement membrane components and dermal fibroblasts. Keratinocytes were grown in organotypic culture for either 9 d (*A–D*) or 14 d (*E–H*) in the absence (*C,D,G,H*) or presence (*A,B,E,F*) of pre-existing basement membrane components. In the presence of basement membrane components and fibroblasts, a fully stratified epithelium was seen that demonstrated normal morphologic differentiation and tissue architecture (*B,F*), whereas cultures were considerably thinner without fibroblasts (*A,E*). In the absence of pre-existing basement membrane components, cultures underwent greater stratification with fibroblasts (*D*) than without fibroblasts (*C*), but both conditions showed altered tissue architecture characterized by disorganization of basal cells. These architectural alterations were more evident in 14 d cultures (*G,H*).

membrane structure was seen by the presence of a more continuous lamina densa in AlloDerm cultures grown for 14 d without fibroblasts (**Fig 3*D***). Hemidesmosomes were seen at regularly spaced intervals (**Fig 3*D***, *dark arrows*) and anchoring fibrils were seen adjacent to the lamina densa (**Fig 3*D***, *white arrow*). This demonstrated that, whereas fibroblasts could accelerate basement membrane maturation, they were not required for the development of structured basement membrane as long as pre-existing basement membrane components were present. Cultures grown in the presence of fibroblasts for 14 d showed a lamina densa that was more electron dense and continuous than that seen in 9 d AlloDerm cultures with fibroblasts (**Fig 3*E***). Interestingly, the electron-dense material of the lamina densa in these 9 and 14 d AlloDerm cultures was similar to that seen on the surface of AlloDerm that was analyzed after it was prepared and not placed in culture (**Fig 3*F***). This suggested that basement membrane organization took place on this surface, which served as a structural template for the assembly of basement membrane. It was concluded that pre-existing basement membrane components, but not dermal fibroblasts, were required for the assembly of structured basement membrane and hemidesmosomes. As seen in collagen raft cultures, however, the presence of fibroblasts alone was not permissive for the generation of a structured basement membrane.

Normalized deposition of hemidesmosomal components is dependent upon pre-existing basement membrane components and is accelerated by dermal fibroblasts The role of basement membrane components and dermal fibroblasts in the assembly of basement membrane was also characterized by determining the distribution of laminin 5 and its receptor, $\alpha 6\beta 4$ integrin, by immunohistochemical stain. Basement membrane normalization was assessed by the degree to which these proteins were deposited in a polarized, linear pattern at the basement membrane zone. In the absence of dermal fibroblasts, 9 d AlloDerm cultures demonstrated a patchy, discontinuous deposition of laminin 5 at the dermal–epidermal interface (**Fig 4*A***). In contrast, cultures grown on AlloDerm in the presence of fibroblasts for 9 d demonstrated continuous and

Table I. Summary of morphology, basement membrane components, and assembly, growth, and differentiation of organotypic epithelia

	+ BM + HFF		+ BM − HFF		− BM + HFF		− BM − HFF	
	9d	14d	9d	14d	9d	14d	9d	14d
Tissue stratification	*****	*****	**	**	***	***	**	**
Tissue architecture	normal	normal, well-polarized basal cells	normal	normal	aberrant, loss of polarity	aberrant	aberrant, flat basal cell layer	aberrant, flat basal cell layer, parakeratin
Basement membrane assembly	+ HD + LD[a]	+ HD + LD[a]	+ HD + LD[b]	+ HD + LD[a]	− HD − LD	ND	ND	ND
Laminin 5	linear	linear	patchy	linear	patchy	patchy	patchy/pc	patchy/faint
α6 integrin	linear	linear	linear/pc/sb	linear	patchy	linear/pc	linear/pc	patchy/faint
Filaggrin	+++	+++	++	+++	+++	++	+++	++
Brdu (LI)	43%	18%	18%	0%	26%	0%	24%	0%

BM – basement membrane, HFF – human foreskin fibroblasts.
***** – full stratification, *** – moderate stratification, ** – little stratification.
HD – hemidesmosome, LD – Lamina densa. [a]linear, [b]focal.
pc – pericellular staining only, sb – suprabasal staining.
ND – not determined.
+++ – strong staining, ++ – moderate staining.

linear deposition of laminin 5 that was strictly polarized along the basement membrane zone (**Fig 4*B***). This suggested that the normalized deposition and organization of laminin 5 was accelerated when fibroblasts were incorporated into AlloDerm cultures. In contrast, a discontinuous pattern of laminin 5 deposition was seen for cultures grown on collagen rafts in the absence of pre-existing basement membrane components both without or with fibroblasts. In the absence of fibroblasts, laminin 5 was limited to the cytoplasm of basal cells and was not deposited in the basement membrane zone after 9 d (**Fig 4*C***). The addition of fibroblasts to these cultures resulted in the extracellular deposition of laminin 5, but the staining distribution remained punctate and discontinuous (**Fig 4*D***).

Even in the absence of fibroblasts, AlloDerm cultures showed a polarized and linear distribution of laminin 5 after 14 d (**Fig 4*E***). This supports the view that normalized laminin 5 deposition and basement membrane formation did not require dermal fibroblasts, as long as keratinocytes were grown on an interface containing pre-existing basement membrane proteins. In contrast, cultures grown without basement membrane components but with fibroblasts for 14 d continued to show patchy deposition of laminin 5 (**Fig 4*G,H***). When these cultures were grown without fibroblasts, only faint laminin 5 staining was seen, suggesting that this protein had been degraded in the absence of fibroblasts (**Fig 4*G***). It appears that, whereas laminin 5 was synthesized in the absence of pre-existing basement membrane components, these components were needed to direct the deposition of laminin 5 into the assembling basement membrane.

The distribution of the a6 integrin subunit closely paralleled that of laminin 5 (**Table I**). Cultures grown on AlloDerm without fibroblasts for 9 d demonstrated staining that was both linear, yet pericellular in the suprabasal layers (**Table I**). Five days later (day 14), cultures grown without fibroblasts showed further basement membrane maturation as evidenced by the restriction of a6 integrin to a linear and polarized distribution at the basement membrane zone (**Fig 4*I***). This linear pattern was similar to that seen when cultures were grown in the presence of pre-existing basement membrane proteins and dermal fibroblasts, both at 9 d (**Table I**) and 14 d (**Fig 4*J***), suggesting that the presence of dermal fibroblasts accelerated the normalized distribution of this protein. In contrast, cultures grown in the absence of pre-existing basement membrane components demonstrated a pericellular distribution of α6 subunit without fibroblasts and a patchy, extracellular deposition with fibroblasts (**Table I**). These findings demonstrated that the spatial and temporal deposition of laminin 5 and a6 integrin were similar during the maturation of the basement membrane. Thus, the normalized deposition of this integrin-ligand pair was fibroblast independent, but required the presence of pre-existing basement membrane components. The progressive maturation of basement membrane seen by the transition from the pericellular and patchy, to the linear, polarized deposition of these components in AlloDerm cultures, closely matched the temporal sequence of events through which ultrastructural assembly of basement membrane occurred.

Sustained keratinocyte growth requires fibroblasts and basement membrane, whereas normalized differentiation is fibroblast independent Growth of keratinocytes in organotypic cultures was determined by measuring the percentage of basal cells that incorporated BrdU during a 8 h pulse [labeling index (LI)]. Two day after seeding, keratinocyte cultures demonstrated elevated levels of proliferation regardless of the presence of dermal fibroblasts or basement membrane components (**Fig 5**). These cultures showed LI between 28 and 36%, suggesting that the initial growth of keratinocytes was independent of mesenchymal stimulation. Only keratinocytes cultured in the presence of AlloDerm and fibroblasts, however, were able to maintain proliferative activity after 14 d in culture. Keratinocytes grown directly on collagen rafts, with or without fibroblasts, as well as cells grown on AlloDerm without fibroblasts, showed a 1.5–2-fold decrease in LI after 9 d and nearly complete suppression of growth 14 d after seeding (**Fig 5**). In contrast, AlloDerm cultures grown for 14 d with fibroblasts showed a LI that continued to decrease to a range that was more similar to that seen *in vivo*, suggesting that full maturation of basement membrane structure was coupled to the normalization of keratinocyte growth. This demonstrated that the presence of both structured basement membrane and dermal fibroblasts were required to sustain keratinocyte growth in organotypic culture.

Normalization of keratinocyte differentiation was independent of dermal fibroblasts and basement membrane. When grown with fibroblasts for 9 d and 14 d, filaggrin was expressed in the upper third of the epithelium in a pattern similar to that seen in human skin. This was the case for both AlloDerm cultures grown for 9 d (**Fig 6*A***) and 14 d (**Fig 6*B***) and for collagen raft cultures grown for 9 d (**Fig 6*C***). In the absence of dermal fibroblasts, AlloDerm cultures (**Fig 6*D,E***) and collagen raft cultures (**Fig 6*F***) grown for 9 and 14 d were considerably thinned, but demonstrated a normal pattern of filaggrin distribution. These findings showed that sustained keratinocyte growth was dependent on the presence of both structured

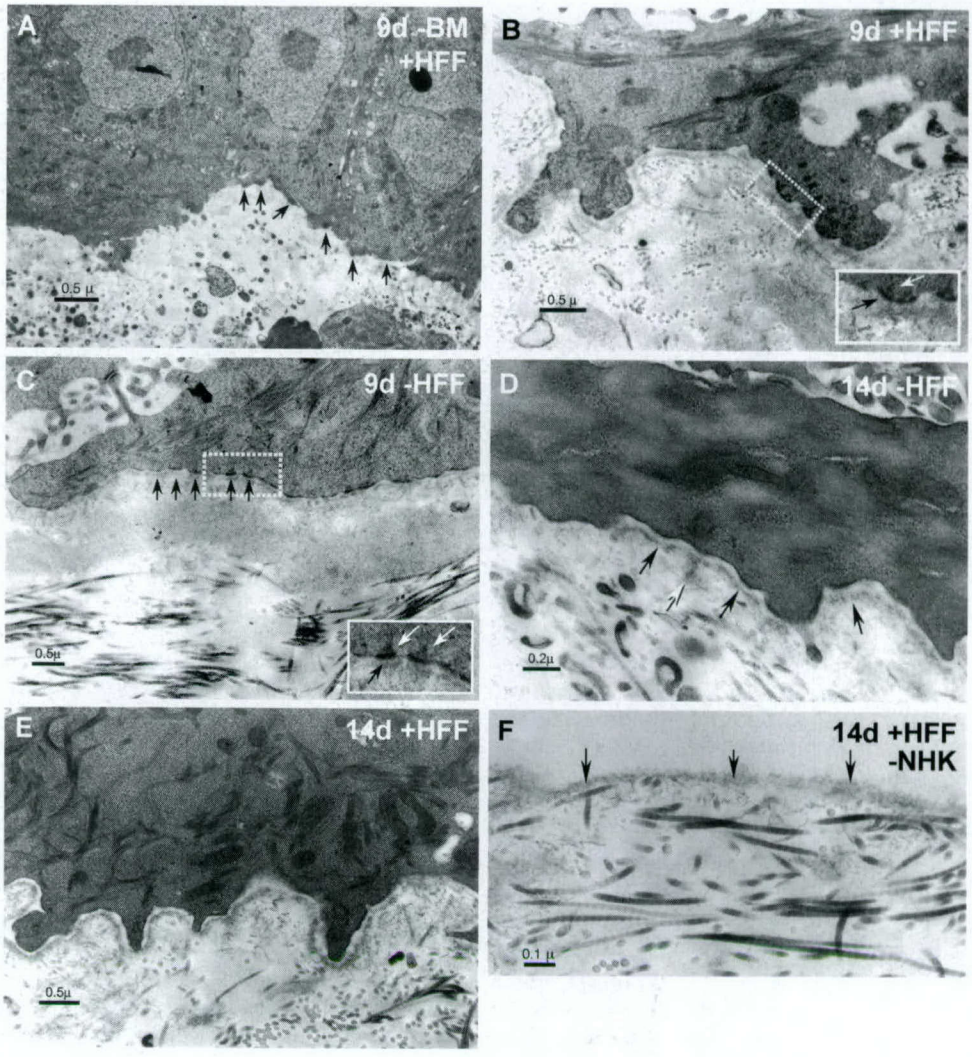

Figure 3. Ultrastructural assembly of the basement membrane zone in organotypic cultures. Cultures grown either in the absence (*A*) or presence of pre-existing basement membrane components (*B–E*) were studied after 9 d (*A–C*) and 14 d (*D,E*). Cultures were grown either with both keratinocytes and fibroblasts (*A,B,E*) or with keratinocytes and no fibroblasts (*C,D*). AlloDerm was also analyzed after it was freshly prepared without growing it in culture (*F*). Electron-dense condensations are seen in the absence of pre-existing basement membrane components (*A, arrows*) but no other basement membrane structures were seen (*A*). Lamina densa and hemidesmosomes were seen in (*B*), as evidenced by electron-dense plaques (*inset*) showing intracellular (*white arrow*) and extracellular (*black arrow*) filamentous structures. Focal areas of well-organized lamina densa and hemidesmosomes were seen in (*C*) (*black arrows*). Under higher magnification, these areas showed regularly spaced, electron-dense plaques (*inset*), which were associated with intracellular bundles of keratin filaments (*inset, white arrow*) and filamentous structures, which extended to the lamina densa (*inset, black arrow*). A more continuous basement membrane demonstrating anchoring fibrils (*white arrow*) and hemidesmosomes (*black arrow*) were seen in (*D*), whereas a continuous lamina densa was seen in (*E*). Electron-dense material was seen on the upper surface of freshly prepared AlloDerm, which was not used in cultures (*F, arrows*).

basement membrane and dermal fibroblasts, whereas normalized differentiation was independent of both of these microenvironmental factors.

DISCUSSION

We have developed novel organotypic cultures of human stratified squamous epithelium to investigate how microenvironmental factors such as pre-existing basement membrane components and dermal fibroblasts direct the organization, assembly, and maturation of basement membrane and modulate epidermal phenotype. Using these engineered human tissues, we have found that these components play a co-ordinated part in the generation of a well-structured basement membrane, regulate keratinocyte growth and differentiation, and normalize epithelial tissue architecture. In the absence of pre-existing basement membrane components such as laminin 1 and type IV and VII collagen, fibroblasts were not sufficient to generate structured basement membrane or to normalize epithelial phenotype. When these proteins were present at the time keratinocytes were seeded (AlloDerm cultures), a well-structured basement membrane formed both with and without dermal fibroblasts. The incorporation of fibroblasts into the AlloDerm cultures accelerated basement membrane assembly, sustained keratinocyte growth, and normalized epidermal tissue architecture. We have achieved this by repopulating an acellular human dermis with viable fibroblasts that migrated from an underlying contracted type I collagen gel. This novel, human tissue model recapitulates the morphology of the *in vivo* tissue to a large degree and contributes to our understanding of the role of epithelial–mesenchymal cross-talk in the normalization of basement membrane structure and the morphogenesis of human skin.

Our ultrastructural and immunohistochemical evidence clearly point to the rapid assembly of basement membrane when keratinocytes were cultured on AlloDerm that was repopulated with fibroblasts. Structured basement membrane was seen at 9 d as a nearly continuous lamina densa and was paralleled by the linear and polarized distribution of laminin 5 and the α6 integrin subunit. In the absence of fibroblasts, basement membrane assembly

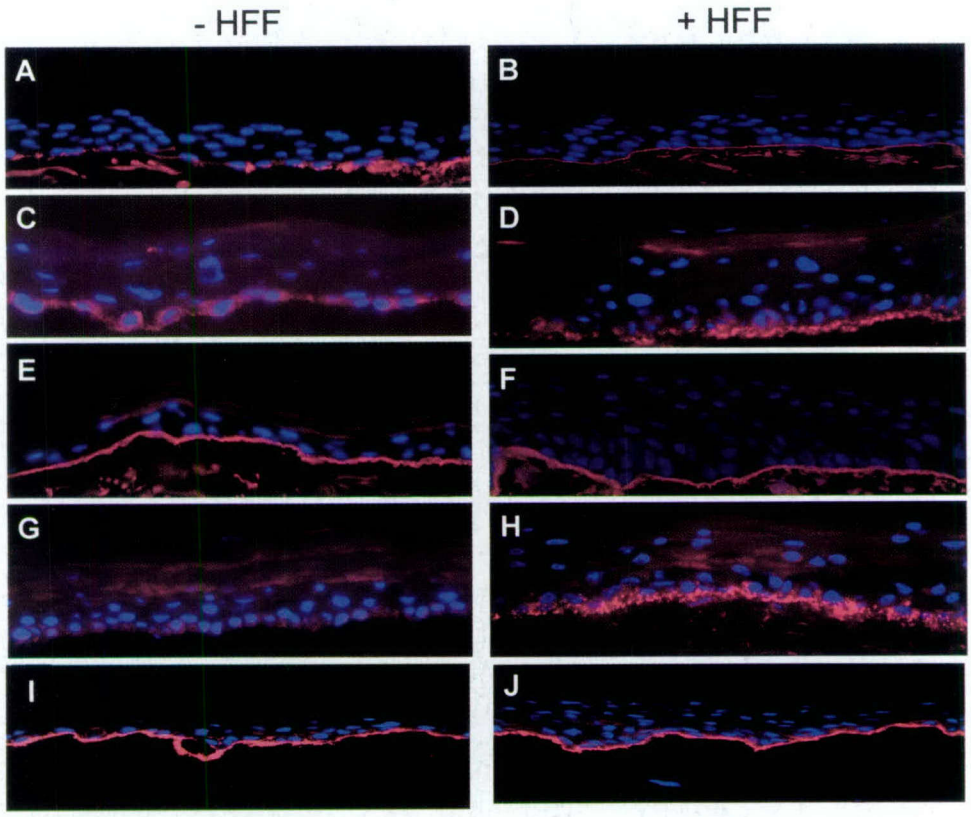

Figure 4. Pre-existing basement membrane components and fibroblasts enhance the deposition and polarization of laminin 5 and the a6 integrin subunit. Immunofluorescent stain for laminin 5 was performed on 9 and 14 d organotypic cultures in the presence of pre-existing basement membrane components with (*B,F*) and without (*A,E*) fibroblasts and in the absence of pre-existing basement membrane with (*D,H*) and without (*C,G*) fibroblasts. Staining for the a6 integrin subunit was performed on 14 d organotypic cultures in the presence of pre-existing basement membrane components with (*J*) and without (*I*) fibroblasts. Nine day cultures grown in the presence of pre-existing basement membrane without fibroblasts (*A*) demonstrated a patchy, discontinuous pattern of laminin 5 compared with cultures grown in the presence of fibroblasts (*B*), which showed continuous and linear deposition of laminin 5. Linear deposition was seen in 14 d cultures that contained pre-existing basement membrane components grown both with (*F*) or without (*E*) fibroblasts. In contrast, cultures grown in the absence of pre-existing basement membrane components with (*D,H*) and without (*C,G*) fibroblasts demonstrated laminin 5 expression that was discontinuous and pericellular at both 9 and 14 d. The linear deposition of a6 integrin subunit was seen in a pattern similar to laminin 5 when 14 d cultures were grown without (*I*) and with (*J*) fibroblasts in the presence of pre-existing basement membrane components.

was initially seen as regularly spaced areas of lamina densa adjacent to hemidesmosomes, which may represent nucleation sites for basement membrane assembly. The patchy, but linear distribution of laminin 5 and α6 integrin seen by immunohistochemical stain supports the view that initial basement membrane organization can occur at discrete sites (Fleischmajer *et al*, 1998). It is thought that formation of structured basement membrane is a self-assembly process (Smola *et al*, 1998b; Colognato and Yurchenco, 2000), which occurs as the local concentration of basement membrane proteins reaches a critical threshold and enables these components to interact physically (Yurchenco and O'Rear, 1994). Marinkovich *et al* (1993) have shown that fibroblasts play a part in this process by secreting proteins that reorganize the extracellular matrix or stabilize previously assembled basement membrane. This study showed that when grown in organotypic culture with human foreskin keratinocytes, dermal fibroblasts synthesized and deposited three major components of basement membrane: laminin 1 and collagen types IV and VII (Marinkovich *et al*, 1993). It has been shown that these components need to be assembled prior to the formation of a mature basement membrane in order to bind to cell surface integrins and serve as nucleation sites for the self-assembly of basement membrane (Fleischmajer *et al*, 1998).

Our finding of discrete sites of basement membrane organization in the absence of fibroblasts strongly suggests that the pre-existing basement membrane components present on AlloDerm cultures provided a template on which basement membrane development could rapidly occur. It has recently been shown that hemidesmosomes form around pre-existing anchoring fibrils when foreskin keratinocytes were grown on a de-epidermalized bovine tongue connective tissue without fibroblasts (Hildebrand *et al*, 2002). Similarly, cell suspensions (Friend *et al*, 1982) and viable sheets of adult rabbit corneal epithelium (Gipson *et al*, 1983; Payne *et al*, 2000) have been shown to assemble hemidesmosomes rapidly when grown on corneal stroma that contains intact basal laminae. It was found that hemidesmosome assembly occurred at sites where pre-existing anchoring fibrils inserted into the lamina densa, suggesting that these were likely nucleation sites for hemidesmosome organization (Gipson *et al*, 1983). We observed that no basement membrane assembly was seen when keratinocytes were grown in organotypic culture without pre-existing basement membrane components, even when fibroblasts were incorporated. Thus, the presence of these pre-existing basement membrane proteins provides an important permissive cue for the rapid formation and maturation of ultrastructurally complete basement membrane.

We have incorporated fibroblasts into our tissue model by facilitating their migration to repopulate a previously acellular dermis. These fibroblasts moved from the underlying contracted, type I collagen gel and were retained in the reticular dermis (Lee *et al*, 2000). We have shown that epidermal morphogenesis and growth were significantly compromised by the absence of dermal fibroblasts. Similarly, previous studies have shown that keratinocyte growth and differentiation were improved when fibroblasts were incorporated into dermal equivalents (Limat *et al*,

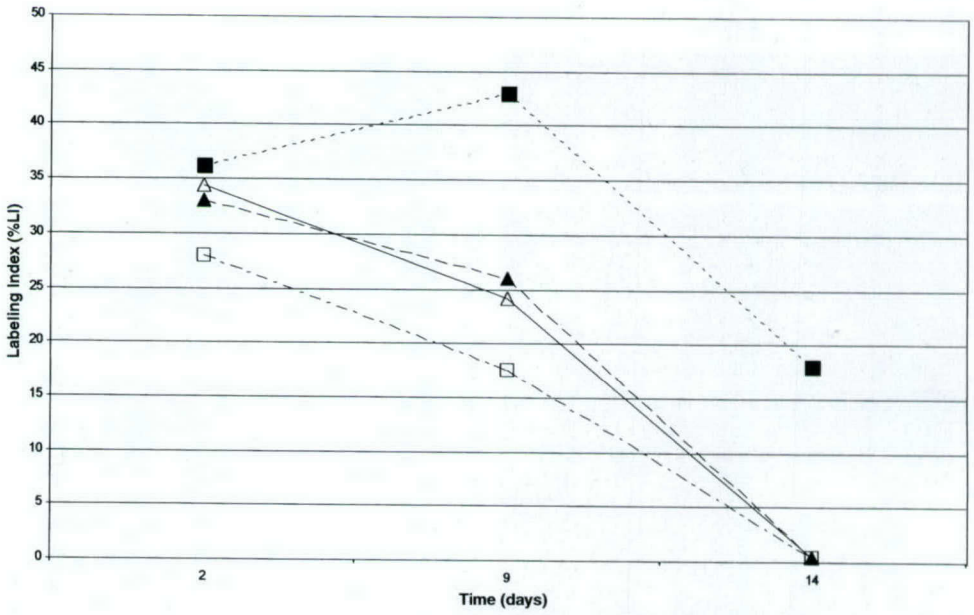

Figure 5. Keratinocyte growth is sustained by fibroblasts and basement membrane interactions. Organotypic cultures were grown for 2, 9, and 14 d and pulsed with 10 mM BrdU for their last 8 h. LI was determined by counting BrdU-positive, basal cell nuclei after immunohistochemical stain with an anti-BrdU antibody. Only cultures containing both assembled basement membrane and fibroblasts were able to sustain keratinocyte growth for 14 d (■ ... ■ ... ■). Cultures grown with fibroblasts and without basement membrane components (▲ ... ▲ ... ▲), without fibroblasts and with basement membrane components (△ ... △ ... △), and without either fibroblasts and basement membrane components (□ ... □ ... □) showed elevated growth initially, but no proliferative activity at 14 d.

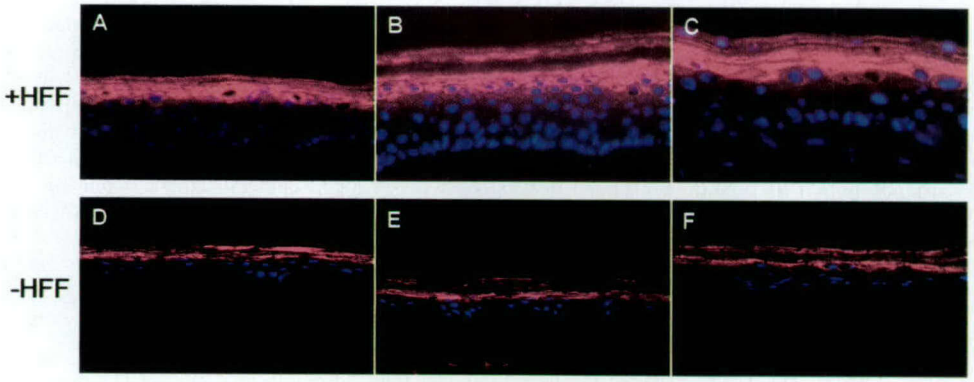

Figure 6. Differentiation of organotypic cultures is independent of pre-existing basement membrane components and dermal fibroblasts. Immunofluorescent stain for filaggrin demonstrated a normal pattern of expression limited to the stratum granulosum and stratum corneum when cultures were grown in the presence of fibroblasts both with (*A,B*) or without (*C*) pre-existing basement membrane components and when cultures were grown in the absence of fibroblasts with (*D,E*) or without (*F*) pre-existing basement membrane components.

1989; Rosdy and Clauss, 1990; Ponec and Kempenaar, 1995). In addition to the role of fibroblasts in the production of basement membrane components, it has been shown that diffusible factors produced by fibroblasts play a part in extracellular matrix metabolism and modulate keratinocyte production of basement membrane components (Smola *et al*, 1998b). This may help explain the more rapid assembly of basement membrane on AlloDerm grown in the presence of fibroblasts when compared with cultures from which fibroblasts were excluded. The cooperation between specific fibroblast-derived soluble factors and basement membrane assembly has recently been established (Li *et al*, 2001).

Organotypic tissue models have previously been adapted to study epithelial–mesenchymal interactions (Boxman *et al*, 1993; Smola *et al*, 1994; Berking and Herlyn, 2001) on a variety of connective tissue substrates that served as dermal equivalents. A well-stratified epithelium was seen when cultures were grown on dermal equivalents fabricated as type 1 collagen gels, which were populated with fibroblasts (Bell *et al*, 1981; Asselineau *et al*, 1989; Parenteau *et al*, 1991). Porous membranes seeded with fibroblasts or coated with extracellular matrix proteins have been used to generate skin-like organotypic cultures (Rosdy and Clauss, 1990). Alternatively, fibroblasts have been incorporated into a three-dimensional scaffold, where these cells could secrete and organize an extracellular matrix (Fleischmajer *et al*, 1998). Whereas organotypic cultures of stratified epithelium have been shown to express basement membrane components in organotypic culture (Prunieras *et al*, 1983; Bohnert *et al*, 1986; Grinnell *et al*, 1986; Contard *et al*, 1993; Ohji *et al*, 1994), limited success has been achieved in attaining structured basement membrane (Marinkovich *et al*, 1993; Zieske *et al*, 1994; Smola *et al*, 1998). As it is known that basement membrane components play a functional part in the regulation of epidermal growth and differentiation (Stoker *et al*, 1990), it is important to generate cultures that have a well-structured basement membrane. Furthermore, it has previously been shown that the correct spatial organization and polarity of basal cells was associated with functional hemidesmosomes and basement membrane integrity (Dowling *et al*, 1996). Our findings support these observations as only tissues with well-structured basement membrane showed optimal epithelial tissue architecture.

The goal of organotypic cultures of human skin is to fabricate and maintain a stratified epithelium that demonstrates *in vivo*-like features of epidermal morphology, growth, and differentiation (Berking and Herlyn, 2001). We have optimized these cultures by combining the two components thought to be critical in epidermal normalization: dermal fibroblasts and structured basement membrane. Dermal fibroblasts were required to stimulate stratification and accelerate basement membrane formation, whereas pre-existing basement membrane components were required to initiate and promote basement membrane assembly. Both of these microenvironmental factors were needed to sustain keratinocyte growth and optimize epithelial architecture. Our cultures demonstrated significantly improved basement membrane organization, stratification, growth, and differentiation when compared with cultures that lacked human fibroblasts, pre-existing basement membrane proteins or both of these components. This novel, composite culture system mimics the essential morphologic features of human skin to a high degree and demonstrates that this human culture model will be a valuable tool for future studies.

We would like to thank Sujata Pawagi, Michael Scalia, Heather Sawka, Nadav Segal, Lina Nguyen, and Larry Pfeiffer for technical assistance, Dr Lorne Taichman for critical comments, Jackie Garfield for performing transmission electron microscopy and to Karen Henrickson for preparation of illustrations. In addition, we thank Dr G. Meneguzzi for his generous gift of laminin 5 antibodies. This work was supported by grants no. DAMMD17-01-1-0688 from the US Army Medical Research and Materiel Command and no. 2RO1DE011250-06 from the National Institutes of Dental and Craniofacial Research.

REFERENCES

Asselineau D, Bernard BA, Bailly C, Darmon M: Retinoic acid improves epidermal morphogenesis. *Dev Biol* 133:322–335, 1989

Bell E, Ehrich P, Butte DJ, Nakatsuji T: Living tissue formed *in vitro* and accepted as skin-equivalent tissue of full thickness. *Science* 211:1052–1054, 1981

Berking C, Herlyn M: Human skin reconstruct models: A new application for studies of melanocyte and melanoma biology. *Histol Histopathol* 16:669–674, 2001

Bohnert A, Hornung J, Mackenzie IC, Fusenig NE: Epithelial–mesenchymal interactions control basement membrane production and differentiation in cultured and transplanted mouse keratinocytes. *Cell Tissue Res* 244:413–429, 1986

Boxman I, Lowik C, Aarden L, Ponec M: Modulation of IL-6 production and IL-1 activity by keratinocyte–fibroblast interaction. *J Invest Dermatol* 101:316–324, 1993

Champliaud MF, Lunstrum GP, Rousselle P, Nishiyama T, Keene DR, Burgeson RE: Human amnion contains a novel laminin variant, laminin 7, which like laminin 6, covalently associates with laminin 5 to promote stable epithelial-stromal attachment. *J Cell Biol* 132:1189–1198, 1996

Christiano AM, Uitto J: Molecular complexity of the cutaneous basement membrane zone: Revelations from the paradigms of epidermolysis bullosa. *Exp Dermatol* 5:1–11, 1996

Colognato H, Yurchenco PD: Form and function: The laminin family of heterotrimers. *Dev Dyn* 218:213–234, 2000

Contard P, Bartel RL, Jacobs L, *et al*: Culturing keratinocytes and fibroblasts in a three-dimensional mesh results in epidermal differentiation and formation of a basal lamina-anchoring zone. *J Invest Dermatol* 100:35–39, 1993

Dipersio CM, Hodivala-Dilke KM, Jaeniscld ED, Perlish R, Kreidberg JA, Hynes RO: α3β1 integrin is required for normal development of the epidermal basement membrane. *J Cell Biol* 137:729–742, 1997

Dowling J, Yu Q-C, Fuchs E: ß4 integrin is required for hemidesmosome formation, cell adhesion and cell survival. *J Cell Biol* 134:559–572, 1996

Fleischmajer R, Kuhn K, Sato Y, *et al*: There is temporal and spatial expression of alpha1 (IV), alpha2 (IV), alpha5 (IV), alpha6 (IV) collagen chains and beta1 integrins during the development of the basal lamina in an "*in vitro*" skin model. *J Invest Dermatol* 109:527–533, 1997

Fleischmajer R, MacDonald ED, Contard P, Perlish JS: Immunochemistry of a keratinocyte-fibroblast co-culture model for reconstruction of human skin. *J Histochem Cytochem* 41:1359–1366, 1993

Fleischmajer R, Utani A, MacDonald ED, *et al*: Initiation of skin basement membrane formation at the epidermo-dermal interface involves assembly of laminins through binding to cell membrane receptors. *J Cell Sci* 111 14:1929–1940, 1998

Friend J, Kinoshita S, Thoft RA, Eliason JA: Corneal epithelial cell cultures on stromal carriers. *Invest Ophthalmol Vis Sci* 23:41–49, 1982

Fusenig NE: Epithelial–mesenchymal interactions regulate keratinocyte growth and differentiation *in vitro*. In: Leigh I, Lane B, Watt F (eds). *The Keratinocyte Handbook*. Cambridge University Press, UK: 1994; p 71–97

Gipson IK, Grill SM, Spurr SJ, Brennan SJ: Hemidesmosome formation *in vitro*. *J Cell Biol* 97:849–857, 1983

Grinnell F, Takashima A, Lamke-Seymour C: Morphological appearance of epidermal cells cultured on fibroblast-reorganized collagen gels. *Cell Tissue Res* 246:13–21, 1986

Hildebrand HC, Hakkinen L, Wiebe CB, Larjava HS: Characterization of organotypic keratinocyte cultures on de-epithelialized bovine tongue mucosa. *Histol Histopathol* 17:151–153, 2002

Jones PH, Harper S, Watt FM: Stem cell patterning and fate in human epidermis. *Cell* 80:83–93, 1995

Lee DY, Ahn HT, Cho KHA: New skin equivalent model: dermal substrate that combines de-epidermized dermis with fibroblast-populated collagen matrix. *J Dermatol Sci* 23:132–137, 2000

Li X, Chen Y, Scheele S, Arman E, Haffner-Krausz R, Ekblom P, Lonai P: Fibroblast growth factor signaling and basement membrane assembly are connected during epithelial morphogenesis of the embryoid body. *J Cell Biol* 153:811–822, 2001

Limat A, Hunziker T, Boillat C, Bayreuther K, Noser F: Post-mitotic human dermal fibroblasts efficiently support the growth of human follicular keratinocytes. *J Invest Dermatol* 92:758–762, 1989

Marinkovich MP, Keene DR, Clytie SR, Burgeson RE: Cellular origin of the dermal-epidermal basement membrane. *Dev Dyn* 197:255–267, 1993

O'Keefe EJ, Woodley DT, Falk RJ, Gammon WR, Briggaman RA: Production of fibronectin by epithelium in a skin equivalent. *J Invest Dermatol* 88:634–639, 1987

Ohji M, SundarRaj N, Hassell JR, Thoft RA: Basement membrane synthesis by human corneal epithelial cells *in vitro*. *Invest Ophthalmol Vis Sci* 35:479–485, 1994

Olsen D, Nagayoshi T, Fazio M, *et al*: Human laminin: Cloning and sequence analysis of cDNAs encoding A, B1 and B2 chains, and expression of the corresponding genes in human skin and cultured cells. *Lab Invest* 60:772–782, 1989

Parenteau NL, Nolte CM, Bilbo P, *et al*: Epidermis generated *in vitro*: Practical considerations and applications. *J Cell Biochem* 45:245–251, 1991

Payne J, Gong H, Trinkhaus-Randall V: Tyrosine phosphorylation: A critical component in the formation of hemidesmosomes. *Cell Tissue Res* 300:401–411, 2000

Ponec M, Kempenaar J: Use of human skin recombinants as an in vitro model for testing the irritation potential of cutaneous irritants. *Skin Pharmacol* 8:49–59, 1995

Prunieras M, Regnier M, Fougere S, Woodley D: Keratinocytes synthesize basal-lamina proteins in culture. *J Invest Dermatol* 81:74s–81s, 1983

Rheinwald JG, Green H: Serial cultivation of strains of human epidermal keratinocytes: The formation of keratinocyte colonies from single cells. *Cell* 6:331–344, 1975

Rosdy M, Clauss L-C: Terminal epidermal differentiation of human keratinocytes grown in chemically defined medium on inert filter substrates at the air–liquid interface. *J Invest Dermatol* 95:409–414, 1990

Rousselle P, Keene DR, Ruggiero F, Champliaud MF, Rest M, Burgeson RE: Laminin 5 binds the NC-1 domain of type VII collagen. *J Cell Biol* 138:719–728, 1997

Smola H, Stark HJ, Thiekotter G, Mirancea N, Krieg T, Fusenig NE: Dynamics of basement membrane formation by keratinocyte–fibroblast interactions in organotypic skin culture. *Exp Cell Res* 239:399–410, 1998

Smola H, Thiekotter G, Baur M, Stark HJ, Breitkreutz D, Fusenig NE: Organotypic and epidermal-dermal cocultures of normal human keratinocytes and dermal cells: Regulation of transforming growth factor α, β1 and β2 mRNA levels. *Toxicol In Vitro* 8:641–650, 1994

Smola H, Thiekotter G, Fusenig NE: Mutual induction of growth factor gene expression by epidermal–dermal cell interaction. *J Cell Biol* 122:417–429, 1993

Stanley JR, Hawley-Nelson P, Yaar M, Martin GR, Katz SI: Laminin and bullous pemphigoid antigen are distinct basement membrane proteins synthesized by epidermal cells. *J Invest Dermatol* 78:456–459, 1982

Stoker AW, Streuli CH, Martins-Green M, Bissell MJ: Designer microenvironments for the analysis of cell and tissue function. *Current Opinion Cell Biol* 2:864–874, 1990

Szabowski A, Maas-Szabowski N, Andrecht S, Kolbus A, Schorpp-Kistner M, Fusenig NE, Angel P: c-Jun and JunB antagonistically control cytokine-regulated mesenchymal–epidermal interaction in skin. *Cell* 103:745–755, 2000

Vaccariello M, Javaherian A, Garlick JA: *A Skin Substitute Model for Wound Healing. Tissue Engineering Methods and Protocols*. Totowa: Humana Press, 1999; p 391–406

Woodley DT, Stanley JR, Reese MJ, O'Keefe EJ: Human dermal fibroblasts synthesize laminin. *J Invest Dermatol* 90:679–683, 1988

Wu Y-J, Parker LM, Binder NE, Beckett MA, Sinard JH, Griffiths CT, Reinwald JG: The mesothelial keratins: A new family of cytoskeletal proteins identified in cultured mesothelial cells nonkeratinizing epithelia. *Cell* 31:693–703, 1982

Yurchenco PD, O'Rear JJ: Basement membrane assembly. *Methods Enzymol* 245: 489–518, 1994

Zieske JD, Mason VS, Wasson ME, *et al*: Basement membrane assembly and differentiation of cultured corneal cells: Importance of culture environment and endothelial cell interaction. *Exp Cell Res* 214:621–633, 1994